Spring 2016

Discrepancy Analysis Between Close-Range Photogrammetry And Terrestrial LiDAR

Sam R. Newsome Jr

DISCREPANCY ANALYSIS BETWEEN CLOSE-RANGE PHOTOGRAMMETRY AND TERRESTRIAL LIDAR

by

SAM R. NEWSOME JR

(Under the Direction of Gustavo Maldonado)

ABSTRACT

This study presents a comparison of building measurements performed on 3D models generated by two different approaches. In one approach, the models were produced via close-range photogrammetry. Such models are based on still-frame photographs that are, post-processed with commercially available photogrammetric software. In the second approach, 3D point-cloud models were generated via laser scanning. For this purpose, three case studies were conducted. The first was a simple one story structure, the second was a multi-story Maya ruin, and the third was an earth filled terrace. Several benchmarks within a closed traverse were established to serve as standard georeference points for all accuracy comparisons. Several physical target points were then marked on the exterior walls of the structure. They are referred here as reference wall points. The reference wall points were then measured with a total-station instrument. After photographs were taken and laser scanning of the structure performed, the coordinates of the reference wall points were also determined from the respective models. The coordinates were then compared with the ones obtained with the total-station instrument. Coordinates and distances from each procedure were compared to determine relative discrepancies and accuracies. The results of this study demonstrate that the close-range photogrammetry can provide accurate enough information

to be used as an alternative for total stations or laser scanners when measuring buildings or other relatively small projects.

INDEX WORDS: Photogrammetry, Laser Scanning, Accuracy, Close-range photogrammetry, Structural, Surveying, Discrepancy Analysis

DISCREPANCY ANALYSIS BETWEEN CLOSE-RANGE PHOTOGRAMMETRY AND TERRESTRIAL LIDAR

by

SAM R. NEWSOME JR

B.S., Georgia Southern University, 2014

A Thesis Submitted to the Graduate Faculty of Georgia Southern University in

Partial Fulfillment of the Requirements for the Degree

MASTER OF SCIENCE

STATESBORO, GEORGIA

DISCREPANCY ANALYSIS BETWEEN CLOSE-RANGE PHOTOGRAMMETRY AND TERRESTRIAL LIDAR

by

SAM R. NEWSOME JR

Major Professor:	Gustavo Maldonado
Committee:	Marcel Maghiar
	N. Mike Jackson

Electronic Version Approved:

May 2016

DEDICATION

To my mother and father

ACKNOWLEDGMENTS

I would like to express my thanks to Dr. Gustavo Maldonado, Dr. Marcel Maghiar, and Dr. N. Mike Jackson for their guidance and knowledge and opportunities that they have given me in my academic career here at Georgia Southern. I would also like to thank the fall 2014, spring 2015, and summer 2015 senior project groups that assisted with the data collection. Finally, I would like to thank the Allen E. Paulson College of Engineering and Information Technology for this opportunity.

TABLE OF CONTENTS

ACKNOWLEDGMENTS VII

FIGURES XIII

TABLES XIV

CHAPTER 1 15

INTRODUCTION 15

Purpose of the study *15*

CHAPTER 2 17

LITERATURE REVIEW 17

Introduction *17*

History of Photogrammetry *17*

Types of Photogrammetry *18*

Comparison Instruments *20*

Science of Photogrammetry *22*

Similar Studies *23*

CHAPTER 3 27

METHODS 27

Equipment *27*

Equipment Cost *29*

Data Analysis Explanation *30*

CHAPTER 4 32

CASE STUDY: RECREATION ACTIVITY CENTER (RAC) STORAGE BUILDING 32

Procedures for Data Collection *32*

Data Analysis *47*

Coordinate Discrepancy Comparison of Photogrammetry Model and Laser Scanner Model to Coordinates Obtained via Total Station 48

Comparison of Distances in the Photogrammetry and Laser Scanner Models Relative to Center Point A066 49

Comparison of Distances in the Photogrammetry and Laser Scanner Models Relative to Center Point B013 52

Comparison of Distances in the Photogrammetry and Laser Scanner Models Relative to Center Point C035 55

Comparison of Distances in the Photogrammetry and Laser Scanner Models Relative to Center Point D022 57

CHAPTER 5 60

CASE STUDY: TEMPLE OF THE SEVEN DOLLS MERIDA, MEXICO 60

Procedures for Data Collection *60*

Data Analysis *72*

Coordinate Discrepancy Comparison of Photogrammetry Model and Laser Scanner Model to Coordinates Obtained via Total Station 73
Comparison of Distances in the Photogrammetry and Laser Scanner Models Relative to Center Point N3..... 74
Comparison of Distances in the Photogrammetry and Laser Scanner Models Relative to Center Point S5 77
Coordinate Distances of Photogrammetry Model and Laser Scanner Model to Center Point E4..... 80
Comparison of Distances in the Photogrammetry and Laser Scanner Models Relative to Center Point W8..... 82
CHAPTER 6 85
CASE STUDY: ZACH S. HENDERSON LIBRARY TERRACE 85
Procedures for Data Collection..... *85*
Data Analysis..... *93*
Coordinate Discrepancy Comparison of Photogrammetry Model and Laser Scanner Model to Coordinates Obtained via Total Station 94
Comparison of Distances in the Photogrammetry and Laser Scanner Models Relative to Center Point A011..... 95
Comparison of Distances in the Photogrammetry and Laser Scanner Models Relative to Center Point B007..... 98
Coordinate Distances of Photogrammetry Model and Laser Scanner Model to Center Point D003 101

Comparison of Distances in the Photogrammetry and Laser Scanner Models Relative to Center Point E007 103

CHAPTER 7 106

CONCLUSIONS AND RECOMMENDATIONS 106

Conclusion *106*

Recommendations *108*

REFERENCES 111

APPENDIX A 113

CASE STUDY: RECREATION ACTIVITY CENTER (RAC) STORAGE BUILDING 113

Raw Total Station, Laser Scanner, and Photogrammetry Data *113*

Coordinate Discrepancy Data *115*

Distance Discrepancy Data *117*

Laser Scanner 117

Photogrammetry 122

APPENDIX B 127

CASE STUDY: TEMPLE OF THE SEVEN DOLLS MERIDA, MEXICO 127

Raw Total Station, Laser Scanner, and Photogrammetry Data *127*

Coordinate Discrepancy Data *129*

Distance Discrepancy Data *131*

Laser Scanner 131

Photogrammetry 136

APPENDIX C 141

CASE STUDY: ZACH S. HENDERSON LIBRARY TERRACE 141

Raw Total Station, Laser Scanner, and Photogrammetry Data *141*

Coordinate Discrepancy Data *144*

Distance Discrepancy Data *146*

Laser Scanner 146

Photogrammetry 151

FIGURES

Figure 4.1 Google Map view of traverse 34
Figure 4.2 Coordinates A, B, C, & D..... 34
Figure 4.3 Align Photo Default Settings Figure 4.4 Build Dense Cloud Default Settings 37
Figure 4.5 Build Texture Default Settings Figure 4.6 Build Mesh Default Settings 38
Figure 4.7 Front view of modeled RAC storage building model 39
Figure 4.8 Left side view of RAC storage building model..... 40
Figure 4.9 Back view of RAC storage building model..... 41
Figure 4.10 Right side view of RAC storage building model..... 42
Figure 4.11 Points marked on RAC storage building model 43
Figure 4.12 Point marking example (reference wall point) for RAC storage building 45
Figure 4.13 Front view of RAC storage building model 46
Figure 4.14 Far view of front of RAC storage building model 46
Figure 4.15 Discrepancies in measured distances for RAC at center point A006..... 50
Figure 4.16 Discrepancies in measured distances for center point B013 53
Figure 4.17 Discrepancies in measured distances for center point C035 56
Figure 4.18 Discrepancies in measured distances for center point D022 58
Figure 5.1 Google Map view of benchmarks around the temple..... 62
Figure 5.2 Coordinates of A, B, C, & D around the temple in the adopted relative coordinate system 63
Figure 5.3 Modeled temple. View toward Southeast..... 67
Figure 5.4 Modeled temple. View toward Northwest..... 68
Figure 5.5 Reference wall points on the temple 68
Figure 5.6 Complete laser scanner model of temple..... 70
Figure 5.7 Trimmed laser model of temple 71
Figure 5.8 Example of reference wall point in virtual model of temple..... 71
Figure 5.9 Discrepancies in measured distances for the temple at center point N3 75
Figure 5.10 Discrepancies in measured distances for the temple at center point S5..... 78
Figure 5.11 Discrepancies in measured distances for temple at center point E4..... 81
Figure 5.12 Discrepancies in measured distances for the temple at center point W8 83
Figure 6.1 Modeled library terrace 89
Figure 6.2 Overhead view of modeled library terrace 90
Figure 6.3 Points marked on library terrace..... 90
Figure 6.4 Point marking example for library terrace..... 92
Figure 6.5 Overhead view of laser scanner library terrace model 92
Figure 6.6 Overhead view of laser scanner library terrace model with point cloud colored..... 93
Figure 6.7 Discrepancies in measured distances for terrace at center point A011 96
Figure 6.8 Discrepancies in measured distances for terrace at center point B007 99
Figure 6.9 Discrepancies in measured distances for terrace at center point D003 102
Figure 6.10 Discrepancies in measured distances for terrace at center point E007..... 104

TABLES

Table 4.1 Final coordinates of traverse benchmarks 35
Table 4.2 Coordinate discrepancy statistical data for RAC with outliers removed 49
Table 4.3 Statistical data of both discrepancies for the RAC at center point A066 with outliers removed 51
Table 4.4 Discrepancies ranges for distance discrepancies of center point A066 52
Table 4.5 Statistical data of both discrepancies for the RAC at center point B013 with outliers removed 54
Table 4.6 Discrepancies ranges for distance discrepancies of center point B013 54
Table 4.7 Statistical data of both discrepancies for the RAC at center point C035 with outliers removed 56
Table 4.8 Discrepancies ranges for distance discrepancies of center point C035 57
Table 4.9 Statistical data of both discrepancies for the RAC at center point D022 with outliers removed 58
Table 4.10 Discrepancies ranges for distance discrepancies of center point D022 59
Table 5.1 Final coordinates of temple benchmarks 64
Table 5.2 Coordinate discrepancy statistical data for temple 74
Table 5.3 Statistical data of distance discrepancies for the temple at center point N3 with outliers removed 76
Table 5.4 Distance discrepancy ranges for the temple at center point N3 77
Table 5.5 Statistical data of distance discrepancies for the temple at center point S5 with outliers removed 79
Table 5.6 Distance discrepancy ranges for the temple at center point S5 79
Table 5.7 Statistical data of distance discrepancies for the temple at center point E4 with outliers removed 81
Table 5.8 Distance discrepancy ranges for temple at center point E4 82
Table 5.9 Statistical data of distance discrepancies for the temple at center point W8 with outliers removed 83
Table 5.10 Distance discrepancy ranges for the temple at center point W8 84
Table 6.1 Coordinate discrepancy statistical data for terrace 95
Table 6.2 Statistical data of distance discrepancies for the terrace at center point A011 with outliers removed 97
Table 6.3 Distance discrepancy ranges for the terrace at center point A011 98
Table 6.4 Statistical data of distance discrepancies for terrace at center point B007 with outliers removed 100
Table 6.5 Distance discrepancy ranges for terrace at center point B007 100
Table 6.6 Statistical data of distance discrepancies for terrace at center point D003 with outliers removed 102
Table 6.7 Distance discrepancy ranges for terrace at center point D003 103
Table 6.8 Statistical data of distance discrepancies for terrace at center point E007 with outliers removed 104
Table 6.9 Distance discrepancy ranges for terrace at center point E007 105

CHAPTER 1

INTRODUCTION

PURPOSE OF THE STUDY

This work involves the study of spatial discrepancies in 3D virtual models generated by two modern approaches, close-range photogrammetry and laser scanning versus positions and distances acquired via classical, laser-based, total-station, surveying instruments. In the photogrammetric approach, the software-generated models were produced from sets of multiple 2D overlapping photographic images, taken from different locations around the structure to be modeled. This technique is now known as close-range photogrammetry and has substantially evolved in the last 30 years. Modern surveying scanning equipment was also employed to create 3D point-cloud models of the same objects using laser scanners. Constant improvements in computer processing times, photographic camera definitions and unmanned aerial vehicles (UAVs) capabilities have increased the use of close-range photogrammetry. It is now becoming a popular alternative for standard surveying techniques, especially in projects where the camera-to-object distances are relatively short. This is because accuracy needs to be within a specified range so the corresponding measurements are acceptable in the surveying industry. If close-range photogrammetry can produce 3D models with accuracies similar to models produced by terrestrial LiDAR and classical total-station instruments, then it could be used as an alternative approach to those methods.

This study compares spatial discrepancies attained via close-range photogrammetry and laser scanning against measurements acquired via total-station instruments. In this work, the total station was used as the control instrument that the others will be judged against. Three case studies

were selected for the mentioned comparison based on the location, size of structure, and type of survey. The first was located near the Recreation Activity Center (RAC) on the campus of Georgia Southern University. This site contained several buildings of varying sizes, but a small brick storage building was chosen for its size and location. The second was located outside the city of Mérida in the Yucatán state of Mexico. The place is a national historical Maya site run by the Mexican National Institute of Anthropology and History (INAH as per its Spanish acronym) called Dzibilchaltun. The Temple of the Seven Dolls at Dzibilchaltun was selected as it was the most complete structure and one of the largest at the site. The last case study was located next to the Zach S. Henderson Library on the Campus of Georgia Southern University. This site was selected as it focused on topography instead of structures.

Several other studies have focused on the accuracy of photogrammetry and laser scanning in past few years. While the studies are similar to this research in some ways they differ greatly. This study placed actual targets (reference wall points) on the structure being measured, which allowed the comparison points to be precisely located in all the models. The other studies used features on the structures to locate their comparison points. The method in which the points were compared also differed. This research used two different approaches, while most others only used one. The first method was the coordinate discrepancy approach that compared the differences in the actual coordinate readings. Even though this coordinate discrepancy method was used by several other the studies, none of them used the second approach, which was the distance discrepancy approach from a center point. In the latter method, distances from several points are calculated from a random center point. The distances acquired from each model are then compared to the distances acquired by a total-station instrument.

CHAPTER 2

LITERATURE REVIEW

INTRODUCTION

The purpose of this study is to compare the accuracy of location and distances in models generated via close-range photogrammetry against spatial measurements obtained with traditional surveying equipment. It is important to understand the technology employed and what others have done in the field. This section covers the background of photogrammetry and the different types that are currently being used. It will also provide some basic information about the laser scanning and total station instruments that are employed as comparison in this study. Next, it includes a general look at the science of photogrammetry. Finally, it explores similar work that others have done related to photogrammetry and laser scanning.

HISTORY OF PHOTOGRAMMETRY

Photogrammetry is not a recent development in technology. In fact, the origins of photogrammetry can be traced back to Leonardo da Vinci's work with optical perceptivity in 1492 (Ghosh 2005, 30). Ghosh indicates that da Vinci's work provided the foundation for photogrammetry that is used today. Another important advancement is credited to John Heinrich Lambert. In 1759, Lambert first introduced the concept of inverse central perspective and space resection of conjugate images in his book "Freie Perspective" (Ghosh 2005, 30). This allowed mathematical principles to be used to find where in space a picture was taken from. According to

Ghosh, Guido Hauck contributed to the field by establishing the relationship between projective geometry and photogrammetry in 1883. Hauck's relationship is considered the most fundamental geometric concept and basis to which most classic analytical photogrammetric developments are based on (Ghosh 2005, 31). In the time period between the turn of the century and the start of World War I, very little developments in analytical photogrammetry were made, even with development of civil aviation (Ghosh 2005, 31-32). Unfortunately, one major setback did occur during this time period. The Dutch government contracted a German company to do mapping of the coast and several islands, but it ultimately failed due to inadequate ground control producing large errors in scale and azimuths (Ghosh 2005, 32). This single handedly set back the practical application of photogrammetry in mapping for almost twenty years in Europe (Ghosh 2005, 32). After World War II, advancements in photogrammetry increased dramatically with the invention of the modern computer being one of main contributors (Ghosh 2005, 34-35).

TYPES OF PHOTOGRAMMETRY

There are two main types of photogrammetry that is used today in civil engineering and surveying, which are close-range and aerial. As the name implies, aerial photogrammetry is accomplished by attaching downward facing cameras to aircraft and flying over the areas of interest. According to Matthews (2008, 5)," Aerial photogrammetry utilizes large-format imagery and ground coordinate information to effectively recreate the geometry of a portion of the earth in a virtual environment. In this virtual environment, reliable horizontal and vertical measurements can be made and recorded (or compiled) directly into a geospatial data file." Aerial

photogrammetry is commonly used for mapping surveys, digital terrain models, and digital orthophotos (Matthews 2008, 8-9).

The other type of photogrammetry is close-range. Close-range photogrammetry is similar to aerial photogrammetry as many of the basic principles apply. The main difference between the two is the distance from the camera to the object. In close-range photogrammetry the object-to-camera distance is less than 1000 ft. or 300 m (Matthews 2008, 11). A variety of different camera configurations and platforms are included under close-range, including low level aerial for light sport aircraft and helium-filled blimps (Matthews 2008, 11). Also included in close-range photogrammetry are photos taken from the ground and from unmanned aerial vehicles (UAVs). Close-range Photogrammetry has not always been a preferred method until recent technology advancements. This is supported by a quote from Matthews describing the Bureau of Land Management's use of close-range photogrammetry in the late 1980's:

> The BLM's [Bureau of Land Management's] national center in Denver has used close-range photogrammetric techniques to document resources since the late 1980s. At that time, although producing high-quality results, the close-range photogrammetric process could be tedious and time-consuming mainly because of the need to apply traditional techniques, workflow, and equipment to close-range image capture and processing. However, recent advances in commercially available and cost-effective three-dimensional measuring and modeling (3DMM) software, high-resolution digital cameras, and high- performance laptop computers have revolutionized the CRP [close-range photogrammetry] process. (Matthews 2008, 11)

This advancement in technology has allowed photogrammetry processing to be moved from the laboratory to the field and from experts to technicians (Matthews 2008, 11). Another difference from aerial photogrammetry is the ability to use standard consumer grade cameras. This mainly due to the advancements in 3D modeling software and digital camera resolution that Mathews

mentioned earlier. Until this advancement in camera and software, close-range relied on the same costly surveying grade camera systems as aerial photogrammetry (Matthews 2008, 5-11). According to Mathews, one of the main advantages of close-range photogrammetry is that it required minimal field equipment and training to produce precise results (Matthews 2008, 2).

COMPARISON INSTRUMENTS

An alternative to close-range photogrammetry modeling is laser scanning. Both technologies are used to collect spatial coordinates from an object in order to generate point clouds, but the way they collect this information is different (Dai, Rashidi, et al. 2013, 69). The type of laser scanner used in this study is a time-of-flight based pulse scanner. Time-of-flight scanners operate by emitting a laser pulse at a target and timing how long it takes the sent light to bounce back to the scanner (Dai, Rashidi, et al. 2013, 70). This allows the scanner to calculate the distance to the target and coordinates of the target. According to Dai et al. (2013, 70), with this technology "high-definition (dense) and accurate point clouds can be achieved." Dai et al. (2013, 70) also made several observations on how certain conditions affected accuracy of laser scanners such as: distance to surface, angle of incidence, reflectivity of materials, humidity, lighting, and roughness of surface. Dai et al. (2013, 70) states that the accuracy of laser scanners decrease as distance increases with accuracy decreasing form 6 mm at 50 m to 20 mm at 100 m. Another condition which affects the accuracy of laser scanners is angle of incidence. The angle of incidence affects the signal intensity by a factor of four when the angle is less than 90 degrees (Dai, Rashidi, et al. 2013, 70). The reflectivity of materials also affects the accuracy by introducing range errors (Dai,

Rashidi, et al. 2013, 70). According to Dai et al. (2013, 70), other conditions such as humidity, lighting, and roughness only had a marginal effect on the accuracy of the laser scanner.

The other instrument used in this study was a total station instrument. Total stations evolved from early theodolites. A total station combines the capabilities of an electronic theodolite with electronic distance measurement (Kavanagh and Mastin 2014, 110). This combination allows the total station to measure horizontal angles, vertical angles, and distances. The ability to measure angles and distances was just one of the capabilities that set the total station apart from its predecessors. According to Kavanagh and Mastin (2014, 115), the microprocessor included in the total station instrument can perform several different mathematical operations including: averaging multiple distance or angle measurements, determining horizontal and vertical distances, and determining X, Y, and Z coordinates. The accuracies of total stations can vary from one instrument to another, but most instruments fall into an angular accuracy range of 0.5 to 5 seconds and are capable of measuring distances up to 3,000 m with one prism (Kavanagh and Mastin 2014, 115). This level of accuracy is possible due to the included dual axis compensator. The dual axis compensator allows the instrument to correct for lateral and longitudinal errors in leveling (Kavanagh and Mastin 2014, 115). In the past, surveyors would have had to measure the angles in both faces of the instrument and average the results to minimize any tilt errors. Now with dual axis compensators, the instrument's microprocessor can automatically remove any errors and adjust the measurement accordantly (Kavanagh and Mastin 2014).

SCIENCE OF PHOTOGRAMMETRY

Photogrammetry is a surveying technique that uses data extracted from two-dimensional photo images and aligns them into a three-dimensional model (Dai and Lu 2010, 242). This technique relies on the collinearity equations that allow the image coordinates to be related to the object coordinates (Dai and Lu 2010, 243). The basic principle of the equations is that the object point, camera center, and image point lie on a straight line (Yakar, Yilmaz and Mutluoglu 2010, 87). Dia and Lu (2010, 243) state, "If a camera's internal parameters are known, any spatial point can be fixed by intersection of two rays of light that are projected from two different camera stations." This is the basic principle of how photogrammetry software algorithms work to align pictures and produce models. However, there are two major factors that can affect the accuracy of the resulting model. The first is a system error due to lens distortion (Dai and Lu 2010, 243). Dia and Lu (2010, 243) state that "measurements errors due to camera lens distortion can be treated as the system error with a consistent effect." This error causes the point to shift from its true position to a skewed position (Dai and Lu 2010, 243). This is due to a combination of decentering distortion and radial distortion (Dai and Lu 2010, 244). Decentering distortion is caused by the camera lenses not being perfectly centered in relation to each other (Dai and Lu 2010, 243). Radial distortion is a distortion in each lens, this distortion causes points that are further from the center of the lens to have a greater distortion (Dai and Lu 2010, 243). This type of error is easily corrected by the photogrammetry software. The second type of errors according to Dai and Lu (2010, 243) are errors due to human factors. Most human errors are attributed to the imprecise marking of points in two different photos. This can be overcome by marking the points in three or more photos (Dai and Lu 2010, 243). This is why most programs require the points to be marked in at least three photos.

SIMILAR STUDIES

Several research studies similar to this one have been performed in recent years. Some of the studies deal with accuracy comparisons, while others take a more general look at photogrammetry and laser scanning. The first is a study performed by Dal et al. entitled "Comparison of Image-Based and Time-of-Flight-Based Technologies for Three-Dimensional Reconstruction of Infrastructure." In this study, Dal et al. compares photogrammetry and laser scanning accuracy, quality, time efficiency, and cost. The proposed methodology of this study was to produce models using photogrammetry and laser scanning and compare the spatial coordinates against those obtained by a total station (Dai, Rashidi, et al. 2013). One notable different between Dai's et al. study and this research is the method of point comparison. Dai et al. (2013, 72) used the corners of the infrastructure and other feature points on the surface for the comparison points, while this study uses physical targets placed on the structure. Their study employed a ground truth model that was created using the total station data. This was then used as the reference for the accuracy comparison by registering the point clouds produced by laser scanning and photogrammetry into same coordinate frame as the ground truth model (Dai, Rashidi, et al. 2013, 72) Three types of photogrammetry software were used by Dai, et al. (2013, 71) in addition to the laser scanner. They conducted several case studies to obtain the necessary data, which were a concrete beam bridge, a stone building, and concrete arch bridge. The concrete beam bridge produced an average error of between 6.44 cm and 14.06 cm for the photogrammetry and 0.48 cm to 0.56 cm for the laser scanner (Dai, Rashidi, et al. 2013, 74). The stone building had similar results with an average error between 6.83 cm to 10.46 cm for the photogrammetry and

0.59 cm to 0.67 cm for the laser scanner (Dai, Rashidi, et al. 2013, 75). In the last case study, only the photogrammetry was compared against the ground truth model. The photogrammetry model had an average error between 6.52 cm and 9.48 cm (Dai, Rashidi, et al. 2013, 76). Dai et al. also made note of the point density that each model produced. The photogrammetry models had a point density between 3,200 and 10,000 points per square meter, while the laser scanner consistently had over 10, 000 points per square meter (Dai, Rashidi, et al. 2013, 74-76). Dai et al. (2013, 77) concluded that photogrammetry and laser scanning produce dense point clouds that were satisfactory for visualization and photogrammetry offered a good alternative to laser scanning when accuracies required were greater than 8 cm.

Another notable study in close-range photogrammetry was done by Yakar, Yilmaz and Mutluoglu (2010) called "Close range photogrammetry and robotic total station in volume calculation." In this study, Yakar, Yilmaz and Mutluoglu (2010, 88) conducted a volume calculation comparison between close-range photogrammetry and a robotic total station. However, they used the robotic total station in a manner similar to a laser scanner. The robotic total station was set to scan a sand pile at a spacing of 20 cm to produce a point cloud (Yakar, Yilmaz and Mutluoglu 2010, 90). They performed two additional scan with the robotic total station, one was at a 40 cm interval and the other was at a 100 cm interval (Yakar, Yilmaz and Mutluoglu 2010, 90). All three of the robotic total station models and the photogrammetry model were compared to the known volume that was obtained using a lorry (Yakar, Yilmaz and Mutluoglu 2010, 88). The photogrammetry model had a 93.63 percent accuracy, while the 20 cm total station model had a 96.35 percent accuracy (Yakar, Yilmaz and Mutluoglu 2010, 95). The two other total station models had slightly lower accuracies, but both were still above 90 percent. After the base line was established, Yakar, Yilmaz and Mutluoglu (2010, 95) had a known volume

of the material removed from the pile. They recreated the models and compared volume results to the known volume left in the pile. The results obtained by Yakar, Yilmaz and Mutluoglu (2010, 95) were a 96.35 percent accuracy for the total station model, 63.13 percent accuracy for the photogrammetry model, and 89.04 percent accuracy for the geodetic method. They concluded that photogrammetry was a viable solution since it had significant time and cost savings (Yakar, Yilmaz and Mutluoglu 2010, 95).

A study carried out by Sužiedelytė-Visockienė, et al. (2015) focued on the accuracy of close-range photogrammetry for use in deformation of achitectural structures. The study was entiltled "Close-Range Photogrammetry Enables Documentation of Enviroment-Induced Deformation of Achitectural Heritage." The purpose of the study was to find out if close-range photogrammetry had the required accuracy to catalog the current state of achitectural pieces and track its deformation over time. Sužiedelytė-Visockienė, et al. (2015, 1374) used standard photogrammetry software and high end consumer grade digital cameras for the study. The models produced were referenced to estiblished control points for the comparison. Sužiedelytė-Visockienė, et al. (2015, 1378) was able to obtain an accuracy of 1 to 5 µm on two different ornaments inside a heritage achitectural site. They concluded that photogrammerty could be used for documentation and geometric deformation monitoring of cultural heritage sites (Sužiedelytė-Visockienė, et al. 2015, 1378-1379).

Another study titled "Comparison Methods of Terrestrial Laser Scanning, Photogrammetry and Tacheometry Data for Recording of Cultural Heritage Buildings" by Gussenmeyer et al. (2008) fouced on comparing the different technologies and methods of its use. In this study, they used a laser scanner, a total station, and photogrammetry software to capture points on a historic castle. The main difference was that Gussenmeyer et al. (2008) did not do a direct accuracy

comparison. They fouced more on the quality of the models produced and the quality of the points collected. This was accomplished by using the points collected by each system to produce a wireframe that was composed of 21 windows (Grussenmeyer, et al. 2008, 215). A qoute from Grussenmeyer et al. (2008, 214-215) explains why this method was used, "For comparing laser and surveying data, a point to point comparison makes no sence, since laser scanning technique does not allow choosing the point to be measured." This method is no longer nessceary as technology has evloved since this publication. It is now very easy to select exact points from a 3D model for direct point to point comparison. Gurussenmeyer et al. (2008, 216) found using their method that 88 percent of the points fell in a range of -2 cm to 4 cm when comparing diffences in the photogrammetry and laser scanner meshes. They concluded that each system had its own limitations and strengths depending on what the site situtaions demanded, thus one system could not be recommend over the others (Grussenmeyer, et al. 2008, 217)

CHAPTER 3

METHODS

EQUIPMENT

The equipment employed for the photogrammetry part of the project included three cameras, a standard desktop computer, and a photogrammetric processing software. The equipment used for comparison included a laser scanner and total station instrument. The laser scanner required targets, point cloud software, and various tripods. The total station also required additional items such as prisms and tripods.

The three cameras used in this project were a Nikon D800, Canon EOS 5D Mark III, and GoPro Hero 3 Plus Black Edition. The Nikon D800 is a single-lens reflex digital still frame camera with 36.3 effective megapixels. The Nikon D800 was equipped with a fixed wide angle Nikkor 28mm auto focus lens for the duration of the project. The Canon EOS 5D Mark III is a digital single-lens reflex still camera with 22.3 effective megapixels. The Canon was equipped with a fixed wide angle Ultrasonic 20mm auto focus lens for the first seven weeks of the study. After week seven, the Canon was refitted with a fixed wide angle Ultrasonic 24mm auto focus lens with image stabilization. The lens change was necessary to allow the Canon to be mounted in the unmanned aerial vehicle's gimbal assembly for close-range aerial photogrammetry. The GoPro Hero 3 Plus Black Edition is a digital video camera with 12 effective megapixels. The GoPro Hero 3 Plus Black Edition was originally equipped with a fisheye lens from the factory. The fish eye lens was replaced with a fixed wide angle lens to allow the GoPro to be more compatible with the

photogrammetry software and allow for less lens distortion. This is no longer necessary as most software now has built in correction for the GoPro's fish eye lens.

The main component of this study is the software used for 3D model generation. The software used throught out this study was Agisoft's PhotoScan Pro. PhotoScan is a 3D modeling, measuring, and georeferencing software. Three different versions of PhotoScan Pro were used to produce models for this study, which are: version 1.1.0 build 2004, version 1.1.4 build 2021, and version 1.1.6 build 2038. The process used by PhotoScan is photogrammetric triangulation (Features Professional Edition n.d.). PhotoScan includes additional capabilities such as dense point cloud editing and classification, digital elevation modeling, and georeferencing (Features Professional Edition n.d.). PhotoScan has many applications including architecture, engineering, geology, mining, surveying, and many others. In this project, the main focus will be on engineering and surveying applications.

The equipment employed for laser scanning is comprised of three parts. The main part of the system is the actual laser scanner. The scanner owned by Georgia Southern is the Leica Geosystems ScanStation C10. The Leica ScanStation C10 is a ground based laser scanner that is capable of collecting 50,000 points per second at a maximum range of 300 meter (Leica Geosystems 2012). According to Leica Geosystems user manual for the ScanStation C10, the accuracy of the scanner is 6 mm for position, 4 mm for distance, and 12 seconds for horizontal and vertical angles (Leica Geosystems 2012). The next piece of required equipment for the scanner is scanner registration targets. The scanner registration targets are used during the registration process in the scanner software to stitch the different scans together. There are four different types of scanner registration targets that can be used with the ScanStation C10, which are a 6" sphere, 6" black & white tilt and turn target, 6" blue tilt and turn target, and HDS twin target pole system.

Only the HDS twin target pole system, the 6" blue tilt and turn targets, and 6" spheres were used for this study. The last piece of major equipment required to operate the mentioned scanner is the Leica Cyclone software package. Cyclone combines many features into one software package such as point cloud registration, model creation, virtual surveying, and publishing. In this study, the main features used from Cyclone were the point cloud registration, measuring tools, and model creation. Some miscellaneous equipment used included a tripod for the scanner, target poles, and target tripods.

The total-station used for comparison was a Topcon model GPT-3200NW. This total station has an angular accuracy of 7 seconds with a minimum reading of 5 seconds in the horizontal and 10 seconds in the vertical (Topcon GPT 3000 n.d.). This instrument also has a single axis tilt compensator with a correction range of ± 3 minutes (Topcon GPT 3000 n.d.). Some miscellaneous equipment used included a tripod for the total station, prisms, prism poles, and prism pole tripods.

EQUIPMENT COST

The cost of equipment is an important consideration when selecting a modeling system to use. In this section, the list prices for the photogrammetry and laser scanning equipment will be given. Photogrammetry requires a camera and the photogrammetry software. In this study, three cameras were used along with one photogrammetry software. The first camera selected for this study was the Canon EOS 5D Mark III with a Canon EF 24mm lens. The current price for the camera without the lens is $2,799.00 (Canon EOS 5D Mark III 2015). The lens has a current price of 599.99 (Canon EF 24mm f/2.8 IS USM 2015). The next camera used was the Nikon D800 equipped with a fixed wide angle Nikkor 28mm auto focus lens. The price for the camera without

the lens is $2,799.95 (Nikon D800 n.d.). The lens has a current price of $289.95 (AF Nikkor 28mm f/2.8D n.d.). The last camera used was a GoPro Hero 3 Plus Black Edition, which has a current price of $364.99 (GoPro Hero3: Black Edition n.d.). The photogrammetry software used in this study was Agisoft's PhotoScan Professional, which sales for $3,499.00 (Agisoft 2016).

Laser scanning requires a scanner, scanner registration targets, tripods, and software. The current list price for the Leica ScanStation C10 is $102,375.00 (FLT Geosystems 2015). The tripod for the laser scanner is a Leica 5000 series, which has a current price of $309.00 (FTL Geosystems Leica Professional 5000 Series Tripod 2015). The targets used were the Leica HDS Twin Target Poles, but current pricing could not be found without contacting Leica Geosystems. An estimate of $1,500.00 per pole was used based off what Georgia Southern has paid in the past. The target stands used are SECO thumb release tripod, with a current price of 157.00 (FTL Geosystems SECO Thumb Release Tripod 2015). The current price for the Leica Cyclone software is $4,250.00 (Leica Cyclone 3D Point Cloud Processing Software (EA) n.d.)

DATA ANALYSIS EXPLANATION

The objective of this study is to compare point coordinates and the model relative distances collected by the total station to the coordinates generated from the models. The points used for comparison consisted of reference wall points that were applied to the building in random locations. Usually, a total of ten reference wall points were selected at random from each side of the building for a total of forty. Two different methods were used to compare the results from the models to the total station. The first was the coordinate discrepancies method, which is a direct comparison of the differences in the coordinate measurements from the model

to the total-station. Coordinate discrepancies are calculated by subtracting the easting (X), nothing (Y), and elevation (Z) of the total station measurements from the easting, nothing, and elevation of the models. This gives a direct difference in the X, Y, and Z directions. The second method was distance discrepancies from a chosen center point. In this method, a center point is chosen on each side of the building (not necessarily at the center of each side) and several distances are calculated from those center points to other points. The distance equation is used to obtain the distances from the center point to the desired points. These distances are then compared and the discrepancies presented in scatter plots.

CHAPTER 4

CASE STUDY: RECREATION ACTIVITY CENTER (RAC) STORAGE BUILDING

PROCEDURES FOR DATA COLLECTION

The focus of this section will be on the procedures used to obtain the data presented in the recreation activity center storage building case study. This section includes information about the work site and how surveying control is obtained. It also includes each instrument's detailed procedures that were used during the data collection process. Finally, it includes how the photogrammetry and laser scanner data was collected and processed to produce models.

The site selected for the model accuracy comparison is located near the Recreation Activity Center (RAC) on the Campus of Georgia Southern University. A small brick storage building with a metallic roof was selected for this purpose. This location was chosen as it had relatively little tree cover and no bushes near the building. Trees and bushes have a tendency to distort or produce holes in the models, especially the photogrammetry models, and should be avoided when possible. The small size of the building was another important characteristic that led to this location selection. The smaller size allowed multiple trials to be run without a significant investment in time. This allowed for the best procedure with the highest accuracy to be found in the time frame that was required. The only negative characteristic of this site was the lack of known nearby benchmarks for survey control. Since the location of the building prevented the use known benchmarks on campus, a closed traverse was completed to establish four benchmarks near the selected structure. After the control benchmarks were established, 299 reference wall points

were added to the structure. The reference wall points were marked with stickers on the exterior walls of the structure.

Surveying control is the ground work that allows comparisons between the different models to be done with a certain degree of confidence in accuracy. In order to compare the resulting 3D models, a control system was needed around the RAC storage building. Four benchmarks were established with nails around the building and a closed traverse was performed. The four points are shown in figures 4.1 and 4.2. They were labeled A, B, C, and D. The position of bench mark A was assumed to be 20 ft. in the X direction (easting) and 40 ft. in the Y direction (northing). It was important to establish the benchmarks with high accuracy as this would serve as the control for the whole study. Since the project was spread out over several months, divots were drilled into the nails to increase point location precision. This allowed the tip of the poles to be placed in the same position every time on the nail. The internal and external angles of the closed traverse were measured by "closing-the-horizon" and employing the "direct" and "reverse" modes of the instrument. After local corrections at each vertex, the final angular error of closure was 21 sec. When the distances were measured, the reflectorless (non-prism) mode was selected on the total station and the distance was collected as close to the ground as possible to avoid pole verticalization errors.

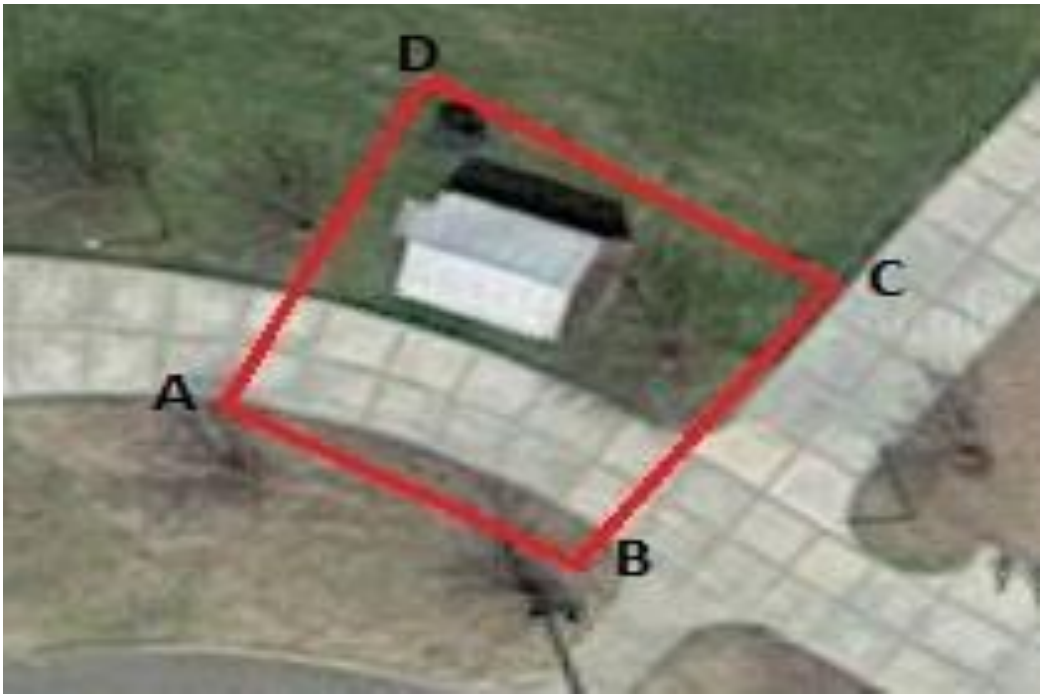

Figure 4.1 Google Map view of traverse

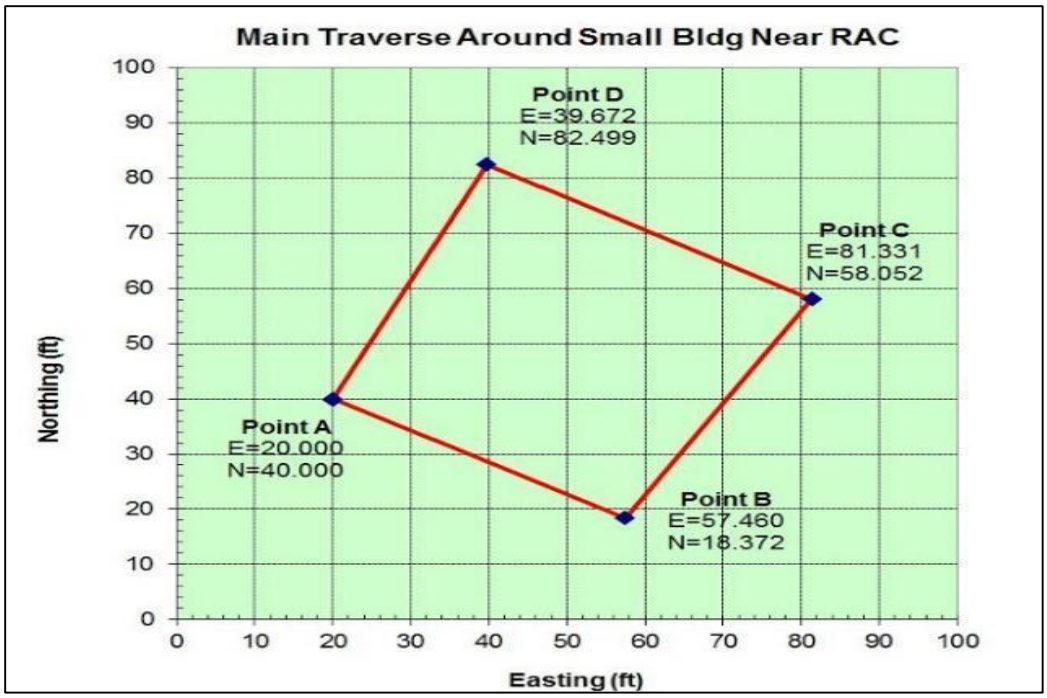

Figure 4.2 Coordinates A, B, C, & D

The final longitudinal error of closure in the traverse was 0.003 ft., which corresponded to an approximate longitudinal precision of 1 (one) unit in 59,000 units. To complete the coordinates of the reference benchmarks, the relative elevations of points A, B, C, and D were determined using a modern auto-level instrument. Since point C is the lowest point of the four, it was selected to be at a reference elevation of 10 ft. The elevations of the remaining points were then computed from this arbitrary datum. The adopted final elevations were the average of two complete closed loops. The determined final coordinates for the benchmarks are listed in table 4.1.

Table 4.1 Final coordinates of traverse benchmarks

Final Coordinates of Benchmarks			
Point	X (ft.)	Y (ft.)	Z (ft.)
A	20.000	40.000	12.461
B	57.460	18.372	11.524
C	81.331	58.052	10.000
D	39.672	82.499	11.783

The total station was the first instrument used in this study, as it was also used to establish the control benchmarks. The total station was employed as the control instrument that all other measurements would be compared to. The purpose was to compare a trusted standard instrument to the newer available technology. When collecting the points from the building, the total station occupied one of the control benchmarks. The northing, easting, and elevation coordinates of the point would be entered into the instrument along with the known azimuth to another point. This would set the instrument to the reference coordinate system and give the instrument the direction

of north. The operator would then aim the instrument at points on the building and obtain the coordinates of that point using reflectorless mode. The operator would continue collecting points until the instrument need to be moved and the set up process repeated for a new point.

The photogrammetry model was the next deliverable produced. As stated earlier, the photogrammetry software selected for this accuracy comparison was Agisoft's PhotoScan Professional Edition, version 1.1.6. Several other options were evaluated, but PhotoScan was selected as it had the required features for the scope of this study. Four different models were produced of the RAC storage building, one from each of the three cameras and a combined photo set from the Cannon and Nikon cameras. The Cannon 5D Mark III camera model was selected as it produced the clearest model of the structure. The RAC storage building model used for the comparison was created using 118 pictures. The photo set consisted of 60 pictures from ground level and 58 pictures from a ladder placed close to the building near the center of each of the four sides. The camera was set at the highest megapixel setting of 22.3 with JPEG selected as the file compression format. The camera to object distances for this case study are less than 20 ft. When preparing PhotoScan to process the pictures, the default settings were used for each process. The standard processes used were "align photos," "build dense cloud," "build mesh," and "build texture." The standard settings for the align photos operation were accuracy set to high with pair preselection disable under the general options. Under the advanced options the key point limit was set to 40,000 and tie point limit to 1,000 with constrain features by mask disabled. Refer to figure 4.3 for an example of the default settings for the align photos operation. The following default settings were used for the build dense cloud operation, quality set to medium, depth filtering to aggressive, and reuse depth maps disabled. Figure 4.4 displays the default setting for the build dense cloud operation of PhotoScan.

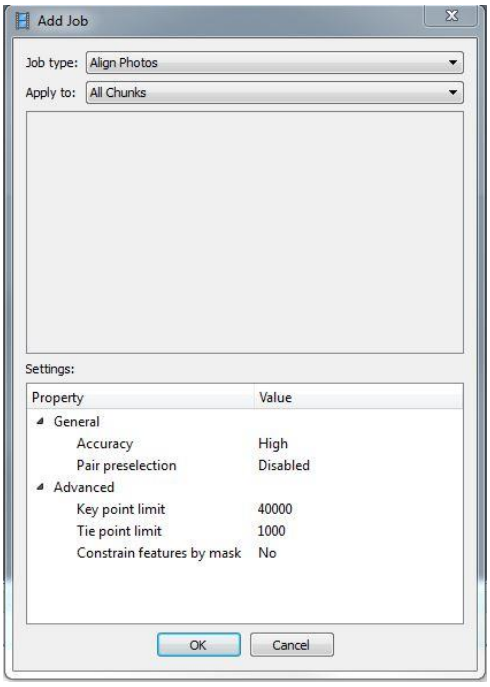

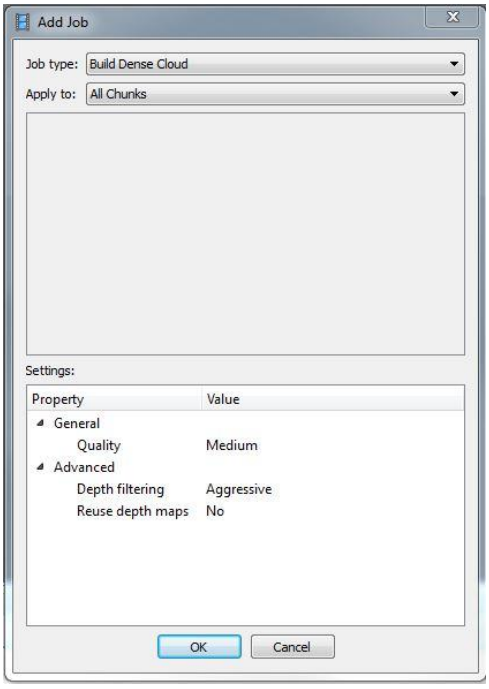

Figure 4.3 Align Photo Default Settings **Figure 4.4 Build Dense Cloud Default Settings**

Under the general tab of the build mesh operation the settings were arbitrary surface type, dense cloud source data, medium face count and 200,000 custom face count. The advanced tab had two additional setting for interpolation and point classes, both were left at the default setting of enable and all respectively. The final operation was build texture. In the general settings of build texture, mapping mode was set to generic, texture from was set to all cameras, blending mode to mosaic, texture size to 4096 and texture count to 1. Under the advance tap, there was only one setting, color correction was set to no. Figures 4.5 and 4.6 displays examples of the default settings for the build mesh and build texture operations.

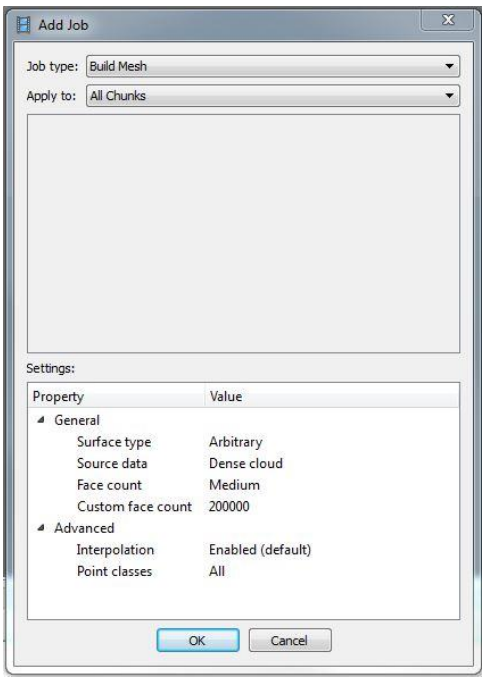

Figure 4.5 Build Texture Default Settings

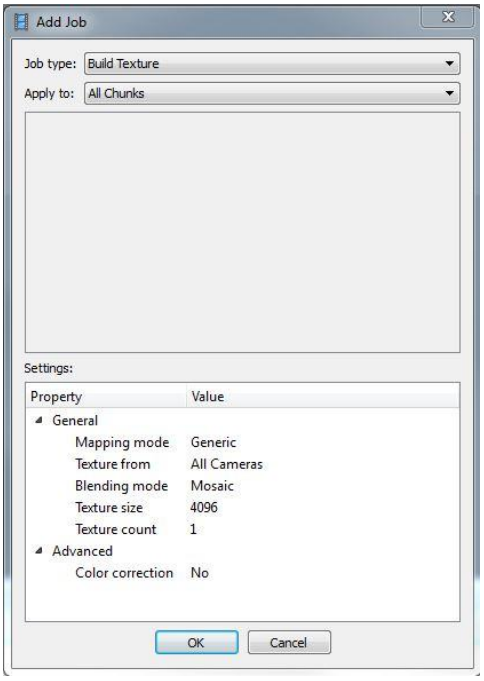

Figure 4.6 Build Mesh Default Settings

The processed model is shown in figures 4.7, 4.8, 4.9, and 4.10. After the model was created using PhotoScan, it had to be georeferenced to the relative coordinate system that was used by the total station. The georeferencing is necessary since the photogrammetry software creates its own relative coordinate system when the models are generated. Without relating one coordinate system to the other, it would be impossible to compare the coordinates of the points across multiple technologies. The photogrammetry model was georeferenced by selecting, on the walls of the structure, four of the reference wall points that were measured with the total station. The selected points were then marked in PhotoScan by placing markers in three or more photos containing each point. The purpose of marking the points in multiple photos is to allow the software to triangulate the locations of the point using the camera locations that have already been processed. After the points were marked in PhotoScan, the coordinates of the points from total station were entered.

This method of georeferencing was necessary as the control benchmarks were cut from the model by the photogrammetry program. It would have been preferable to use the control benchmarks. This is because the employed method can introduce error from total station. The cause of error stems from using points picked at random to do the georeferencing. By doing this, the researchers assumed all the points collected by the total station are accurate, which may not always be the case. After the model was georeferenced, the coordinates of the other points were collected by placing markers on the model at the location of the selected point. After all the markers were placed, the view estimated command in PhotoScan was used to calculate the coordinates of the marked points. Figure 4.11 demonstrates a marked and referenced model.

Figure 4.7 Front view of modeled RAC storage building model

Figure 4.8 Left side view of RAC storage building model

Figure 4.9 Back view of RAC storage building model

Figure 4.10 Right side view of RAC storage building model

Figure 4.11 Points marked on RAC storage building model

The laser scanner used for this project was the Leica Geosystems ScanStation C10. The scanner registration targets employed were the Leica HDS twin target pole system and the Leica 6" blue tilt and turn target. A total of six targets were used when the scanning was performed. The Leica HDS twin target poles were placed on the four benchmarks and two Leica 6" blue tilt and turn targets were placed in various locations depending on the scanner location. A total of four scans were performed with the scanner placed at each corner of the building at approximately a 6 ft. distance from the structure. This allowed the scanner to collect two sides of the building and at least three targets. The scanner was set to high resolution to ensure enough point density was achieved for point collection. This was the only time a complete project was done using high resolution scans. The high resolution scans are not needed in most situations. This is because superposed multiple medium resolution scans will increase the density of the resulting point cloud. Also high resolution scans require additional time over medium resolution scans. A high

resolution normally takes about twenty-seven minutes to complete, while a medium resolution only takes six minutes to complete. The high resolution scans were used in this case because of the corner location selected for the scanner, with smaller angle of incidence as wall segments were scanned farer from the scanner station. Since the building was small, the scanner was placed at the corners which allowed the operators to reduce the number of scans required for this building. If each face of the building were scanned individually, it would have required a minimum of eight scans and additional scanner registation target locations as it would have been impossible to see three common targets in each scan. The four high resolution scans were registered using Leica Geosystems' Cyclone software. The registration process combines the scans together using the scanner registration targets that are in each scan. Registration requires a minimum of three common targets between two scans for those scans to be stitched together. The software continues stitching corresponding scans together until all the scans are combined. After all the scans are registered together, the resulting model must be georeferenced to the total station coordinate system. Georeferencing in Cyclone is accomplished by importing a comma delimited text file containing the coordinates of the benchmarks. Cyclone uses the information in the text file to create a control scanworld. The control scanworld is then registered with the previous complete registration which georeferences the model to the correct coordinate frame. As with any process there is always some error involved. The error in the registration for this model after georeferencing was 0.013 ft. or 0.156 in. and 0.007 ft. or 0.084 in. before georeferencing. With the model georeferenced, the coordinates of the comparison points were collected from the virtual model. This was accomplished by selecting a model point that was at the center of one of the reference wall points on the model. The coordinates were recorded at that point and this was

repeated until all reference wall points were collected. An example of the point collection process can be found in figure 4.12. Also the completed model can be seen in figures 4.13 and 4.14.

Figure 4.12 Point marking example (reference wall point) for RAC storage building

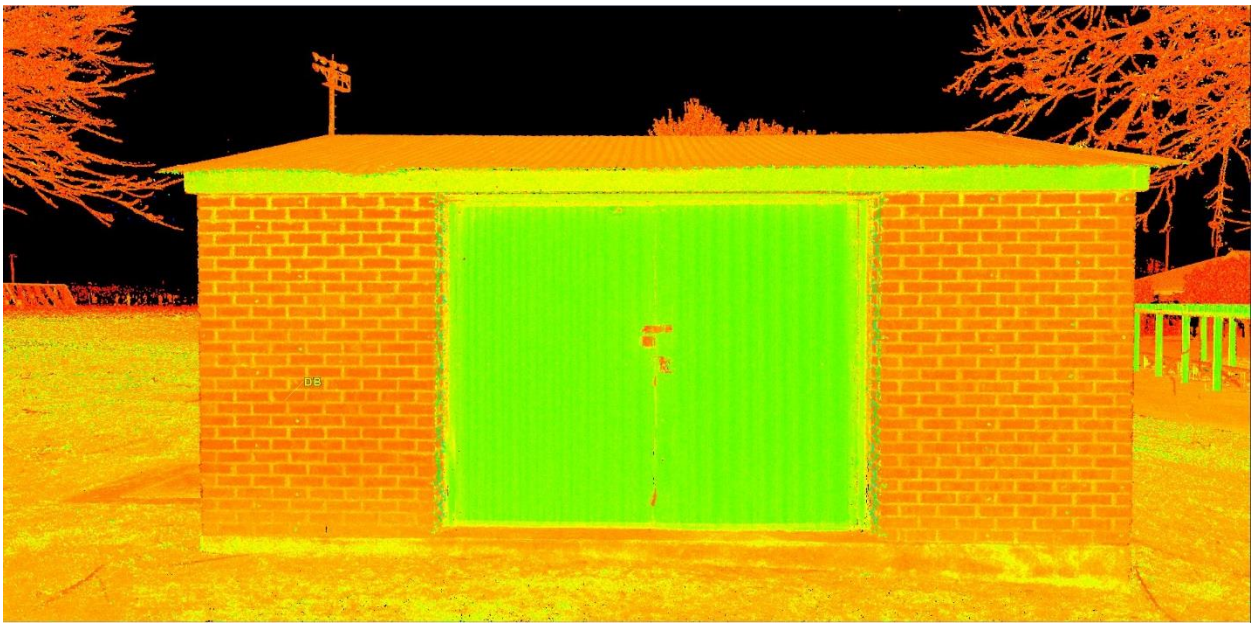

Figure 4.13 Front view of RAC storage building model

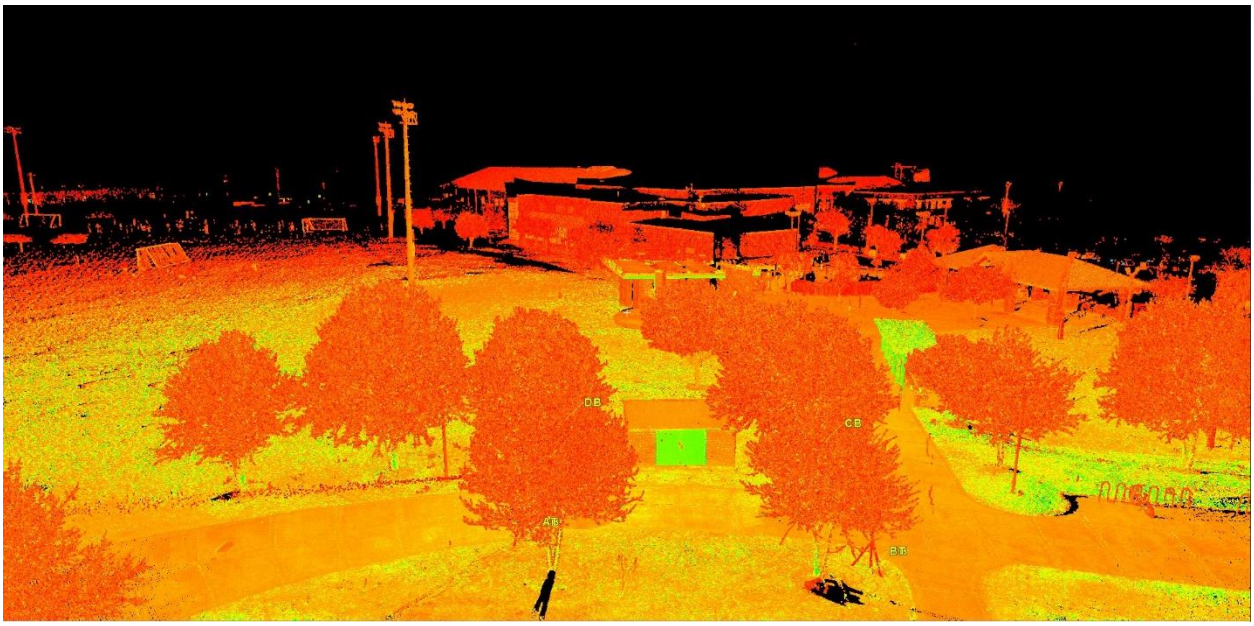

Figure 4.14 Far view of front of RAC storage building model

DATA ANALYSIS

The objective was to compare point coordinates (at reference wall points) generated from photogrammetry and laser scanner models to the same point coordinates obtained via the total-station instrument. Ten points on each wall were selected from the two hundred ninety-nine points for comparison. Results were determined by using two different methods, coordinate discrepancies and distance discrepancies from a chosen center point. In both methods discrepancies were calculated by subtracting the total station results from the results of either the laser scanner or photogrammetry model. The results are presented in the following sections, depending on the comparison being made. The first section contains a summary of the results from the coordinate discrepancy approach for the laser scanner and photogrammetry models respectively. This section also includes the maximum discrepancies, minimum discrepancies, mean values, root mean square (RMS) values and standard deviations. The next four sections focus on the distance discrepancies from the four center points. Each section discusses the results from a center point that was selected from side A, B, C, or D (corresponding to south, east, north and west facing wall). In these sections, a center point was chosen and then equation (1) was used to find the distance from comparison point to center point.

$$D_i = \sqrt{(x_i - x_c)^2 + (y_i - y_c)^2 + (z_i - z_c)^2} \qquad (1)$$

$$x_i, y_i, \& \, z_i = coordinates\ of\ comparison\ point$$

$$x_c, y_c, \& \, z_c = coordinates\ of\ center\ point$$

Then, the maximum discrepancies, minimum discrepancies, mean values, root mean square (RMS) values and standard deviations are then calculated as in the first section. Additionally, the percentage of distance discrepancies between discrepancy ranges were found by adding the

number of values falling in that range. Several ranges were used for grouping, which were less than 0.001 ft. (0.012 in) ,0.001 ft. to 0.005 ft. (0.012in to 0.06in), and progressed in increments of 0.005 ft. until 0.030 ft. (0.36 in).

Coordinate Discrepancy Comparison of Photogrammetry Model and Laser Scanner Model to Coordinates Obtained via Total Station

This section presents the comparison of the selected point coordinates from the laser scanner and photogrammetry models versus the total station point coordinates. The actual raw data was not included in this section due to its large size, but can be found in Appendix A. However, the statistical results are given in table 4.2. In the X coordinate, the maximum discrepancy for the laser scanner model was 0.0810 ft., while the photogrammetry model was 0.0.0876 ft., which is a difference of 0.0792 in. The mean for the X coordinate of the laser scanner model was 0.0097 ft., while the photogrammetry model mean was 0.0169 ft., about 0.09 in. in difference. The Y coordinate had similar results, but the minimum value for the photogrammetry model was slightly higher at 0.0004 ft. The Z coordinate of both the laser scanner and the photogrammetry had the largest discrepancy. The discrepancy of the laser scanner model was 0.5750 ft. or 6.9 in., while the photogrammetry model was 0.6015 ft. or 7.218 in.

Table 4.2 Coordinate discrepancy statistical data for RAC with outliers removed

Statistical Data for Coordinate Discrepancies with Outliers Removed						
Item	Laser Scanner -Total Station			Photogrammetry - Total Station		
	X	Y	Z	X	Y	Z
Maximum Value (ft.)	0.0810	0.0480	0.5750	0.0876	0.0470	0.6015
Minimum Value (ft.)	0.0000	0.0000	0.0000	0.0002	0.0004	0.0009
Mean Value (ft.)	0.0097	0.0090	0.0741	0.0169	0.0103	0.0913
RMS Value (ft.)	0.0188	0.0140	0.2003	0.0223	0.0144	0.2095
Standard Deviation (ft.)	0.0163	0.0109	0.1885	0.0147	0.0102	0.1910
Outliers Removed	A047, C006			C039		

Comparison of Distances in the Photogrammetry and Laser Scanner Models Relative to Center Point A066

In this section, distances from several reference wall points to the center point A066 are compared. In figure 4.15, the laser scanner and photogrammetry model distances were compared to the distances collected by the total station. The result of each comparison are displayed in a combined figure for each center point. In the figure, the horizontal axis is the distance from the center point to the selected point, while the vertical axis presents the discrepancy values. Most of the points in the figure, fall close to the zero-ordinate value corresponding to the location of the horizontal axis with a spread of less than 0.04 ft. or about a 0.5 in. The photogrammetry points are slightly more scattered then the laser scanner. The largest distance discrepancies results were consistently points D009 and D010, which generated discrepancies larger than 0.08 ft. or roughly

1 in. This was most likely caused by human error when the coordinates were recorded from the total station. Two of the points in figure 4.15 that are greater than 0.10 ft. are the result of these errors, but the two additional photogrammetry points are not. The two additional points greater than 0.10 ft. in the photogrammetry model have no definite explanations. The two points affected were D012 and D014, which are at the center top and middle corner of the building respectively. The model was examined at the two points to verify that distortion of the model had not caused the problems with the coordinate data. After the model was inspected, it was found to have some distortion at point D014. Also point D014 marker was located slightly off of the center of the point. As for point D012, there appears to be no problem with distortion or the marker and thus no definite conclusion can be made regarding them.

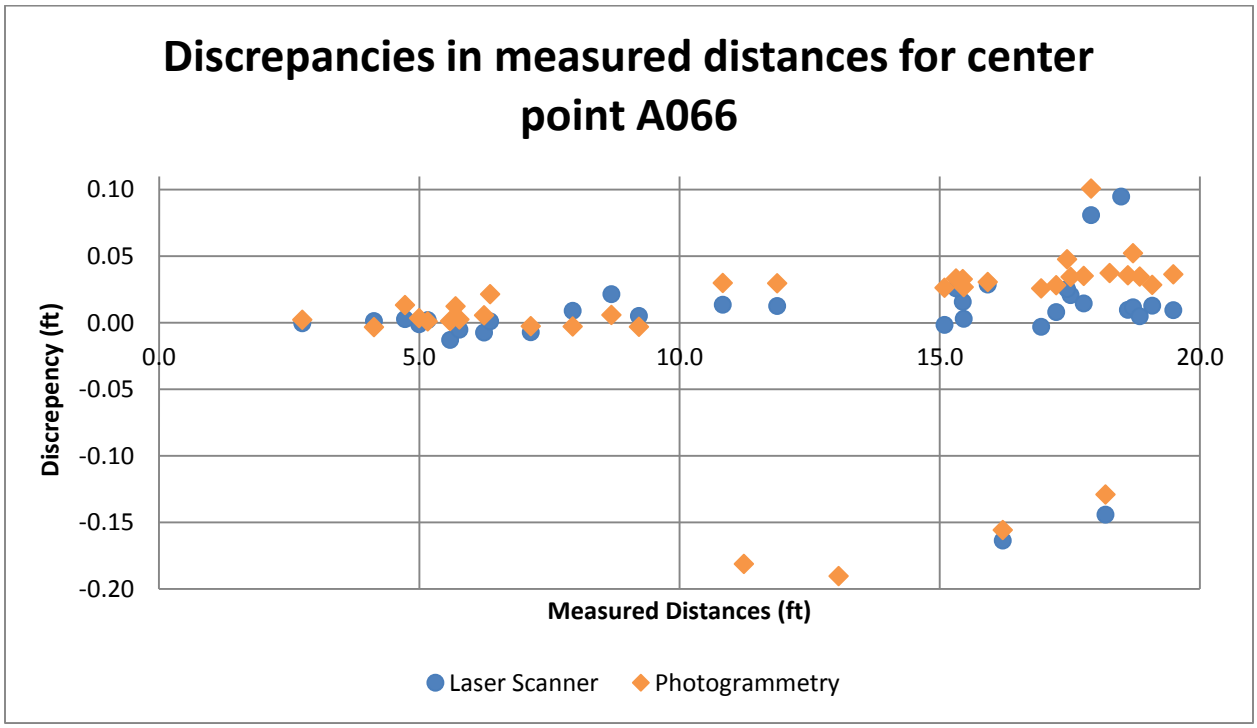

Figure 4.15 Discrepancies in measured distances for RAC at center point A006

The statistical results for center point A066 are in table 4.3. In this set of results, the laser scanner model produced higher discrepancies than the photogrammetry model. The maximum discrepancy value for the laser scanner model was almost 2 ft., due to the potential introduction of human errors. In the other three center points the laser scanner model discrepancies are less than 1 ft. The minimum value for both models were at or below 0.001 ft. For the Mean Value, RMS value and the standard deviation the laser scanner model was one magnitude of error more than the photogrammetry model. When the outliers in the laser scanner and photogrammetry data are removed, the maximum discrepancies are similar. The laser scanner generated a maximum discrepancy of 0.2293 ft. with reference wall points A047 and C006 removed. The photogrammetry model produced a similar result of 0.2063 ft. with point C039 removed.

Table 4.3 Statistical data of both discrepancies for the RAC at center point A066 with outliers removed

Item	Laser Scanner - Total Station	Photogrammetry - Total Station
Maximum Value (ft.)	0.2293	0.2063
Minimum Value (ft.)	0.0003	0.0010
Mean Value (ft.)	0.0389	0.0455
RMS Value (ft.)	0.0756	0.0697
Standard Deviation (ft.)	0.0666	0.0556
Outliers Removed	A047, C006	C039

In table 4.4 below, the discrepancies for center point A066 are placed into discrepancies ranges. For the laser scanner model, 64% of the discrepancies were less than 0.02 ft. or about 0.25 in. The photogrammetry model was less accurate with only 33% falling in that range. Nine points for the laser scanner model's discrepancies were greater than 0.03 ft., while 18 points (46%) of the

photogrammetry model's points were greater 0.03 ft. In all four center points, the laser scanner model consistently had more or equal points with discrepancies of less than 0.005 ft. For center point A066, the laser scanner model had 26% of its points below 0.005 ft., while the photogrammetry model only had 23% in that range.

Table 4.4 Discrepancies ranges for distance discrepancies of center point A066

Discrepancy Ranges for Center Point A066								
Item	Laser Scanner - Total Station				Photogrammetry - Total Station			
Discrepancy ranges (ft.)	# falling in that range	% at each range	% Less Than	% Greater Than	# falling in that range	% at each range	% Less Than	% Greater Than
<0.001	1	3%	3%	97%	0	0%	0%	100%
0.001<d<0.005	9	23%	26%	74%	9	23%	23%	77%
0.005<d<0.010	8	21%	46%	54%	2	5%	28%	72%
0.010<d<0.015	6	15%	62%	38%	2	5%	33%	67%
0.015<d<0.020	1	3%	64%	36%	0	0%	33%	67%
0.020<d<0.025	2	5%	69%	31%	1	3%	36%	64%
0.025<d<0.030	3	8%	77%	23%	7	18%	54%	46%
0.030<d	9	23%	100%		18	46%	100%	
SUM	39				39			

Comparison of Distances in the Photogrammetry and Laser Scanner Models Relative to Center Point B013

The distance discrepancies at point B013 outperformed the other three center points in most of the statistical data for both, the laser scanner and photogrammetry models. Figure 4.16 displays the discrepancies in measured distances for this center point, which is similar to the figure of center point A066 in the previous section minus the outliers at points D009 and D010.

The statistical data for center point B013 is presented in table 4.5 and the respective discrepancies range are in table 4.6. The photogrammetry model at this point had the smallest maximum discrepancy 0.1044 ft. It also had the lowest amount of discrepancies greater than 0.03 ft. at only 23% of the points. The laser scanner model had the lowest statistical data at this center point. The laser scanner model also had more points below 0.02 ft. at 85%, while the photogrammetry model only had 46% below. The mean value for the laser scanner model and photogrammetry model was the lowest at this point, at 0.0119 ft. and 0.0230 ft. respectively. The laser scanner model had the greatest amount of points below 0.005 ft. at 15 points or 38% for this center point.

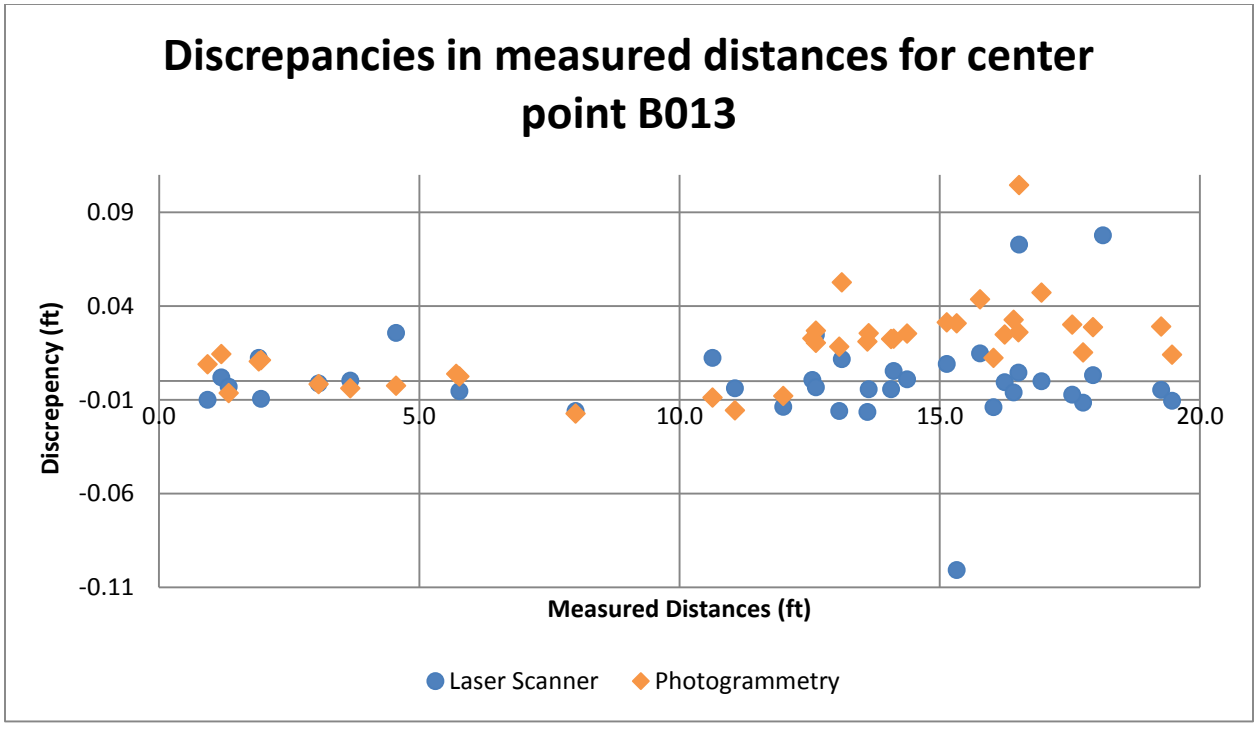

Figure 4.16 Discrepancies in measured distances for center point B013

Table 4.5 Statistical data of both discrepancies for the RAC at center point B013 with outliers removed

Item	Laser Scanner -Total Station	Photogrammetry - Total Station
Maximum Value (ft.)	0.0776	0.1044
Minimum Value (ft.)	0.0001	0.0016
Mean Value (ft.)	0.0119	0.0230
RMS Value (ft.)	0.0202	0.0286
Standard Deviation (ft.)	0.0169	0.0186
Outliers Removed	A047, C006	C039

Table 4.6 Discrepancies ranges for distance discrepancies of center point B013

Discrepancy Ranges for Center Point B013								
Item	Laser Scanner - Total Station				Photogrammetry - Total Station			
Discrepancy ranges (ft.)	# falling in that range	% at each range	% Less Than	% Greater Than	# falling in that range	% at each range	% Less Than	% Greater Than
<0.001	5	13%	13%	87%	0	0%	0%	100%
0.001<d<0.005	10	26%	38%	62%	5	13%	13%	87%
0.005<d<0.010	6	15%	54%	46%	4	10%	23%	77%
0.010<d<0.015	9	23%	77%	23%	5	13%	36%	64%
0.015<d<0.020	3	8%	85%	15%	4	10%	46%	54%
0.020<d<0.025	1	3%	87%	13%	6	15%	62%	38%
0.025<d<0.030	1	3%	90%	10%	6	15%	77%	23%
0.030<d	4	10%	100%		9	23%	100%	
SUM	39				39			

Comparison of Distances in the Photogrammetry and Laser Scanner Models Relative to Center Point C035

Center Point C035 also performed well, especially the laser scanner model. Figure 4.17 looks similar to the other figures, except there are is more points above the 0.05 ft. Just like the other two center points, there are a couple of outliers in the data. The points in question all come from side D of the models. The affected points in this center point were D009, D010, D012, and D013. This suggest that there was a problem when using the total station to collect the points for side D of the RAC building.

The Statistics for point C035 are in table 4.7 and the distance discrepancy ranges are given in table 4.8. The laser scanner model once again had more points below 0.02 ft. at 69%, while the photogrammetry model only had 41% below.

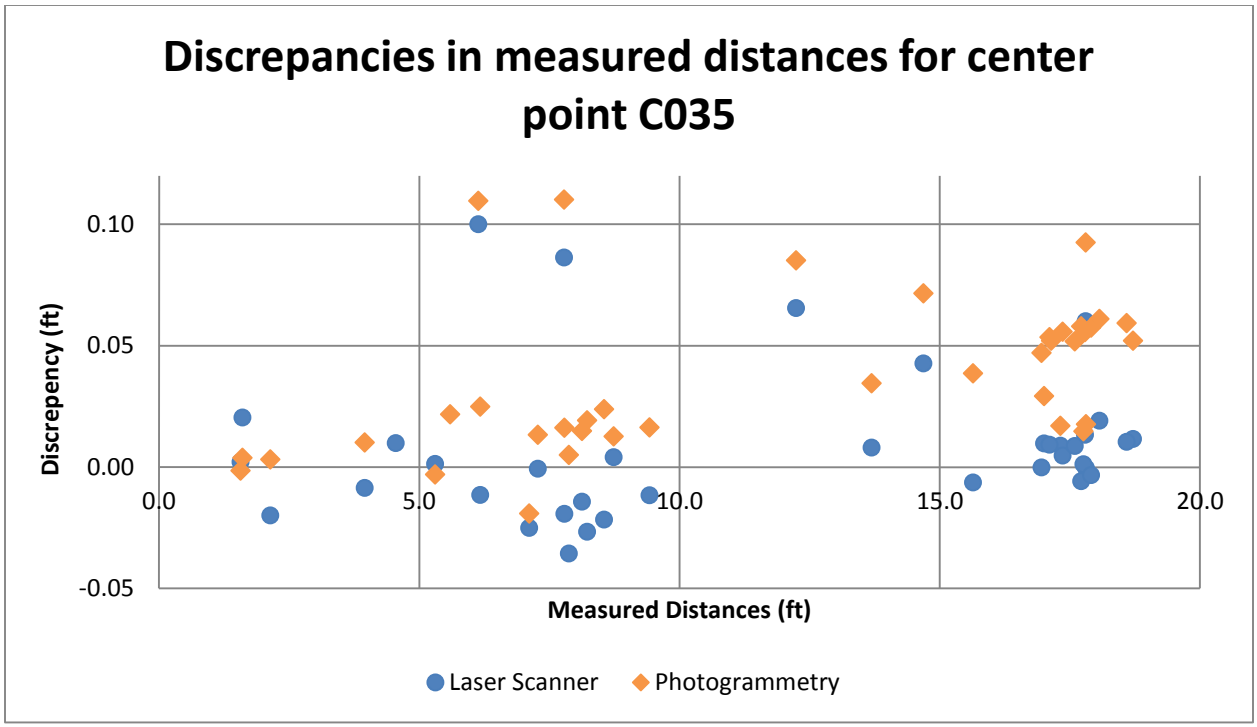

Figure 4.17 Discrepancies in measured distances for center point C035

Table 4.7 Statistical data of both discrepancies for the RAC at center point C035 with outliers removed

Item	Laser Scanner -Total Station	Photogrammetry - Total Station
Maximum Value (ft.)	0.1000	0.1102
Minimum Value (ft.)	0.0001	0.0015
Mean Value (ft.)	0.0191	0.0389
RMS Value (ft.)	0.0300	0.0467
Standard Deviation (ft.)	0.0238	0.0297
Outliers Removed	A047, C006	C039

Table 4.8 Discrepancies ranges for distance discrepancies of center point C035

Discrepancy Ranges for Center Point C035								
Item	Laser Scanner - Total Station				Photogrammetry - Total Station			
Discrepancy ranges (ft.)	# falling in that range	% at each range	% Less Than	% Greater Than	# falling in that range	% at each range	% Less Than	% Greater Than
<0.001	3	8%	8%	92%	0	0%	0%	100%
0.001<d<0.005	6	15%	23%	77%	4	10%	10%	90%
0.005<d<0.010	9	23%	46%	54%	1	3%	13%	87%
0.010<d<0.015	6	15%	62%	38%	5	13%	26%	74%
0.015<d<0.020	3	8%	69%	31%	6	15%	41%	59%
0.020<d<0.025	3	8%	77%	23%	3	8%	49%	51%
0.025<d<0.030	1	3%	79%	21%	1	3%	51%	49%
0.030<d	8	21%	100%		19	49%	100%	
SUM	39				39			

Comparison of Distances in the Photogrammetry and Laser Scanner Models Relative to Center Point D022

The last section of distances discrepancies is for the center point D022. Figure 4.18 is similar to the other figures with the exception of a large discrepancy for point D013 for the photogrammetry model. Additionally, both models had a discrepancy of larger than 0.01 ft. for point D014. This confirms that the data collected by the total station on side D was flawed due to operator error. The statistics for point D022 are provided in Table 4.9 and the distance discrepancy ranges are in Table 4.10. The laser scanner at this center point had 69% of the distance discrepancies less than 0.02 ft. The photogrammetry model had 49% of its discrepancies less than 0.02 ft., which was the highest of all the center points.

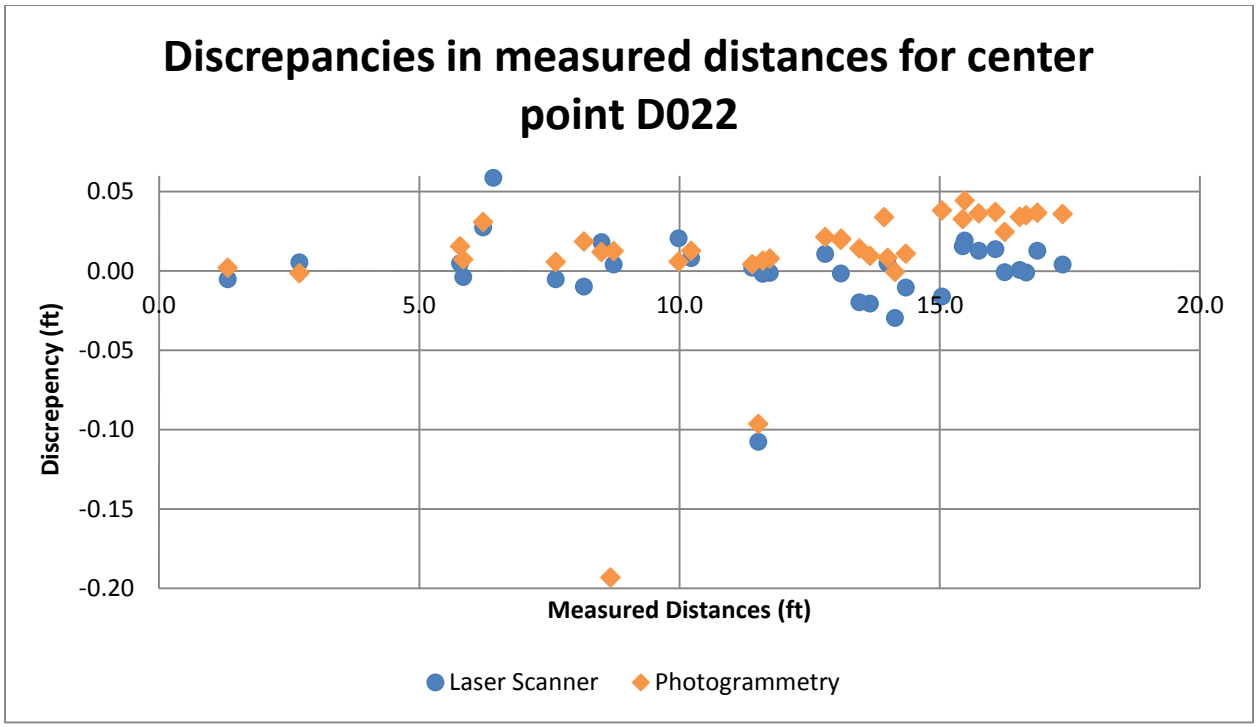

Figure 4.18 Discrepancies in measured distances for center point D022

Table 4.9 Statistical data of both discrepancies for the RAC at center point D022 with outliers removed

Item	Laser Scanner -Total Station	Photogrammetry - Total Station
Maximum Value (ft.)	0.5570	0.5804
Minimum Value (ft.)	0.0006	0.0004
Mean Value (ft.)	0.0522	0.0610
RMS Value (ft.)	0.1297	0.1316
Standard Deviation (ft.)	0.1218	0.1214
Outliers Removed	A047, C006	C039

Table 4.10 Discrepancies ranges for distance discrepancies of center point D022

Discrepancy Ranges for Center Point D022								
Item	Laser Scanner - Total Station				Photogrammetry - Total Station			
Discrepancy ranges (ft.)	# falling in that range	% at each range	% Less Than	% Greater Than	# falling in that range	% at each range	% Less Than	% Greater Than
<0.001	2	5%	5%	95%	1	3%	3%	97%
0.001<d<0.005	10	26%	31%	69%	3	8%	10%	90%
0.005<d<0.010	5	13%	44%	56%	7	18%	28%	72%
0.010<d<0.015	5	13%	56%	44%	5	13%	41%	59%
0.015<d<0.020	5	13%	69%	31%	3	8%	49%	51%
0.020<d<0.025	2	5%	74%	26%	3	8%	56%	44%
0.025<d<0.030	2	5%	79%	21%	0	0%	56%	44%
0.030<d	8	21%	100%		17	44%	100%	
SUM	39				39			

CHAPTER 5

CASE STUDY: TEMPLE OF THE SEVEN DOLLS MERIDA, MEXICO

PROCEDURES FOR DATA COLLECTION

The focus of this section will be on the procedures used to obtain the data presented in the temple of the seven dolls case study. This section includes information about the work site and how surveying control is obtained. It also presents each instrument's detailed procedures that were used during the data collection process. Finally, it includes how the photogrammetry and laser scanner data was collected and processed to produce models.

The site selected for this model accuracy comparison was located outside the town of Mérida in the Yucatán state of Mexico. The location is a national historical Maya site run by the Mexican National Institute of Anthropology and History (INAH as per its Spanish acronym) called Dzibilchaltun. This project was a partnership between Georgia Southern University, Universidad Anahuac Mayab, and INAH. The *Temple of the Seven Dolls* at Dzibilchaltun was selected as it was the most complete structure and one of the largest at the site. The temple was also chosen due to the preservation work INAH is conducting at the structure. An added bonus to this building was that INAH had already done substantial underbrush and tree removal around the structure. As stated earlier, trees and underbrush make it difficult to obtain complete models. This was the largest structure modeled for this study. The temple consisted of a three tiered structure with small ruins around it. The bottom section was of a pyramidal shape with stairs leading up to the second section. The second section consisted of a square structure with four windows, four doors, and an inner camber. The inner camber protruded through the roof of the second tier forming the third.

The third tier was also square, but significantly smaller with just one exit to the roof on the southern side. Similar to the RAC case study, there were no known benchmarks located near the structure. Since there were no known benchmarks in the area, a closed traverse was completed to establish four benchmarks around the temple. After the control benchmarks were established, 40 target reference points were located on the structure. These target reference points were marked by blue painter's tape with a black crosshair in the center of the tape. Later, it was realized this was not a good choice of colors.

Surveying control is the ground work that allows comparisons between the different models to be done with a certain degree of confidence in accuracy. In order to compare the resulting 3D models and acquire accurate data for INAH, a control system was needed around the temple. Four benchmarks were established with rebar stakes around the temple and a closed traverse was performed. The four control benchmarks are shown in figures 5.1 and 5.2. They were labeled A, B, C, and D. The position of bench mark A was assumed to be 600 ft. in the X direction (easting) and 300 ft. in the Y direction (northing). It was important to establish the benchmarks with high accuracy as this would serve as the control for the whole study. Since the project was spread out over a month, divots were drilled into the rebar stakes to increase point location precision. This allowed the tip of the poles to be placed in the same position every time on the rebar stakes. The internal and external angles of the closed traverse were measured by employing the "closing-the-horizon" procedure in "direct" and "reverse" modes of the instrument. The initial azimuth from point A to B was approximately measured with a hand compass. Therefore, the orientation of the traverse is just approximate, within ±5°. After local corrections at each vertex, the final angular error of closure was 5 sec. When the distances were measured,

the reflectorless (non-prism) mode was selected on the total station and the distance was collected as close to the ground as possible to avoid pole verticalization errors.

Figure 5.1 Google Map view of benchmarks around the temple

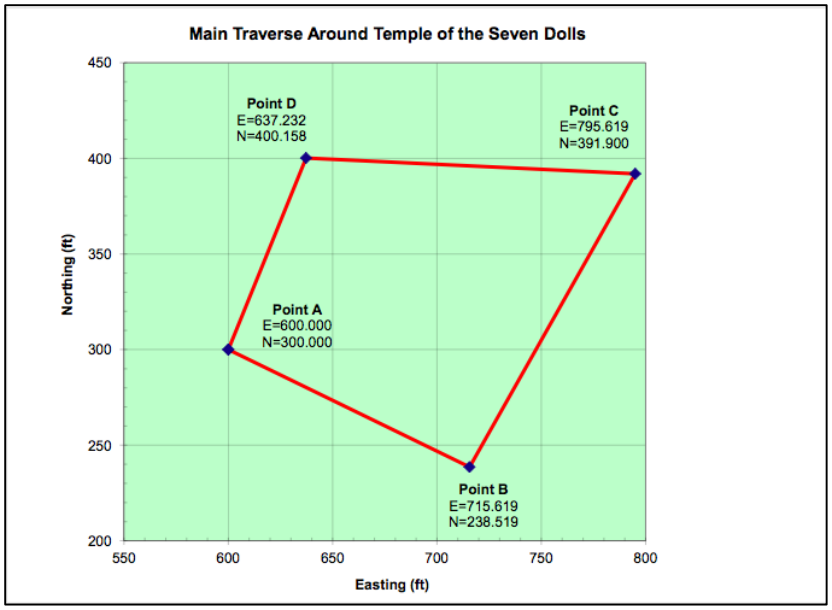

Figure 5.2 Coordinates of A, B, C, & D around the temple in the adopted relative coordinate system

The final longitudinal error of closure in the traverse was 0.0226 ft., which corresponded to an approximate longitudinal precision of 1 (one) unit in 25,184 units. To complete the coordinates of the reference benchmarks, the relative elevations of points A, B, C, and D were determined using a modern auto-level instrument. Since point A was the starting point, it was selected to be at a reference elevation of 32.808 ft. or 10 m. The elevations of the remaining points were then computed from this arbitrary datum. The determined final coordinates for the benchmarks are listed in table 5.1.

Table 5.1 Final coordinates of temple benchmarks

Final Coordinates of Benchmarks			
Point	X (ft.)	Y (ft.)	Z (ft.)
A	600.000	300.000	32.808
B	715.619	238.519	32.802
C	795.014	391.900	33.038
D	637.232	400.158	33.947

The total station was the first instrument used in this study, as it was also used to establish the control benchmarks. The total station was employed as the control instrument that all other measurements would be compared to. The purpose was to compare a trusted standard instrument to the newer available technology. When collecting the points from the temple, the total station occupied one of the control benchmarks. The northing, easting, and elevation coordinates of the point would be entered into the instrument along with the known azimuth to another point. This would set the instrument to the reference coordinate system and give the instrument the direction of north. The operator would then aim the instrument at points on the building and obtain the coordinates of that point using reflectorless mode. The operator would continue collecting points until the instrument need to be moved and the set up process repeated for a new point.

The photogrammetry model was the next deliverable produced. As stated earlier, the photogrammetry software selected for this accuracy comparison was Agisoft's PhotoScan Professional Edition, version 1.1.6. In this case study only one model was produced, unlike in the RAC case study. This was in part due to the number of photos needed to model such a large structure in great detail. The cameras used to produce the model were the Nikon D800 and the

GoPro Hero 3 Black Edition. The Nikon was used to collect photos of the first and second tiers of the structure from the ground. The GoPro was attached to a custom built quadcopter and used to obtain downward vertical photos and photos of the third tier. The temple model used for comparison was created using a total of 2433 pictures. The photo set consisted of 1166 pictures for the Nikon on the ground and 1267 pictures from the GoPro in the air. Both cameras were set to their maximum resolutions, which were 36.3 megapixels for the Nikon and 12 megapixels for the GoPro. The camera to object distances for this case were 75 ft. or less, since the wide angle lenses used required greater distance to capture large sections of the temple. Unfortunately, with this case study, the standard PhotoScan settings were not adequate to process the pictures. The standard processes such as "align photos," "build dense cloud," "build mesh," and "build texture" were used, but they required the default setting to be modified before a successful model was produced. In the align photos process, the key point limit was set to zero and the tie point limit was set 100,000. Setting the key point limit to zero allowed the software to target the maximum number of feature points in each photo. Increasing the tie point limit from 1,000 to 100,000 maximized the number of possible matches between photos. These two modifications reduced the possibility of photo alignment problems showing up in the later processing steps. This was necessary due to the distance that the photos were taken from. Under the build dense cloud settings, the quality was set to medium and the depth filtering was set to mild. The first test models produced were done with the quality set to lowest, which allowed for shorter processing time. The finial model used for the comparison was done at medium quality and required thirty-four days to process. The processing time was partly dependent on the computer hardware used. For this study, the computer selected was a Lenovo ThinkCentre with an Intel i7 3.40 GHz cpu and 32 gigabytes of memory. The depth filtering was set to mild instead of aggressive as some of the test models

had a severe lack of detail. Once the depth filtering was set to mild it eliminated the problems with parts of the structure losing detail. The depth filtering setting controls how many small details are included in the models. The settings for the build mesh were only modified on the face count. The face count controls the maximum number of polygons in the final mesh and was set to high in this model. This was done to help with creation of the model and to help sharpen the lines of the model. In the final processing step, build texture, the default settings were used. The final step just applies texture to the mesh and thus has little effect on the actual model. If a texture problem is found, the settings can be adjusted to correct it, but expect an extremely long processing time. The final photogrammetry model can be seen in figures 5.3 and 5.4. After the model was created using PhotoScan, it had to be georeferenced to the relative coordinate system that was used by the total station. The georeferencing is necessary since the photogrammetry software creates its own relative coordinate system when the models are generated. Without relating one coordinate system to the other, it would be impossible to compare the coordinates of the points across multiple technologies. The photogrammetry model was georeferenced by selecting four of the reference wall points that were measured with the total station. The selected points were then marked in PhotoScan by placing markers in roughly 20 photos containing each point. The four points selected from the model for georeferencing were N8, S2, E4, and W8. After the points were marked in PhotoScan, the coordinates of the points obtained via a total station were entered. This method of georeferencing was necessary as the control benchmarks were cut from the model by the photogrammetry program. It would have been preferable to use the control benchmarks as this method can introduce errors from the measurements produced by the total station instruments. After the model was georeference, the coordinates of the other points were collected by again marking the points in 20 photos. This method of marking the comparison points was used since

the reference wall points were not visible on the finished model unlike the RAC model. The loss of the reference wall points is due to two causes. The first problem was the distance that the photos were taken from and the second was the type of reference wall points used on the building. The blue tape used for the reference wall points had a really low reflectivity, which led to the tape disappearing in both the photogrammetry and laser scanner models. After all the markers were placed on the reference wall points, the "view estimated" command in PhotoScan was used to calculate the coordinates of the marked points. Figure 5.5 demonstrates a marked and referenced model of the temple.

Figure 5.3 Modeled temple. View toward Southeast

Figure 5.4 Modeled temple. View toward Northwest

Figure 5.5 Reference wall points on the temple

The laser scanner used for this project was the Leica Geosystems ScanStation C10. The scanner registration targets employed were Leica HDS twin target pole systems and Leica 6" blue

tilt and turn targets. The Leica 6" blue tilt and turn targets were placed at the benchmarks, but since there were only three available targets they had to be moved between the four benchmarks. A total of ten Leica HDS twin target pole systems were used during the scanning of the temple. These targets were moved to multiple locations around the temple as the scanning progressed. There were a total of 17 target locations used around the temple; three on the north side, two on the south side, three on the east side, five on the west side and the four on the benchmarks. This case study required more scans than any other project or case study conducted by the civil engineering department at Georgia Southern University. The total number of scans required to complete the temple was 63. The size and particular geometric shape of the structure required a relatively large number of scans and target locations. Unlike the RAC case study, the scanner was set to medium resolution. Medium resolution was acceptable in this case due to the amount of overlap from scan to scan. Medium resolution was also preferred due to shorter scan time of six minutes versus twenty-seven minutes for a high resolution. The 63 medium resolution scans were registered using Leica Geosystems' Cyclone software. The registration process combines the scans together using the targets that are in each scan. Registration requires a minimum of three common targets between two scans for those scans to be stitched together. The software continues stitching corresponding scans together until all the scans are combined. After all the scans are registered together, the resulting model must be georeferenced to the total station coordinate system. Georeferencing in Cyclone is accomplished by importing a comma delimited text file containing the coordinates of the benchmarks. Cyclone uses the information in the text file to create a control scanworld. The control scanworld is then registered with the previous complete registration which georeferences the model to the correct coordinate plane. As with any process, there is always some error involved. The error in the registration for this model after

georeferencing was 0.01 ft. or 0.12 in. With the model georeferenced, the coordinates of the comparison points were collected from the model. This was accomplished by locating the desired reference wall point on the model and picking a single point in the center of the cross-shaped mark. This was made difficult due to the blue tape and black cross used on the reference wall points. Blue and black have lower reflectivity, which makes it difficult for the scanner to get a return when the laser hits the point. This made it difficult to locate the exact center of the reference wall point. The difficultly led to a lower accuracy for the laser scanner in this case study. The final model is displayed in figures 5.6 and 5.7 and an example of a reference wall point in figure 5.8.

Figure 5.6 Complete laser scanner model of temple

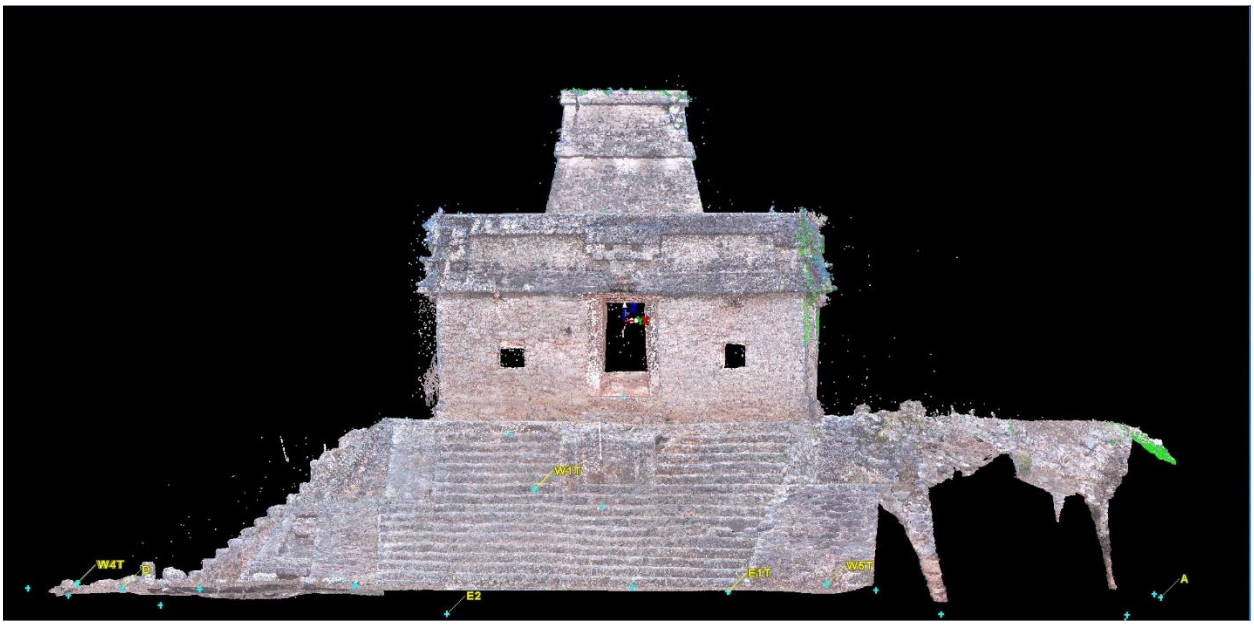

Figure 5.7 Trimmed laser model of temple

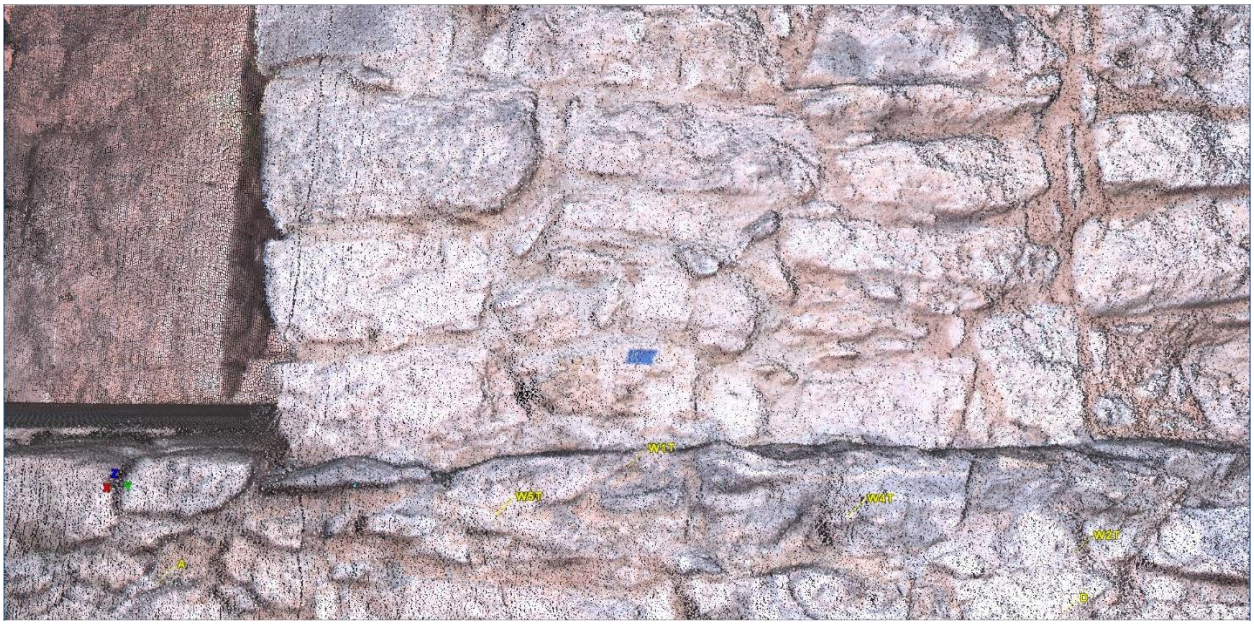

Figure 5.8 Example of reference wall point in virtual model of temple

DATA ANALYSIS

The objective was to compare point coordinates generated from the photogrammetry and laser scanner models to the control point coordinates obtained by the total-station instrument. All 40 points collected were used for this case study, but they were not evenly distributed between the sides. The north side included eight points and the east side had twelve points. The other two sides included ten points each. Results were determined by using two different methods, coordinate discrepancies and distance discrepancies between points from a chosen center point. In both methods discrepancies were calculated by subtracting the total station results from the results of either the laser scanner or photogrammetry model. The results are presented in the following sections, depending on the comparison being made. The first section contains a summary of the results from the coordinate discrepancy approach for the laser scanner and photogrammetry models respectively. This section also includes the maximum discrepancies, minimum discrepancies, mean values, root mean square (RMS) values and standard deviations. The next four sections focus on the distance discrepancies from the four center points. Each section discusses the results from a center point that was selected from each side of the structure, S, E, N, or W (corresponding to south, east, north and west facing walls). In these sections, a center point was chosen and then equation (1), from the previous case study, was used to find the distances from several points (reference wall points) to the selected center point (also a reference wall point). Then, the maximum discrepancies, minimum discrepancies, mean values, root mean square (RMS) values and standard deviations are calculated as in the first section. Additionally, the percentage of distance discrepancies between defined discrepancy ranges were found by considering the number of values falling in those ranges. Several ranges were used for grouping, which were less

than 0.001 ft. (0.012 in) ,0.001 ft. to 0.005 ft. (0.012in to 0.06in), and progressed in increments of 0.005 until 0.030 ft. (0.36 in).

Coordinate Discrepancy Comparison of Photogrammetry Model and Laser Scanner Model to Coordinates Obtained via Total Station

This section presents the comparison of the selected point coordinates from the laser scanner and photogrammetry models versus the coordinates acquired with total station instruments. The actual raw data was not included in this section due to its large size, but can be found in Appendix B. However, the statistical data without outliers is given in table 5.2. The outliers can be found in the raw data included in Appendix B. In the X coordinate, the maximum discrepancy for the laser scanner model was 0.1510 ft., while the photogrammetry model was 0.1208 ft. which is a difference of 0.0202 ft. The mean for the X coordinate of the laser scanner model was 0.0521 ft., while the photogrammetry model mean was 0.0400 ft., about 0.15 in. in difference. The Y coordinate had similar results, but the photogrammetry model had a larger maximum value instead of the laser scanner model. The mean for the Z coordinate of the laser scanner model performed worse than that of the photogrammetry model. It is also important to note that the photogrammetry models minimum values are skewed due to the fact several coordinates were inputted at the reference wall points to georeference the model.

Table 5.2 Coordinate discrepancy statistical data for temple

Statistical Data for Coordinate Discrepancies						
Item	Laser Scanner - Total Station			Photogrammetry - Total Station		
	X	Y	Z	X	Y	Z
Maximum Value (ft.)	0.1510	0.0812	0.5697	0.1208	0.0885	0.4964
Minimum Value (ft.)	0.0029	0.0083	0.0027	0.0000	0.0000	0.0000
Mean Value (ft.)	0.0521	0.0301	0.0289	0.0400	0.0282	0.0230
RMS Value (ft.)	0.0756	0.0367	0.0899	0.0540	0.0394	0.0780
Standard Deviation (ft.)	0.0520	0.0216	0.0865	0.0352	0.0267	0.0756
Outliers Removed		N7, W2			S7, W2	

Comparison of Distances in the Photogrammetry and Laser Scanner Models Relative to Center Point N3

In this section, the distances from several points to the selected center point N3 are compared. In figure 5.9, the laser scanner and photogrammetry model distances were compared to the distances collected by the total station. The result of each comparison are displayed in a combined figure for each center point. In the figure, the horizontal-axis is the distance from the center point to the selected point, while the vertical-axis presents the discrepancy values. Most of the points in the figure, fall close to the zero-discrepancy, horizontal axis with a spread of less than 0.1 ft. or about 1.2 in. The photogrammetry points and laser scanner points clearly follow a similar pattern in figure 5.9. This tends to suggest there could be a problem with the total station data that was collected. The largest distance discrepancies result was point W2, which generated

discrepancies larger than 0.3 ft. or roughly 3.6 in. This was most likely caused by human error when the coordinates were recorded from the total station, since the photogrammetry and laser scanner models both had the point above 0.3 ft. Additionally, three other points had discrepancies between 0.1 ft. and 0.15 ft., which were points E9, E10, and E11. The problem with these three points steams from their location on the temple. Unlike most of the points, these points were located on the stairs of the temple instead of the actual structure. This led to a difficult identification of the points in the models and this could have resulted in inaccurate coordinates.

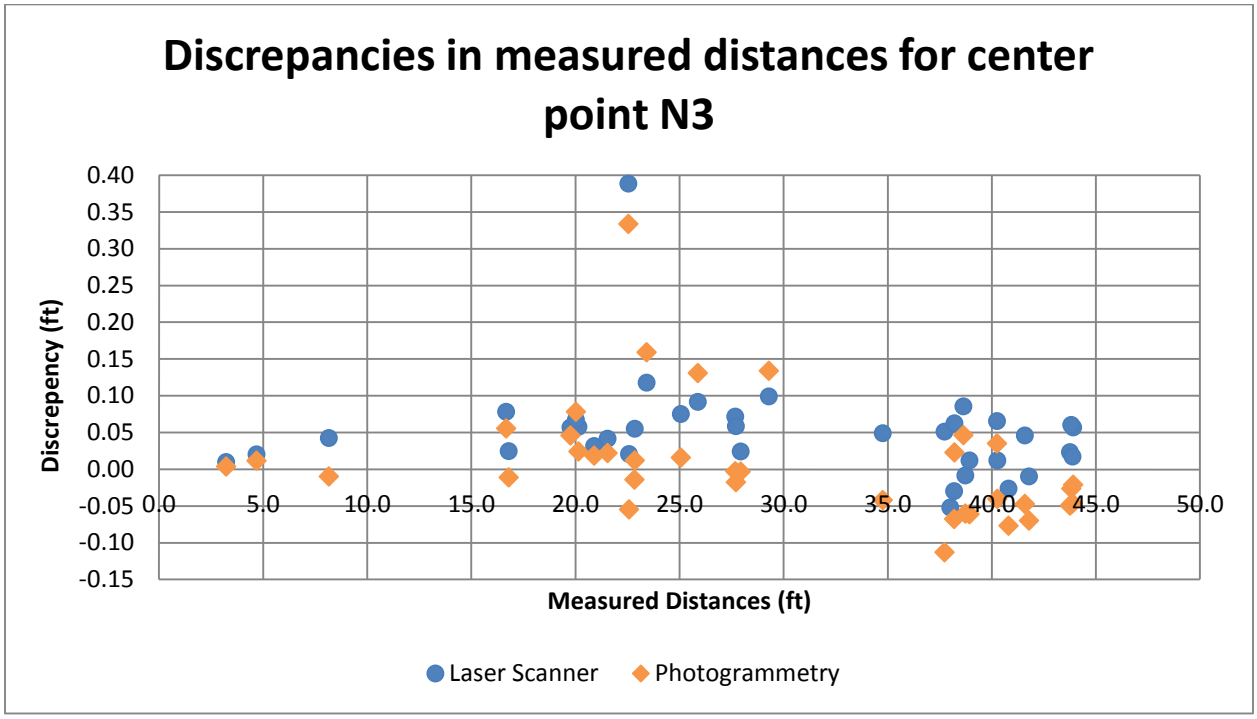

Figure 5.9 Discrepancies in measured distances for the temple at center point N3

The statistical results for center point N3 are in table 5.3. In this set of results, the photogrammetry model produced higher discrepancies than the laser scanner model. The

maximum discrepancy value for the photogrammetry model was almost 3.2 ft., due to the potential introduction of human errors. This problem repeated again in center point E3, but not with the same magnitude. In the other two center points the laser scanner and photogrammetry models discrepancies are less than 1 ft. In this center point and E3, both the laser scanner and the photogrammetry models had discrepancies large that 1 ft. Additionally, the same two points are causing the problems. The offending points are S7 for the photogrammetry model and N7 for the laser scanner model. When the outliers are removed from the laser scanner and photogrammetry model data, the maximum discrepancies are 0.2178 ft. and 0.2350 ft. respectively. The minimum value for both models were at or below 0.009 ft. For the Mean Value, RMS value and the standard deviation the laser scanner model was had about half the error of the photogrammetry model.

Table 5.3 Statistical data of distance discrepancies for the temple at center point N3 with outliers removed

Item	Laser Scanner - Total Station	Photogrammetry - Total Station
Maximum Value (ft.)	0.2178	0.2350
Minimum Value (ft.)	0.0084	0.0026
Mean Value (ft.)	0.0522	0.0534
RMS Value (ft.)	0.0641	0.0694
Standard Deviation (ft.)	0.0391	0.0492
Outliers Removed	N7, W2	S7, W2

In table 5.4 below, the discrepancies for center point N3 are placed into discrepancies ranges. For the laser scanner model, 15% of the discrepancies were less than 0.02 ft. or about 0.25

in. The photogrammetry model was more accurate with 28% falling in that range. Twenty-six points for the laser scanner model's discrepancies were greater than 0.03 ft., while only 23 points (59%) of the photogrammetry model's points were greater 0.03 ft. In this center point, the photogrammetry model had more points with discrepancies of less than 0.005 ft. For center point N3, the laser scanner model had 0% of its points below 0.005 ft., while the photogrammetry model had 8% in that range.

Table 5.4 Distance discrepancy ranges for the temple at center point N3

Discrepancy Ranges for Center Point N3								
Item	Laser Scanner - Total Station				Photogrammetry - Total Station			
Discrepancy ranges (ft.)	# falling in that range	% at each range	% Less Than	% Greater Than	# falling in that range	% at each range	% Less Than	% Greater Than
<0.001	0	0%	0%	100%	0	0%	0%	100%
0.001<d<0.005	0	0%	0%	100%	3	8%	8%	92%
0.005<d<0.010	3	8%	8%	92%	1	3%	10%	90%
0.010<d<0.015	2	5%	13%	87%	4	10%	21%	79%
0.015<d<0.020	1	3%	15%	85%	3	8%	28%	72%
0.020<d<0.025	5	13%	28%	72%	4	10%	38%	62%
0.025<d<0.030	2	5%	33%	67%	1	3%	41%	59%
0.030<d	26	67%	100%		23	59%	100%	
SUM	39				39			

Comparison of Distances in the Photogrammetry and Laser Scanner Models Relative to Center Point S5

The distance discrepancies at point S5 performed better than those at center point N3 in all of the statistical data for both, the laser scanner and photogrammetry models. Figure 5.10 displays the discrepancies in measured distances for this center point, which is similar to the figure for

center point N3 in the previous section minus the outlier at point S7. It is important to note that point N7 did reappear in this center point once again with a higher than normal discrepancy. It also was the maximum discrepancy for the scanner at this center point.

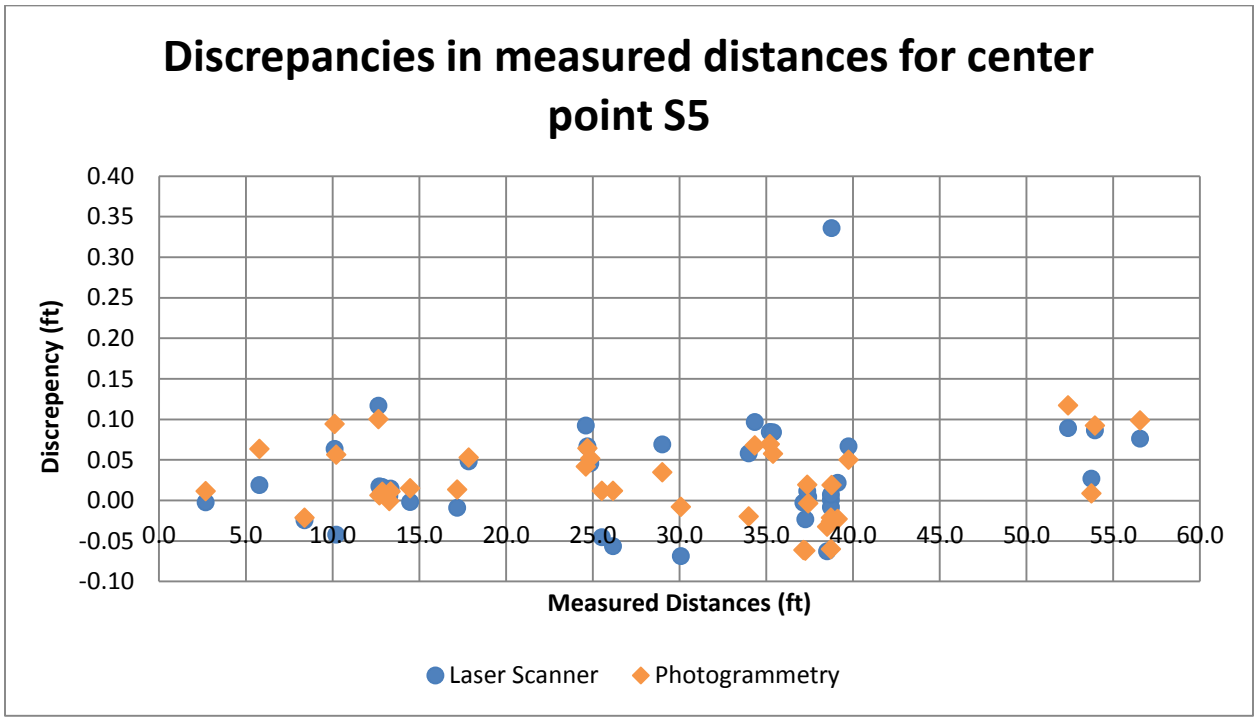

Figure 5.10 Discrepancies in measured distances for the temple at center point S5

The statistical data for center point S5 is presented in table 5.5 and the respective discrepancies range are in table 5.6. The photogrammetry model at this point had the smallest maximum discrepancy at 0.0987 ft. It also had the second lowest amount of discrepancies greater than 0.03 ft. at only 51% of the points. The photogrammetry model had more points below 0.02 ft. at 38%, while the laser scanner model only had 36% below. The mean value for the laser scanner model and photogrammetry model was the lowest at this point, at 0.0411 ft. and 0.0378 ft.

respectively. The laser scanner model had the greatest amount of points below 0.01 ft. at 9 points or 23% for this center point.

Table 5.5 Statistical data of distance discrepancies for the temple at center point S5 with outliers removed

Item	Laser Scanner - Total Station	Photogrammetry - Total Station
Maximum Value (ft.)	0.0968	0.0987
Minimum Value (ft.)	0.0008	0.0006
Mean Value (ft.)	0.0411	0.0378
RMS Value (ft.)	0.0509	0.0456
Standard Deviation (ft.)	0.0316	0.0279
Outliers Removed	N7, S1	E9, S1

Table 5.6 Distance discrepancy ranges for the temple at center point S5

Discrepancy Ranges for Center Point S5								
Item	Laser Scanner - Total Station				Photogrammetry - Total Station			
Discrepancy ranges (ft.)	# falling in that range	% at each range	% Less Than	% Greater Than	# falling in that range	% at each range	% Less Than	% Greater Than
<0.001	1	3%	3%	97%	1	3%	3%	97%
0.001<d<0.005	4	10%	13%	87%	1	3%	5%	95%
0.005<d<0.010	4	10%	23%	77%	3	8%	13%	87%
0.010<d<0.015	2	5%	28%	72%	7	18%	31%	69%
0.015<d<0.020	3	8%	36%	64%	3	8%	38%	62%
0.020<d<0.025	3	8%	44%	56%	3	8%	46%	54%
0.025<d<0.030	1	3%	46%	54%	1	3%	49%	51%
0.030<d	21	54%	100%		20	51%	100%	
SUM	39				39			

Coordinate Distances of Photogrammetry Model and Laser Scanner Model to Center Point E4

Center point E4 performed similar to center point N3. Figure 5.11 looks similar to the figure for center point N3, except for the photogrammetry model is evenly distributed about the center line. Most of the points in the figure 5.11, fall close to the zero-value horizontal axis with a spread of less than 0.1 ft. or about a 1.2 in. Just like the other two center points, there are a couple of outliers in the data. The points in question are S7, N7 and W2. Only one of the affected points, W2, is displayed on figure 5.11 due to the scaling on the graph. The other two points S7 and N7 are once again present in this center point. This suggests that there was a problem when using the total station to collect the points S7 and N7 from the temple. Additionally, S7 and N7 have the highest discrepancies at this center point for the photogrammetry and laser scanner models respectively.

The statistics for center point E4 are in table 5.7 and the distance discrepancy ranges are given in table 5.8. The photogrammetry model once again had more points below 0.02 ft. at 44%, while the laser scanner model only had 21% below. The photogrammetry model also had the least amount of points above 0.03 ft. at this center point at 19, while the laser scanner had the most points above at 30.

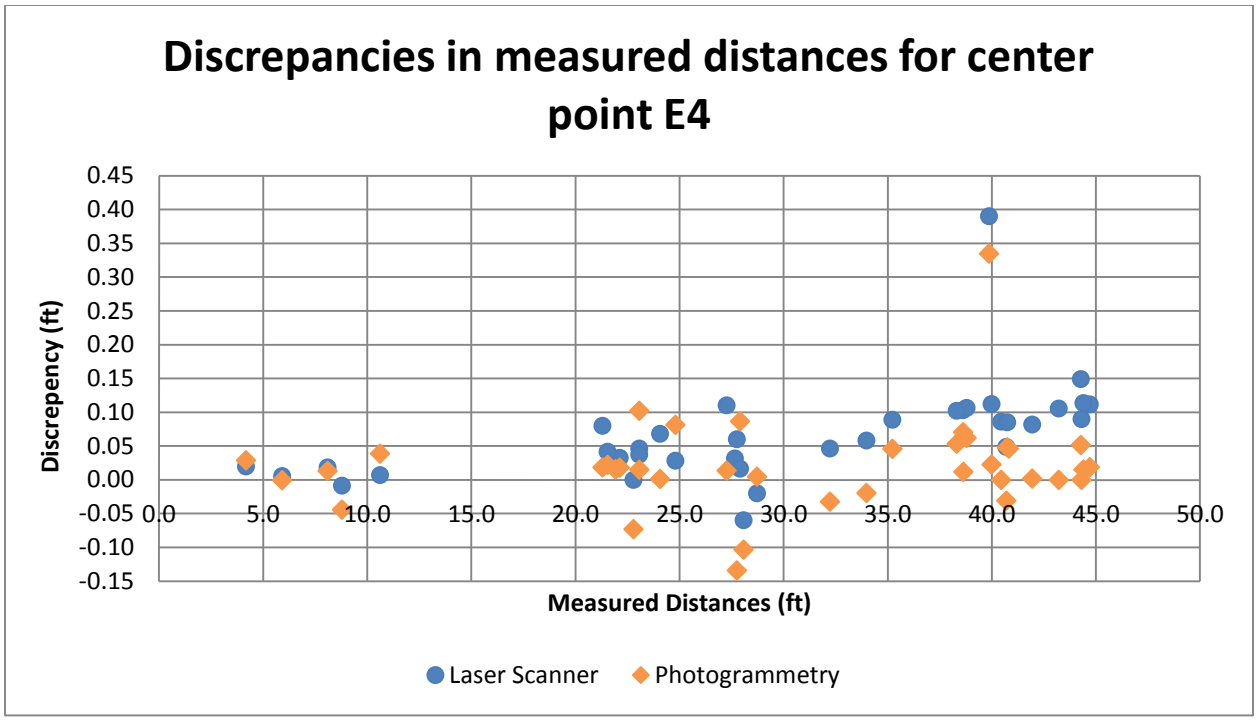

Figure 5.11 Discrepancies in measured distances for temple at center point E4

Table 5.7 Statistical data of distance discrepancies for the temple at center point E4 with outliers removed

Item	Laser Scanner - Total Station	Photogrammetry - Total Station
Maximum Value (ft.)	0.1490	0.1340
Minimum Value (ft.)	0.0001	0.0000
Mean Value (ft.)	0.0614	0.0375
RMS Value (ft.)	0.0714	0.0485
Standard Deviation (ft.)	0.0388	0.0335
Outliers Removed	N7, W2	S7, W2

Table 5.8 Distance discrepancy ranges for temple at center point E4

Discrepancy Ranges for Center Point E4								
Item	Laser Scanner - Total Station				Photogrammetry - Total Station			
Discrepancy ranges (ft.)	# falling in that range	% at each range	% Less Than	% Greater Than	# falling in that range	% at each range	% Less Than	% Greater Than
<0.001	1	3%	3%	97%	4	10%	10%	90%
0.001<d<0.005	0	0%	3%	97%	3	8%	18%	82%
0.005<d<0.010	3	8%	10%	90%	0	0%	18%	82%
0.010<d<0.015	0	0%	10%	90%	3	8%	26%	74%
0.015<d<0.020	4	10%	21%	79%	7	18%	44%	56%
0.020<d<0.025	0	0%	21%	79%	2	5%	49%	51%
0.025<d<0.030	1	3%	23%	77%	1	3%	51%	49%
0.030<d	30	77%	100%		19	49%	100%	
SUM	39				39			

Comparison of Distances in the Photogrammetry and Laser Scanner Models Relative to Center Point W8

The last section of distances discrepancies is for the center point W8. Figure 5.12 is similar to the other figures in that point S7 and N7 have largest discrepancies for the photogrammetry and laser scanner models respectively. This confirms that the S7 and N7 data is flawed in accuracy due to erroneous coordinates acquired with the total station instrument. Additionally, both models had more points in the 0.10 ft. to 0.15 ft. range than other center points. The statistics for center point W8 are provided in Table 5.9 and the distance discrepancy ranges are in Table 5.10. The laser scanner at this center point had 15% of the distance discrepancies less than 0.02 ft. The photogrammetry model had 33% of its discrepancies less than 0.02 ft.

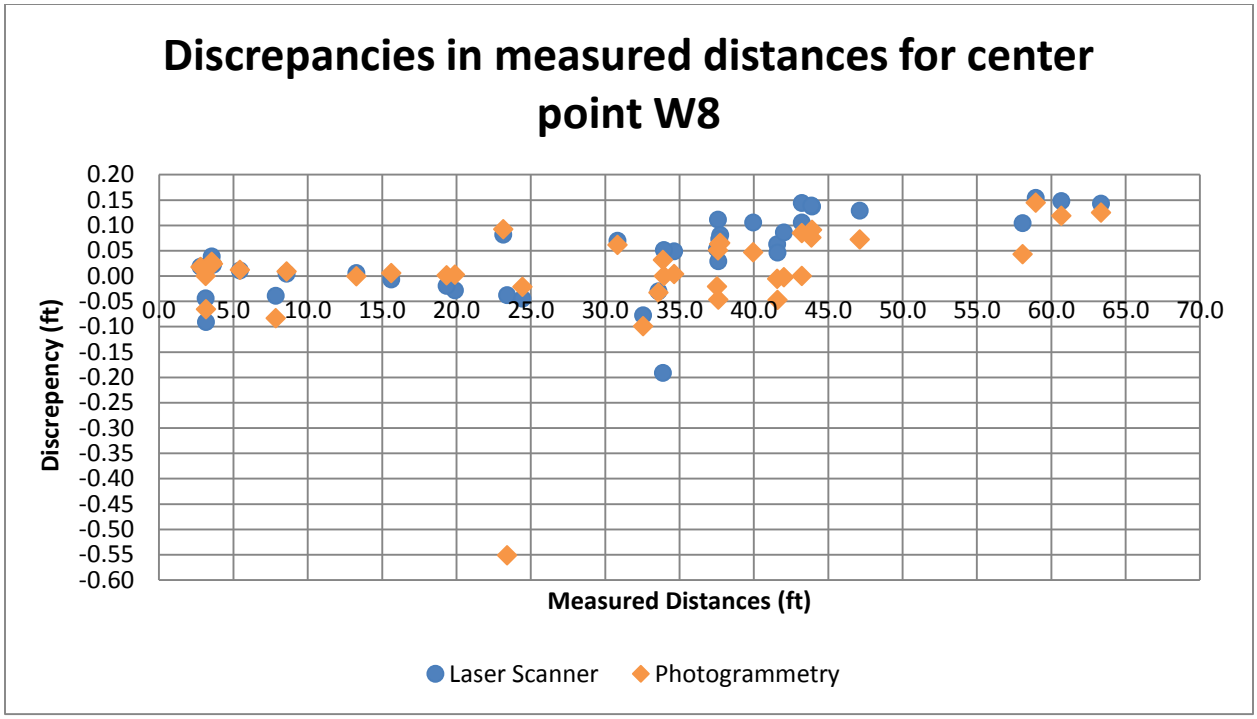

Figure 5.12 Discrepancies in measured distances for the temple at center point W8

Table 5.9 Statistical data of distance discrepancies for the temple at center point W8 with outliers removed

Item	Laser Scanner - Total Station	Photogrammetry - Total Station
Maximum Value (ft.)	0.1478	0.1251
Minimum Value (ft.)	0.0044	0.0000
Mean Value (ft.)	0.0667	0.0441
RMS Value (ft.)	0.0786	0.0547
Standard Deviation (ft.)	0.0441	0.0368
Outliers Removed	N7, E9	S7, E9

Table 5.10 Distance discrepancy ranges for the temple at center point W8

Discrepancy Ranges for Center Point W8								
Item	Laser Scanner - Total Station				Photogrammetry - Total Station			
Discrepancy ranges (ft.)	# falling in that range	% at each range	% Less Than	% Greater Than	# falling in that range	% at each range	% Less Than	% Greater Than
<0.001	0	0%	0%	100%	4	10%	10%	90%
0.001<d<0.005	1	3%	3%	97%	4	10%	21%	79%
0.005<d<0.010	2	5%	8%	92%	3	8%	28%	72%
0.010<d<0.015	1	3%	10%	90%	1	3%	31%	69%
0.015<d<0.020	2	5%	15%	85%	1	3%	33%	67%
0.020<d<0.025	1	3%	18%	82%	3	8%	41%	59%
0.025<d<0.030	2	5%	23%	77%	1	3%	44%	56%
0.030<d	30	77%	100%		22	56%	100%	
SUM	39				39			

CHAPTER 6

CASE STUDY: ZACH S. HENDERSON LIBRARY TERRACE

PROCEDURES FOR DATA COLLECTION

The focus of this section is on the procedures used to obtain the data presented in the Zach S. Henderson Library terrace case study. It presents information about the work site and how surveying control is obtained. It also includes each instrument's detailed procedures that were used during the data collection process. Finally, it presents the photogrammetry and laser scanner data acquisition and post-processing approaches to produce models.

The site selected for the model accuracy comparison is located next to the Zach S. Henderson Library on the Campus of Georgia Southern University. A small concrete paver and soil filled terrace was selected for this purpose. In addition to presenting different elevations, this location was chosen as it had relatively little tree cover and was not obstructed by buildings or other objects. Trees pose a particular problem for terrain models, especially the photogrammetry models, and should be avoided when possible. The small size of the terrace was another important characteristic that led to this location selection. Even though the terrace was small, it still allowed for an adequate amount of elevation difference for a terrain model. The smaller size allowed multiple trials to be run without a significant investment in time. This allowed for the researchers to find an appropriate procedure to produce a terrain model with the least amount of time investment. The only negative characteristic of this site was the lack of known nearby benchmarks for survey control. Since the location of the building prevented the use known benchmarks on

campus and the site was open, the researchers elected to place the total station in the center and just use one station. This allowed the closed traverse to be eliminated. Seventy-five target reference wall points were added to the terrace on the top of the retaining walls. These reference wall points were marked with felt roofing paper nails. These were used as they provide good contrast with the concrete pavers used to make the retaining walls and they allowed for an extended usable life.

Surveying control is the ground work that allows comparisons between the different models to be done with a certain degree of confidence in accuracy. In this case study, survey control in the form of a closed traverse was not need. Instead, the total station was placed at a central location on the terrace and all measurements performed from this one station. This was possible since there were no obstructions that could block the line of sight. This central point was assumed to have coordinates of 200 ft. in the X direction (easting), 300 ft. in the Y direction (northing), and 1000 ft. in elevation. The other models were referenced to this coordinate system by using some of the original reference wall points collected with the total station.

The total station was used as the control instrument that all other measurements would be compared to. The purpose was to compare a trusted standard instrument to the newer available technology. When collecting the points from the terrace, the total station occupied central location on the terrace. The selected northing, easting, and elevation coordinates of the point were entered into the instrument along with the known azimuth to another point. This would set the instrument to the reference coordinate system and give the instrument the direction of the selected reference north (not a magnetic or true north). The operator would then aim the instrument at a reference wall point on the concrete retaining walls and obtain the coordinates of that reference wall point

using reflectorless mode. The operator would continue collecting points from the central point until all points were acquired.

The photogrammetry model was the next deliverable produced. As stated earlier, the photogrammetry software selected for this accuracy comparison was Agisoft's PhotoScan Professional Edition, version 1.1.6. In this case study only one model was produced, unlike in the RAC case study. This was due to the problems encountered in the processing of this model. The camera used to produce the model was the Nikon D800. This camera was used to collect photos from the ground and from the air with a telescopic boom lift. The terrace model used for comparison was created using a total of 522 pictures. The photo set consisted of 376 pictures from the ground and 146 pictures from the telescopic boom lift. The Nikon D800 was set to its maximum resolution of 36.3 megapixels. The camera to object distances for this case study were 20 ft. to 300ft., which was significantly longer that the other case studies due to the use of the telescopic boom lift. Unfortunately, with this case study, the standard PhotoScan settings were not adequate to process the pictures. The standard processes such as "align photos," "build dense cloud," "build mesh," and "build texture" were used, but they required the default setting to be modified before a successful model was produced. In the align photos process, the key point limit was set to zero and the tie point limit was set 100,000. Setting the key point limit to zero allowed the software to target the maximum number of feature points in each photo. Increasing the tie point limit from 1,000 to 100,000 maximized the number of possible matches between photos. These two modifications reduced the possibility of photo alignment problems showing up in the later processing steps. This was necessary due to the distance that the photos were taken from and the inability to positon the camera perpendicular with the ground surface. Under the build dense cloud settings, the quality was set to medium and the depth filtering was set to mild. The depth

filtering was set to mild instead of aggressive as some of the test models had a severe lack of detail. Once the depth filtering was set to mild it eliminated the problems with parts of the structure losing detail. The depth filtering setting controls how many small details are included in the models. The settings for the build mesh were only modified on the face count. The face count controls the maximum number of polygons in the final mesh and was set to high in this model. This was done to help with creation of the model and to help sharpen the lines of the model. In the final processing step, build texture, the default settings were used. The final step just applies texture to the mesh and thus has little effect on the actual model. If a texture problem is found the settings can be adjusted to correct it, but expect an extremely long processing time. The final photogrammetry model can be seen in figures 6.1 and 6.2. After the model was created using PhotoScan, it had to be georeferenced to the relative coordinate system that was used by the total station. The georeferencing is necessary since the photogrammetry software creates its own relative coordinate system when the models are generated. Without relating one coordinate system to the other, it would be difficult to compare the coordinates of the points across multiple technologies. The photogrammetry model was georeferenced by selecting three of the target points that were measured with the total station. The selected points were then marked in PhotoScan by placing markers in every photo containing each point. The three points selected from the model for georeferencing were A009, D010, and F005. After the points were marked in PhotoScan, the coordinates of the points from total station were entered. This method of georeferencing was necessary as control benchmarks were not used for this case study. After the model was georeference, the coordinates of the other points were collected by again marking the points in every photo that contained that particular point. This method of marking the comparison points was used since the targets were not visible on the finished model similar to the temple case study.

The loss of the targets is due to two problems. The first issue was the distance that the photos were taken from and the second was the extreme angles between the camera and the ground surface. The distance and angle problems arose from the use of the telescopic boom lift and ladders used to obtain the photos. The boom lift only had access to one third of the site which cause all photos of the far side to be distorted. The ladders used did not provide enough height to obtain perpendicular photos with the ground surface. This led to most photos being taken at an angle, which produced distortion in the model. After all the markers were placed on the reference wall points, the view estimated command in PhotoScan was used to calculate the coordinates of the marked points. Figure 6.3 demonstrates a marked and referenced model of the terrace.

Figure 6.1 Modeled library terrace

Figure 6.2 Overhead view of modeled library terrace

Figure 6.3 Points marked on library terrace

The laser scanner used for this project was the Leica Geosystems ScanStation C10. The scanning registration targets employed were Leica spheres. These targets were placed at four reference wall points. They are the ones identified as F005, E008, D010, and A021. The total number of scans require to complete the terrace was 18. The size of the terrace and its particular geometric shape increased the number of scans required. Like the temple case study, the scanner was set to medium resolution. Medium resolution was acceptable in this case due to the amount of overlap from scan to scan. Medium resolution was also preferred due to shorter scan time of six minutes verues twenty-seven minutes for a high resolution. The 18 medium resolution scans were registered using Leica Geosystems' Cyclone software. The registration process combines the scans together using the targets that are in each scan. Registration requires a minimum of three common targets between two scans for those scans to be stitched together. The software continues stitching corresponding scans together until all the scans are combined. After all the scans are registered together, the resulting model must be georeferenced to the total station coordinate system. Georeferencing in Cyclone is accomplished by importing a comma delimited text file containing the coordinates of the benchmarks or in this case the target points. Cyclone uses the information in the text file to create a control scanworld. The control scanworld is then registered with the previous complete registration which georeferences the model to the correct coordinate plane. As with any process there is always some error involved. The error in the registration for this model after georeferencing was 0.025 ft. or 0.30 in. With the model georeferenced, the coordinates of the comparison points were collected from the model. This was accomplished by locating the desired reference wall point on the model and picking a single point in the center of the corresponding felt nail. An example of this process can be viewed in figure 6.4 and the final models in figures 6.5 and 6.6.

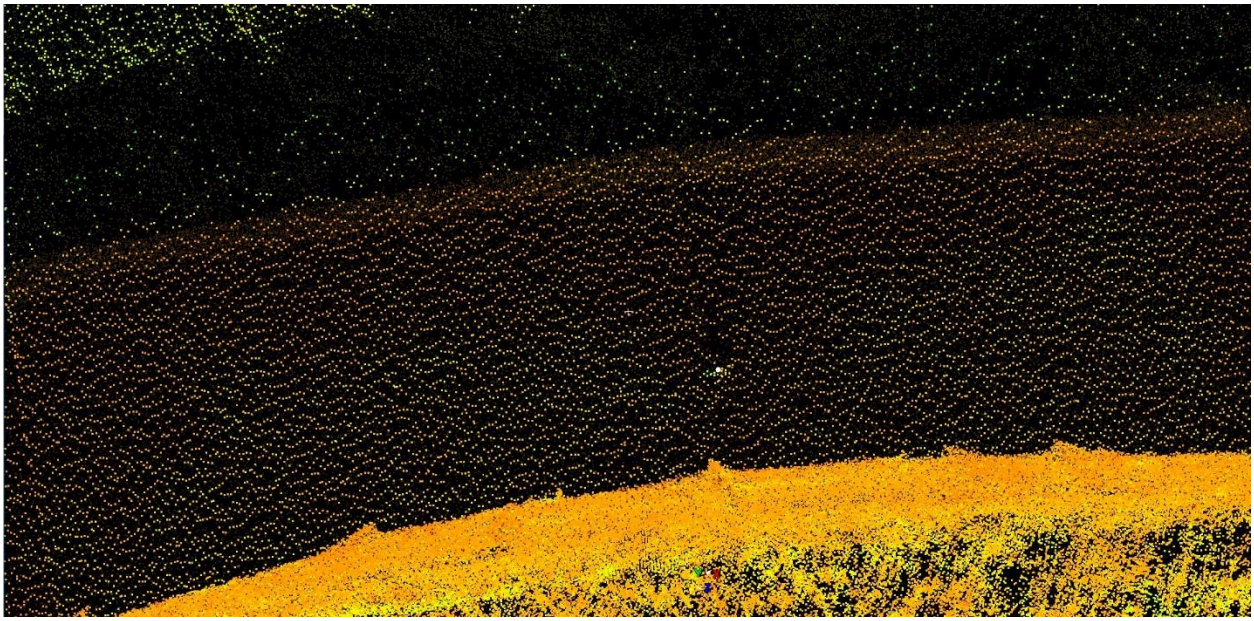

Figure 6.4 Point marking example for library terrace

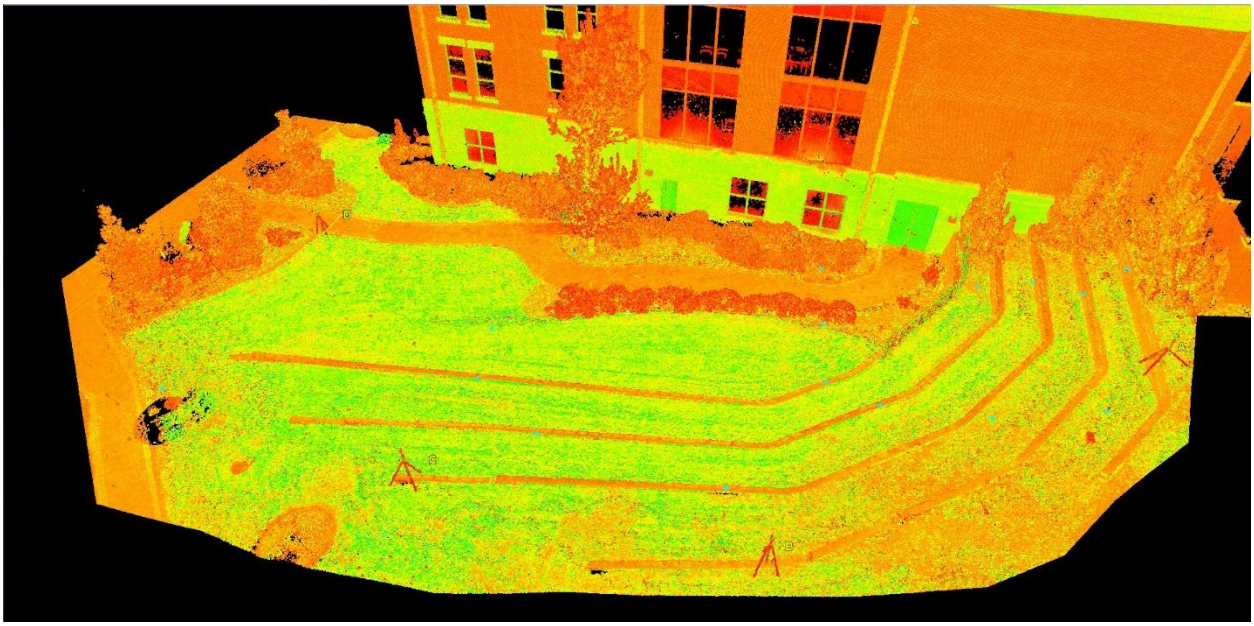

Figure 6.5 Overhead view of laser scanner library terrace model

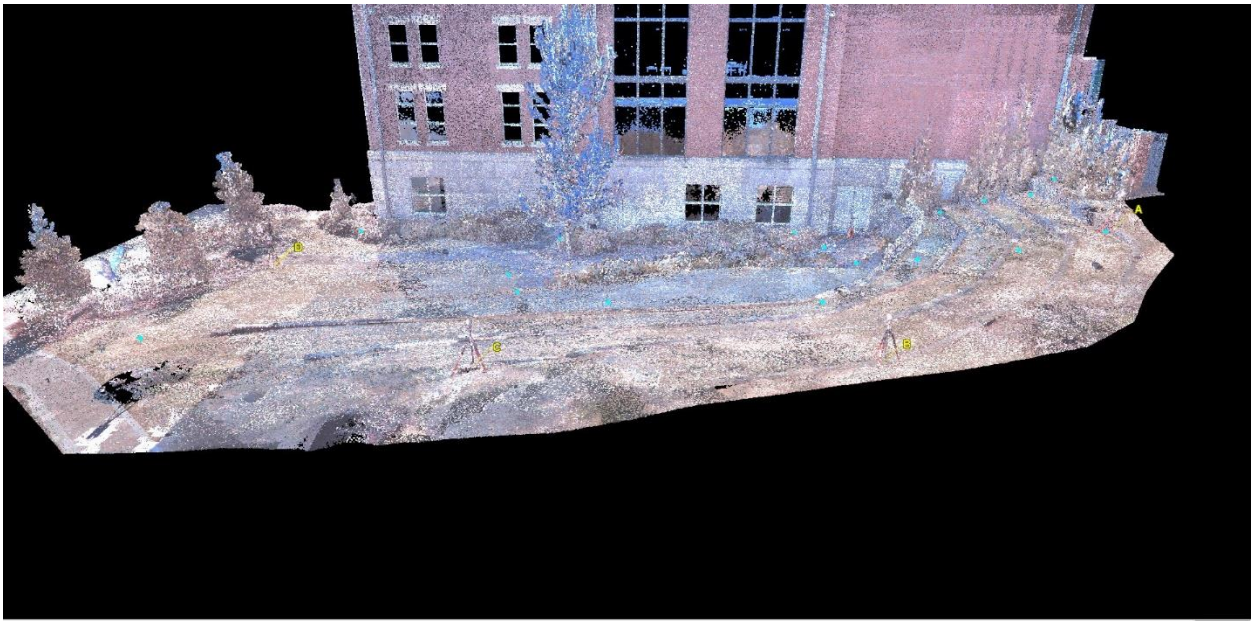

Figure 6.6 Overhead view of laser scanner library terrace model with point cloud colored

DATA ANALYSIS

The objective was to compare point coordinates generated from photogrammetry and laser scanner models to the control point coordinates obtained with a total station instrument. Only 40 of the 75 reference wall points were used for this case study. Since the laser scanner model was done a few months later, some of the original points had disappeared leaving only 48. Results were determined by using two different methods, coordinate discrepancies and distance discrepancies from a chosen center point. In both approaches discrepancies were calculated by subtracting the total station results from the results of either the laser scanner or photogrammetry model. The results are presented in the following sections, depending on the comparison being made. The first section contains a summary of the results from the coordinate discrepancy approach for the laser scanner and photogrammetry models, respectively. This section also

includes the maximum discrepancies, minimum discrepancies, mean values, root mean square (RMS) values and standard deviations. The next four sections focus on the distance discrepancies from the four center points. Each section discusses the results from a center point that was selected at random on the terrace. In these sections, a center point was chosen and then equation (1), from the RAC case study was used to find the distance from comparison point to center point. Then, the maximum discrepancies, minimum discrepancies, mean values, root mean square (RMS) values and standard deviations are then calculated as in the first section. Additionally, the percentage of distance discrepancies between discrepancy ranges were found by considering the number of values falling in that range. Several ranges were used for grouping, which were less than 0.001 ft. (0.012 in) ,0.001 ft. to 0.005 ft. (0.012in to 0.06in), and progressed in increments of 0.005 until 0.030 ft. (0.36 in).

Coordinate Discrepancy Comparison of Photogrammetry Model and Laser Scanner Model to Coordinates Obtained via Total Station

This section presents the comparison of the selected point coordinates from the laser scanner and photogrammetry models versus the total station point coordinates. The actual raw data was not included in this section due to its large size, but can be found in Appendix C. However, the statistical data is given in table 6.1. In the X coordinate, the maximum discrepancy for the laser scanner model was 0.1232 ft., while the photogrammetry model was 0.0964 ft. which is a difference of 0.32 in. The mean for the X coordinate of the laser scanner model was 0.0.0451 ft., while the photogrammetry model mean was 0.0356 ft., about 0.1 in. in difference. The Y

coordinate had similar results as the X coordinate. The maximum value for the Z coordinate of the laser scanner model performed better than that of the photogrammetry model.

Table 6.1 Coordinate discrepancy statistical data for terrace

Statistical Data for Coordinate Discrepancies						
Item	Laser Scanner -Total Station			Photogrammetry- Total Station		
	X	Y	Z	X	Y	Z
Maximum Value (ft.)	0.1232	0.2362	0.0889	0.0964	0.1365	0.1274
Minimum Value (ft.)	0.0000	0.0000	0.0000	0.0025	0.0022	0.0001
Mean Value (ft.)	0.0451	0.0733	0.0337	0.0356	0.0477	0.0351
RMS Value (ft.)	0.0599	0.0965	0.0380	0.0453	0.0593	0.0467
Standard Deviation (ft.)	0.0398	0.0635	0.0177	0.0285	0.0357	0.0311
Outliers Removed		N/A			N/A	

Comparison of Distances in the Photogrammetry and Laser Scanner Models Relative to Center Point A011

In this section, the distances from reference wall marks to the center point A011 are compared. In figure 6.7, the laser scanner and photogrammetry model distances were compared to the distances collected by the total station. The result of each comparison is displayed in a combined figure for each center point. In the figure, the horizontal axis contains the distance from the center point to the selected point, while the vertical axis presents the discrepancy values. Most of the points in the figure, fall close to the horizontal x-axis with a spread of less than 0.2 ft. or

about a 2.4 in. The largest distance discrepancies results were points D003 and E001 from the laser scanner, which generated discrepancies larger than 0.25 ft. or 3 in. This was most likely caused by those points being moved from the time that they were collected by the total station to the time of collection with the scanner a few months later. This is inferred because the laser scanner model was only affected by this error. The photogrammetry model and the coordinates obtained via the total station were acquired at almost the same time.

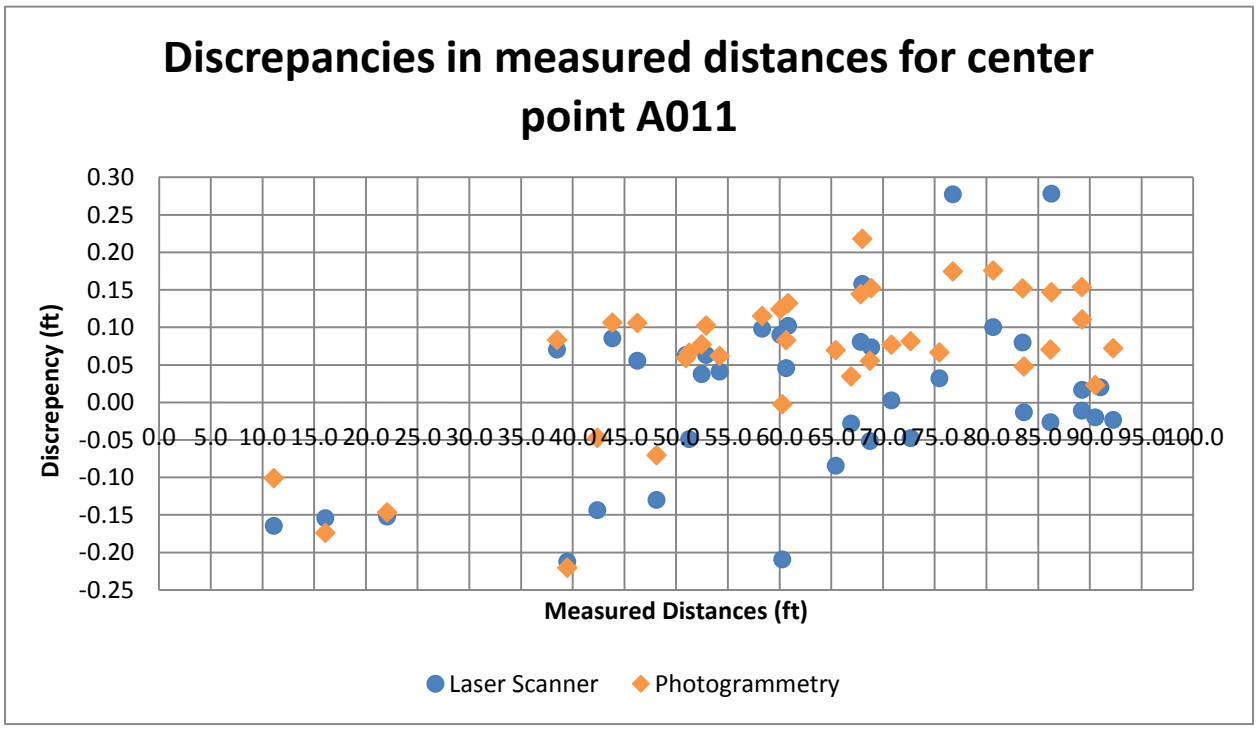

Figure 6.7 Discrepancies in measured distances for terrace at center point A011

The statistical results for center point A011 are in table 6.2. In this set of results, the photogrammetry model produced higher discrepancies than the laser scanner model. The maximum discrepancy value for the photogrammetry model was 0.2178 ft. after removing the

outliers in the data. The minimum value for both models were below 0.003 ft. For the Mean Value, RMS value and the standard deviation the laser scanner model and the photogrammetry model had about the same amount of error.

Table 6.1 Statistical data of distance discrepancies for the terrace at center point A011 with outliers removed

Item	Laser Scanner - Total Station	Photogrammetry - Total Station
Maximum Value (ft.)	0.2124	0.2178
Minimum Value (ft.)	0.0023	0.0028
Mean Value (ft.)	0.0766	0.0995
RMS Value (ft.)	0.0931	0.1090
Standard Deviation (ft.)	0.0558	0.0492
Outliers Removed	E001, D003	F002, A019

In table 6.3 below, the discrepancies for center point A011 are placed into discrepancies ranges. For the laser scanner model, 13% of the discrepancies were less than 0.02 ft. or about 0.25 in. The photogrammetry model was less accurate with only 3% falling in that range. Thirty points for the laser scanner model's discrepancies were greater than 0.03 ft., while thirty-seven points (95%) of the photogrammetry model's points were greater 0.03 ft. In this center point, the photogrammetry and laser scanner models had an equal amount of points with discrepancies of less than 0.005 ft. For center point A011, the laser scanner model and photogrammetry model had 0% of their points below 0.005 ft.

Table 6.2 Distance discrepancy ranges for the terrace at center point A011

Discrepancy Ranges for Center Point A011								
	Laser Scanner - Total Station				Photogrammetry - Total Station			
Discrepancy ranges	# falling in that range	% at each range	% Less Than	% Greater Than	# falling in that range	% at each range	% Less Than	% Greater Than
<0.001	0	0%	0%	100%	0	0%	0%	100%
0.001<d<0.005	1	3%	3%	97%	1	3%	3%	97%
0.005<d<0.010	0	0%	3%	97%	0	0%	3%	97%
0.010<d<0.015	2	5%	8%	92%	0	0%	3%	97%
0.015<d<0.020	2	5%	13%	87%	0	0%	3%	97%
0.020<d<0.025	2	5%	18%	82%	1	3%	5%	95%
0.025<d<0.030	2	5%	23%	77%	0	0%	5%	95%
0.030<d	30	77%	100%		37	95%	100%	
SUM	39				39			

Comparison of Distances in the Photogrammetry and Laser Scanner Models Relative to Center Point B007

The distance discrepancies at point B007 had comparable results to the pervious center point with the exception of the photogrammetry model's maximum value. Figure 6.8 displays the discrepancies in measured distances for this center point. This figure is similar to the pervious one with most of the points contained in a spread of -0.15 ft. to 0.15 ft. This center point does contain an outlier in the photogrammetry model, which is point F002.

The statistical data for center point B013 is presented in table 6.4 and the respective discrepancies range are in table 6.5. The laser scanner model at this point had the smallest maximum discrepancy of 0.1673 ft. It also had the largest amount of discrepancies greater than 0.03 ft. of 87% at this center point. The photogrammetry model had twice as many points as the

laser scanner below 0.02 ft. The mean value for the laser scanner model was the lowest at this point, which was 0.0784 ft.

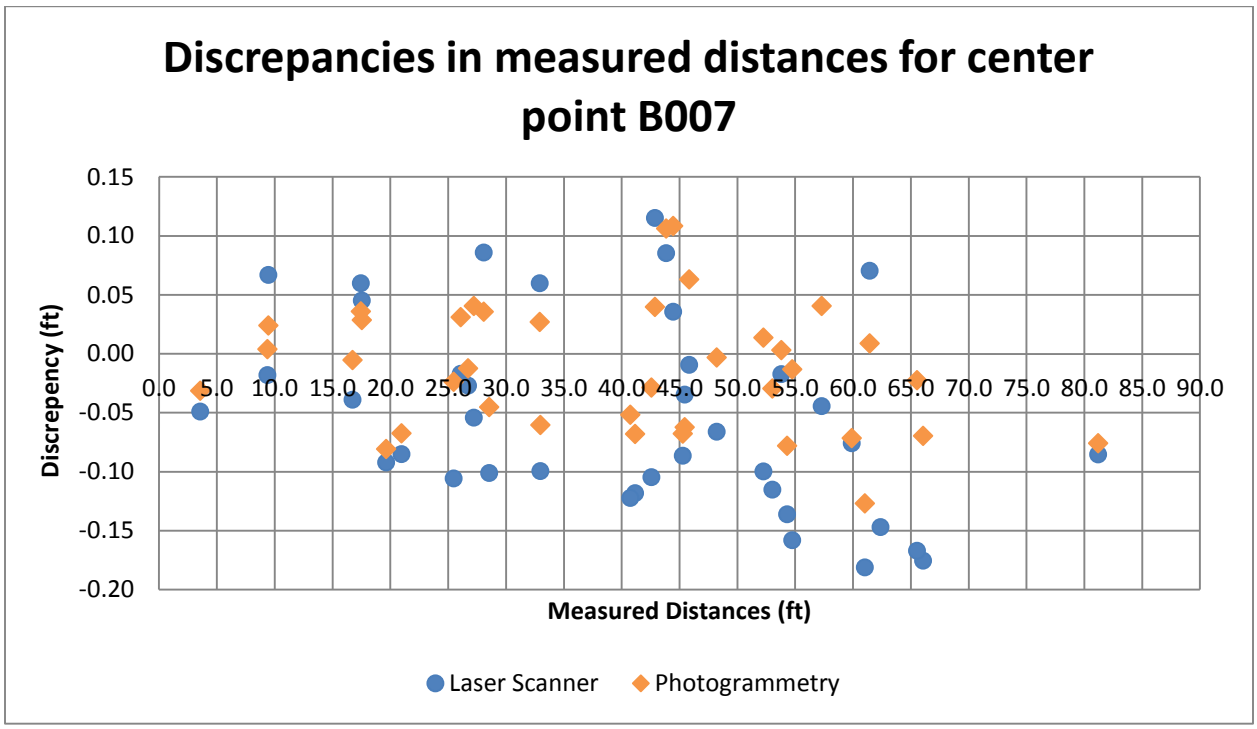

Figure 6.8 Discrepancies in measured distances for terrace at center point B007

Table 6.4 Statistical data of distance discrepancies for terrace at center point B007 with outliers removed

Item	Laser Scanner - Total Station	Photogrammetry - Total Station
Maximum Value (ft.)	0.1673	0.1083
Minimum Value (ft.)	0.0094	0.0030
Mean Value (ft.)	0.0784	0.0427
RMS Value (ft.)	0.0871	0.0504
Standard Deviation (ft.)	0.0410	0.0284
Outliers Removed	F003, F001	F002, F003

Table 6.5 Distance discrepancy ranges for terrace at center point B007

Discrepancy Ranges for Center Point B007								
	Laser Scanner - Total Station				Photogrammetry - Total Station			
Discrepancy ranges	# falling in that range	% at each range	% Less Than	% Greater Than	# falling in that range	% at each range	% Less Than	% Greater Than
<0.001	0	0%	0%	100%	0	0%	0%	100%
0.001<d<0.005	0	0%	0%	100%	3	8%	8%	92%
0.005<d<0.010	1	3%	3%	97%	2	5%	13%	87%
0.010<d<0.015	0	0%	3%	97%	3	8%	21%	79%
0.015<d<0.020	3	8%	10%	90%	0	0%	21%	79%
0.020<d<0.025	0	0%	10%	90%	3	8%	28%	72%
0.025<d<0.030	1	3%	13%	87%	4	10%	38%	62%
0.030<d	34	87%	100%		24	62%	100%	
SUM	39				39			

Coordinate Distances of Photogrammetry Model and Laser Scanner Model to Center Point D003

Center point D003 did not perform as well as some of the other center points. As in center point B007, there is an outlier located at point F002. There appears to be no real reason for this point having a distance discrepancy greater than 1 ft. in center points B007 and D003. It is important to note that there is no problem with point F002 in center point A011. It is also strange that is only displays in the photogrammetry model, which can be viewed in figure 6.9. This error was likely caused by F002 being moved and recollected by the total station. The undergraduate students, who acquired the total station data may have not realized or reported the errors. The photogrammetry pictures were collected right after the reference markers were attached to the concrete retaining walls, so those errors did not affect its model. The points at this center point had the largest range of discrepancies from -0.25 ft. to 0.25 ft.

The Statistical date for center point D003 are in table 6.6 and the distance discrepancy ranges are given in table 6.7. The photogrammetry model had the largest maximum value at this center point, due to the problem described earlier with point F002. The value of the discrepancy at F002 was 1.9833 ft. Even though the maximum value was high for the photogrammetry model, the other data showed that this center point preformed quite well. After removing the outliers in the data, the maximum discrepancies were 0.2491 ft. for the laser scanner model and 0.1560 ft. for the photogrammetry model. The laser scanner model had 18% of its points below 0.02 ft., while the photogrammetry model had 31% below. This was the only center point were the laser scanner model had any points less than 0.001 ft.

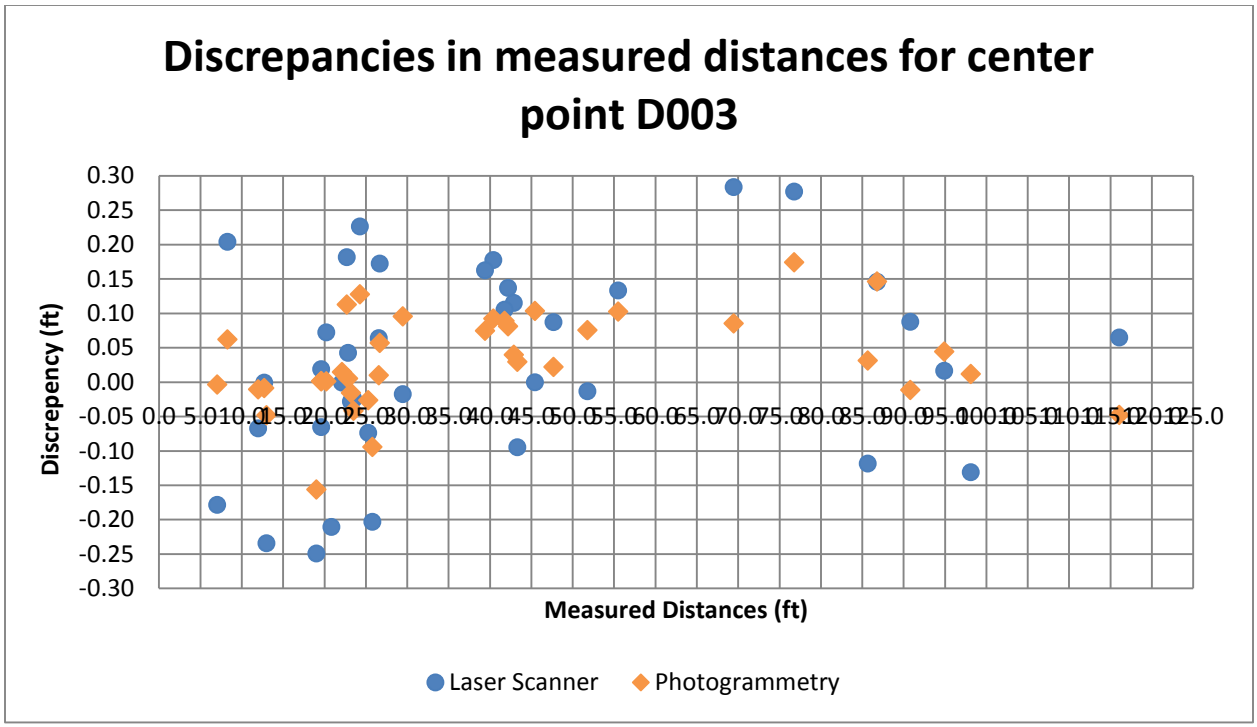

Figure 6.9 Discrepancies in measured distances for terrace at center point D003

Table 6.6 Statistical data of distance discrepancies for terrace at center point D003 with outliers removed

Item	Laser Scanner - Total Station	Photogrammetry - Total Station
Maximum Value (ft.)	0.2491	0.1560
Minimum Value (ft.)	0.0000	0.0011
Mean Value (ft.)	0.1061	0.0536
RMS Value (ft.)	0.1275	0.0682
Standard Deviation (ft.)	0.0747	0.0443
Outliers Removed	E009, A011	F002, A011

Table 6.7 Distance discrepancy ranges for terrace at center point D003

Discrepancy Ranges for Center Point D003								
	Laser Scanner - Total Station				Photogrammetry - Total Station			
Discrepancy ranges	# falling in that range	% at each range	% Less Than	% Greater Than	# falling in that range	% at each range	% Less Than	% Greater Than
<0.001	3	8%	8%	92%	0	0%	0%	100%
0.001<d<0.005	0	0%	8%	92%	4	10%	10%	90%
0.005<d<0.010	0	0%	8%	92%	2	5%	15%	85%
0.010<d<0.015	1	3%	10%	90%	5	13%	28%	72%
0.015<d<0.020	3	8%	18%	82%	1	3%	31%	69%
0.020<d<0.025	1	3%	21%	79%	1	3%	33%	67%
0.025<d<0.030	1	3%	23%	77%	2	5%	38%	62%
0.030<d	30	77%	100%		24	62%	100%	
SUM	39				39			

Comparison of Distances in the Photogrammetry and Laser Scanner Models Relative to Center Point E007

The last section of distances discrepancies is for the center point E007. Figure 6.10 is similar to the other figures with the exception that points have a tighter grouping around the center line. The range of discrepancies for this center point was -0.1 ft. to 0.1 ft., which was the best of any center point. The outlier F002 continues to produce an error greater than 1 ft. in this center point also.

The statistics for point C035 are provided in table 6.8 and the distance discrepancy ranges are in table 6.9. The laser scanner at this center point had 15% of the distance discrepancies less than 0.02 ft. The photogrammetry model had 28% of its discrepancies less than 0.02 ft., which was the second largest behind center point D003. The photogrammetry model also had the smallest number of points above 0.03 ft. at twenty.

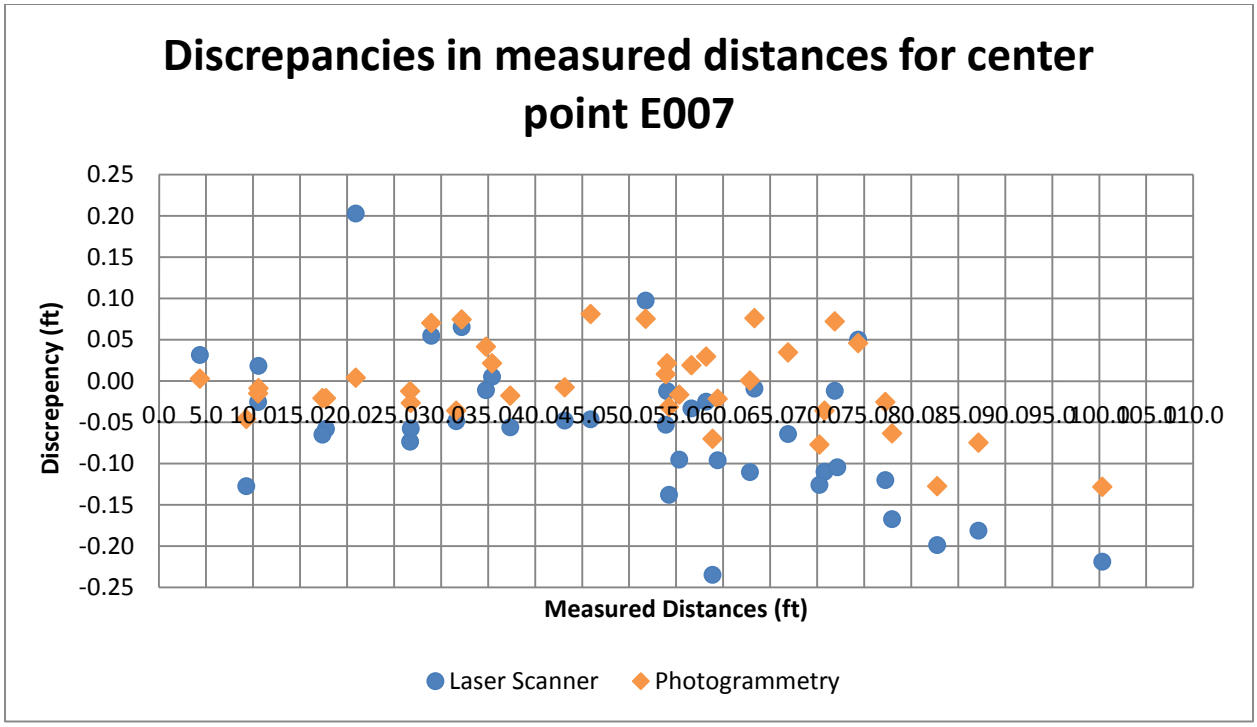

Figure 6.10 Discrepancies in measured distances for terrace at center point E007

Table 6.8 Statistical data of distance discrepancies for terrace at center point E007 with outliers removed

Item	Laser Scanner - Total Station	Photogrammetry - Total Station
Maximum Value (ft.)	0.2029	0.1274
Minimum Value (ft.)	0.0051	0.0004
Mean Value (ft.)	0.0757	0.0387
RMS Value (ft.)	0.0914	0.0479
Standard Deviation (ft.)	0.0541	0.0300
Outliers Removed	C010, A019	F002, A019

Table 6.9 Distance discrepancy ranges for terrace at center point E007

Discrepancy Ranges for Center Point E007								
	Laser Scanner - Total Station				Photogrammetry - Total Station			
Discrepancy ranges	# falling in that range	% at each range	% Less Than	% Greater Than	# falling in that range	% at each range	% Less Than	% Greater Than
<0.001	0	0%	0%	100%	1	3%	3%	97%
0.001<d<0.005	0	0%	0%	100%	2	5%	8%	92%
0.005<d<0.010	2	5%	5%	95%	3	8%	15%	85%
0.010<d<0.015	3	8%	13%	87%	2	5%	21%	79%
0.015<d<0.020	1	3%	15%	85%	3	8%	28%	72%
0.020<d<0.025	1	3%	18%	82%	5	13%	41%	59%
0.025<d<0.030	1	3%	21%	79%	3	8%	49%	51%
0.030<d	31	79%	100%		20	51%	100%	
SUM	39				39			

CHAPTER 7

CONCLUSIONS AND RECOMMENDATIONS

CONCLUSION

The purpose of this study was to compare the accuracy of building measurements performed on 3D models generated by close-range photogrammetry to traditional surveying instruments. If close-range photogrammetry can produce 3D models with accuracies similar to models produced by terrestrial LiDAR and classical total-station instruments, then it could be used as an alternative approach to those methods. In this study, a standard total station instrument was used as the control for the discrepancy comparison. Two different systems for creating 3D models were used, which are close-range photogrammetry and laser scanning. Both systems were compared against the total station by considering coordinate measurements of the same points in all three systems. The raw data was analyzed by using two different approaches. The first approach was coordinate discrepancies and the second was the analysis of distance discrepancies between points.

In the RAC case study, the coordinate discrepancies method had a maximum discrepancy of 0.5750 ft. for the laser scanner model and 0.6015 ft. for the photogrammetry model. In both models, the maximum discrepancy was contained in the z coordinate data. As stated earlier, this was caused by a data collection error on side D of the RAC structure. The maximum discrepancy for the x coordinate was 0.0810 ft. for the laser scanner model and 0.0876 for the photogrammetry model. The y coordinate had similar results, the laser scanner model had a maximum discrepancy of 0.0480 ft., while the photogrammetry model had a maximum of 0.0470 ft. It is important to

note that these discrepancies are only valid when the camera to object distances are less than 20 ft. The distance discrepancies had similar results when compared to the coordinate discrepancies. The laser scanner model had a maximum discrepancy of 0.5570 ft. and the photogrammetry model had a maximum of 0.5804 ft. According to the discrepancy range tables, the laser scanner model had 19% of the points greater than 0.030 ft., while the photogrammetry model had 40%. The laser scanner model also had 72% of the points less than 0.020 ft. and the photogrammetry had 42% less than 0.020ft.

In the temple case study, the coordinate discrepancies method had a maximum discrepancy of 0.5697 ft. for the laser scanner model and 0.4964 ft. for the photogrammetry model. Similar to the RAC case study, both models maximum discrepancies were in the z coordinate. The x and y coordinate maximum discrepancies for the laser scanner model were 0.1510 ft. and 0.0812 ft., respectively. The photogrammetry model had a maximum discrepancy of 0.1208 ft. in the x coordinate and 0.0885 ft. in the y coordinate. The distance discrepancies had similar results when compared to the coordinate discrepancies. The laser scanner model had a maximum discrepancy of 0.2178 ft. and the photogrammetry model had a maximum of 0.2350 ft. The laser scanner model had 22% of the points below 0.020 ft. and 69% above 0.030 ft., while the photogrammetry model had 36% and 54%. The camera to object distances for this case were less than 75 ft.

In the terrace case study, the coordinate discrepancies method had a maximum discrepancy of 0.2362 ft. for the laser scanner model and 0.1365 ft. for the photogrammetry model. Unlike the other two case studies, the maximum discrepancies were in the y coordinate data. The laser scanner model produced a maximum discrepancy of 0.1232 ft. in the x coordinate and 0.0889 ft. in the z coordinate. The photogrammetry model achieved similar results with a maximum discrepancy of 0.0964 ft. in the x coordinate and 0.1274 ft. in the z coordinate. The distance

discrepancies had similar results when compared to the coordinate discrepancies. The laser scanner model had a maximum discrepancy of 0.2491 ft. and the photogrammetry model had a maximum of 0.2178 ft. According to the discrepancy range tables, the laser scanner model had 80% of the points greater than 0.030 ft., while the photogrammetry model had 67%. The laser scanner model also had 14% of the points less than 0.020 ft. and the photogrammetry had 21% less than 0.020ft. The camera to object distances were 20 ft. to 300 ft. in this case, which was significantly longer than the other two case studies.

This research suggests that laser scanning and photogrammetry can be used as alternatives to a standard total station when measuring buildings or relatively small areas. Most of the extreme errors seen were a direct result of operator error and not equipment error. The main advantage that both systems have over the total station was speed during field work and the amount of data collected. However, the photogrammetry approach required large post-processing time. Both systems collect the whole site, while the total station can only collect selected points. This gives personnel at the office additional options when analyzing sites and producing site design options.

RECOMMENDATIONS

In the course of this study, several observations were made pertaining to close-range photogrammetry and laser scanning. The first section explains the observations observed when generating and acquiring the data from the close-range photogrammetry models. The second section contains the observations from the laser scanning model generation and data acquisition.

The photogrammetry models required high resolution clear pictures. The cameras used to produce the models play an important part in the end result. The highest megapixel camera within

budget should be used, especially if equipped with a fixed wide angle lens. As the distance from the object to the lens increases, it causes more information to be packed into a single pixel of the camera. This results in a loss of detail in the picture and in the completed model. It was observed that the wide angle lens would lose detail when it was more than 100 ft. away from the object being photographed. This type of lens should be used as close to the object as possible while still keeping a good field of view. Another observation was that models tend to fail processing when less than sixty percent overlap is used between photos and when the photos are not taken perpendicular to the object. It is recommended by PhotoScan to set the camera to save the pictures in RAW format and then convert them to lossless TIFF format using another program. Additionally, the photogrammetry model will usual require the use of drones if the structure is over one story or if topography is being captured. Currently in the United States, drones can only be used by businesses that have obtained a certificate of authorization from the Federal Aviation Administration. This is important consideration for businesses as they are difficult to obtain and required a significant amount of capital investment. Another important point to consider is how many picture will be necessary to complete a project. The computer used in this study can process 100 to 200 pictures into a model in about an hour. When the photo set grows to over 500 pictures, it can require anywhere from a week to a month to generate the model. The processing time can be reduced by employing workstation or server class computers. Workstations and servers have the option to have multiple processors and over 128 gigabytes of memory, which will significantly reduce the use of the hard drive swap file. The picture limitations observed in this study suggest that photogrammetry tends to be viable only when producing low detail large projects such as terrain mapping or high detail small projects such as the ones presented in this study.

The main observation made when using the laser scanner is how range to the object affected the model. As the scanner moved farther away from the object, the point density would decrease. The decrease in density would increase the difficulty of selecting accurate points and effect the accuracy of the measurements being made. The best recommendation is to keep the laser scanner as close to the object as possible or increase the number of scans when this is not possible. The resolution can also be increased, but that will increase the amount of time per scan. Another option is to scan important sections using a windowed scan with maximum resolution. The type of scanning targets selected influence the overall registration error. The scanning targets used in this study with the highest accuracy were the spheres. The spheres do not have to be readjusted to face the scanner after moving to a new scanner location. This allows for a greater accuracy, since the spheres are not slightly moved with each adjustment. Another important observation is to complete the scanning in one day if possible. Each time targets are repositioned it introduces additional error into the registration as there is always some positioning inaccuracies. Additionally, if the project requires the scanning of blue or black sections expect to increase the resolution or decrease the scanner to object distance. This is due blue and black having a very low reflectance of light. Laser scanners are currently being used to generate point clouds of as-built structures and topography. One of the main uses is in the transportation industry collecting point clouds of roadways and intersections. There many other uses that are not listed here that pertain to other fields of study.

REFERENCES

n.d. *AF Nikkor 28mm f/2.8D.* Accessed April 27, 2015. http://www.nikonusa.com/en/nikon-products/product/camera-lenses/af-nikkor-28mm-f%252f2.8d.html.

2016. *Agisoft.* Accessed April 1, 2016. http://www.agisoft.com/buy/online-store/.

2015. *Canon EF 24mm f/2.8 IS USM.* Accessed April 27, 2015. https://www.usa.canon.com/internet/portal/us/home/products/details/lenses/ef/wide-angle/ef-24mm-f-2-8-is-usm.

2015. *Canon EOS 5D Mark III.* Accessed April 27, 2015. https://www.usa.canon.com/internet/portal/us/home/products/details/cameras/dslr/eos-5d-mark-iii.

Dai, Fei, Abbas Rashidi, Ioannis Brilakis, and Patricio Vela. 2013. "Comparison of Image-Based and Time-of-Flight-Based Technologies for Three-Dimensional Reconstruction of Infastructure." *Journal of Construction Engineering and Management* 69-79.

Dai, Fei, and Ming Lu. 2010. "Assessing the Accuracy of Applying Photogrammetry to Take Geometric Measurements on Building Products." *Journal of Construction Engineering and Management* 242-250.

n.d. "Features Professional Edition." *Agisoft.* Accessed 11 1, 2015. http://www.agisoft.com/features/professional-edition/.

2015. *FLT Geosystems.* Accessed April 27, 2015. http://www.fltgeosystems.com/laser-scanners-3d/used-leica-c10-3d-laser-scanner-used-leica-c10/.

2015. *FTL Geosystems Leica Professional 5000 Series Tripod.* Accessed April 27, 2105. http://www.fltgeosystems.com/tripods-bipods/leica-gst20-professional-series-tripod-296632-lca296632/.

2015. *FTL Geosystems SECO Thumb Release Tripod.* Accessed April 27, 2015. http://www.fltgeosystems.com/tripods-bipods/seco-original-thumb-release-prism-pole-tripod-5218-02-sec5218-02-red/.

Ghosh, Sanjib K. 2005. *Fundamentals of Computational Photogrammetry*. New Delhi: Concept Pubishing Company.

n.d. *GoPro Hero3: Black Edition.* Accessed April 2, 2016. http://www.amazon.com/GoPro-CHDHX-301-HERO3-Black-Edition/dp/B009TCD8V8.

Grussenmeyer, P, T Landes, T Voegtle, and K Ringle. 2008. "Comparison Methods of Terrestrial Laser Scanning, Photogrammetry, and Techeometry Data for Recording of Cultural Heritage Buildings." *The International Archives of the Photogrammetry, Remote Sensing and Spatial Information Sciences* 213-218.

Kavanagh, Barry F, and Tom B Mastin. 2014. *Surveying : Principles and Applications.* Boston: Pearson.

n.d. *Leica Cyclone 3D Point Cloud Processing Software (EA).* Accessed April 1, 2016. http://www.fltgeosystems.com/software/leica-hds-software/leica-cyclone-3d-point-cloud-processing-software-lca760728/.

Leica Geosystems. 2012. *Leica Scanstion C10/C5 User Manual.* Heerburg: Leica Geosystems AG.

Matthews, Neffra A. 2008. *Aerial and Close-Range Photogrammetric Technology: Providing Resource Documentation, Interpretation, and Preservation.* Technical Note 428, Denver: U.S. Department of the Interior, Bureau of Land Management.

n.d. *Nikon D800.* Accessed April 27, 2015. http://www.nikonusa.com/en/nikon-products/product-archive/dslr-cameras/d800.html.

Sužiedelytė-Visockienė, Jūratė, Renata Bagdžiūnaitė, Naglis Malys, and Vida Maliene. 2015. "Close-Range Photogrammetry Enables Documentation of Environment-Induced Deformation of Architectural Heritage." *Environmental Engineering and Management Journal* 1371-1381.

n.d. "Topcon GPT 3000." *Survey Equipment.* Accessed 11 1, 2015. http://www.surveyequipment.com/PDFs/topcon-gpt-3000-manual.pdf.

Yakar, M, H M Yilmaz, and O Mutluoglu. 2010. "Close range photogrammerty and robotic total station in volume calculation." *International Journal of the Physical Sciences* 86-96.

APPENDIX A

CASE STUDY: RECREATION ACTIVITY CENTER (RAC) STORAGE BUILDING

This sections includes the raw data that was collected during Recreation Activity Center storage building case study. The data is split into three sections according to the type of data. The first is section is for the actual raw data collected from each method. The second section is the discrepancies from the coordinate discrepancy method and the third contains the discrepancies from the distance discrepancy method.

RAW TOTAL STATION, LASER SCANNER, AND PHOTOGRAMMETRY DATA

Point		Easting (X)			Northing (Y)			Elevation (Z)		
		TS (ft.)	Laser (ft.)	Photo (ft.)	TS (ft.)	Laser (ft.)	Photo (ft.)	TS (ft.)	Laser (ft.)	Photo (ft.)
A1	A008	45.100	45.098	45.113	66.050	66.045	66.043	15.125	15.138	15.086
A2	A013	44.695	44.699	44.703	64.965	64.983	64.960	16.705	16.703	16.682
A3	A016	44.695	44.698	44.708	64.980	64.981	64.970	14.440	14.438	14.417
A4	A028	43.755	43.744	43.748	62.475	62.467	62.463	17.805	17.801	17.772
A5	A047	42.930	42.926	42.907	60.235	60.274	60.245	17.815	15.577	17.783
A6	A053	42.420	42.421	42.390	58.860	58.899	58.862	18.930	18.916	18.892
A7	A062	41.885	41.871	41.859	57.445	57.447	57.448	17.800	17.802	17.757
A8	A064	41.890	41.869	41.865	57.465	57.468	57.462	15.550	15.553	15.504
A9	A066	41.965	41.950	41.957	57.695	57.692	57.702	12.810	12.813	12.764
A10	A070	41.085	41.072	41.055	55.320	55.336	55.327	17.795	17.793	17.746
B1	B007	42.095	42.085	42.070	54.810	54.803	54.809	18.475	18.477	18.449
B2	B008	42.060	42.063	42.033	54.825	54.825	54.830	17.100	17.107	17.054
B3	B009	42.055	42.054	42.034	54.825	54.828	54.829	15.780	15.790	15.727
B4	B013	42.815	42.812	42.797	54.535	54.542	54.542	17.560	17.561	17.519
B5	B014	42.820	42.808	42.800	54.545	54.540	54.541	16.225	16.229	16.190
B6	B054	54.545	54.563	54.549	50.085	50.079	50.085	18.920	18.926	18.921
B7	B055	54.555	54.558	54.558	50.090	50.111	50.088	17.570	17.573	17.568
B8	B056	54.550	54.548	54.554	50.095	50.115	50.089	16.225	16.224	16.223
B9	B060	55.975	55.979	55.974	49.555	49.565	49.553	18.690	18.689	18.699
B10	B061	55.965	55.966	55.971	49.550	49.580	49.558	17.795	17.796	17.799
D1	D009	58.690	58.690	58.698	62.455	62.451	62.465	18.135	17.571	17.571

Point		Easting (X)			Northing (Y)			Elevation (Z)		
		TS (ft.)	Laser (ft.)	Photo (ft.)	TS (ft.)	Laser (ft.)	Photo (ft.)	TS (ft.)	Laser (ft.)	Photo (ft.)
D2	D010	56.175	56.170	56.175	63.380	63.384	63.402	18.145	17.590	17.564
D3	D012	51.165	51.156	51.173	65.265	65.272	65.295	18.150	17.575	17.552
D4	D013	48.670	48.674	48.682	66.205	66.206	66.233	18.160	17.589	17.564
D5	D014	45.635	45.636	45.650	67.340	67.332	67.368	17.255	16.688	16.654
D6	D021	58.700	58.706	58.721	62.435	62.433	62.445	14.880	14.887	14.883
D7	D022	56.175	56.176	56.196	63.380	63.380	63.386	14.860	14.862	14.859
D8	D028	56.165	56.180	56.189	63.380	63.371	63.390	13.540	13.547	13.537
D9	D031	48.625	48.635	48.638	66.205	66.200	66.231	13.565	13.565	13.538
D10	D037	51.110	51.112	51.128	65.275	65.271	65.297	12.820	12.802	12.797
C1	C006	57.645	57.646	57.647	51.250	51.251	51.237	19.600	16.599	19.611
C2	C007	57.455	57.460	57.462	50.730	50.731	50.714	18.020	18.018	18.018
C3	C016	58.520	58.531	58.549	53.555	53.549	53.551	16.435	16.437	16.439
C4	C023	59.095	59.087	59.105	55.100	55.072	55.096	19.610	19.612	19.611
C5	C028	59.285	59.355	59.373	55.740	55.748	55.760	16.915	16.917	16.911
C6	C035	59.610	59.609	59.636	56.440	56.431	56.442	18.905	18.902	18.919
C7	C036	60.075	60.066	60.089	57.640	57.639	57.636	18.010	18.010	18.013
C8	C039	60.315	60.396	59.999	58.470	58.461	57.349	14.895	14.896	13.755
C9	C044	61.080	61.075	61.102	60.280	60.277	60.277	15.560	15.560	15.571
C10	C047	60.920	60.923	60.946	59.895	59.847	59.848	12.830	12.835	12.839

COORDINATE DISCREPANCY DATA

Point	Total Station - Laser Scanner			Total Station - Photogrammetry		
	X	Y	Z	X	Y	Z
A1	-0.0020	-0.0050	0.0130	0.0126	-0.0068	-0.0390
A2	0.0040	0.0180	-0.0020	0.0078	-0.0051	-0.0228
A3	0.0030	0.0010	-0.0020	0.0130	-0.0097	-0.0232
A4	-0.0110	-0.0080	-0.0040	-0.0073	-0.0119	-0.0329
A5	-0.0040	0.0390	-2.2380	-0.0226	0.0105	-0.0318
A6	0.0010	0.0390	-0.0140	-0.0303	0.0022	-0.0384
A7	-0.0140	0.0020	0.0020	-0.0262	0.0027	-0.0435
A8	-0.0210	0.0030	0.0030	-0.0252	-0.0030	-0.0456
A9	-0.0150	-0.0030	0.0030	-0.0080	0.0065	-0.0465
A10	-0.0130	0.0160	-0.0020	-0.0301	0.0072	-0.0486
AVG=	0.0088	0.0134	0.2283	0.0183	0.0066	0.0372
B1	-0.0100	-0.0070	0.0020	-0.0248	-0.0011	-0.0258
B2	0.0030	0.0000	0.0070	-0.0267	0.0051	-0.0458
B3	-0.0010	0.0030	0.0100	-0.0209	0.0043	-0.0527
B4	-0.0030	0.0070	0.0010	-0.0177	0.0070	-0.0415
B5	-0.0120	-0.0050	0.0040	-0.0200	-0.0044	-0.0351
B6	0.0180	-0.0060	0.0060	0.0036	0.0004	0.0014
B7	0.0030	0.0210	0.0030	0.0032	-0.0017	-0.0022
B8	-0.0020	0.0200	-0.0010	0.0037	-0.0060	-0.0018
B9	0.0040	0.0100	-0.0010	-0.0013	-0.0021	0.0085
B10	0.0010	0.0300	0.0010	0.0059	0.0081	0.0044
AVG=	0.0057	0.0109	0.0036	0.0128	0.0040	0.0219
C1	0.0010	0.0010	-3.0010	0.0023	-0.0131	0.0113
C2	0.0050	0.0010	-0.0020	0.0074	-0.0157	-0.0019
C3	0.0110	-0.0060	0.0020	0.0285	-0.0044	0.0039
C4	-0.0080	-0.0280	0.0020	0.0102	-0.0036	0.0011
C5	0.0700	0.0080	0.0020	0.0876	0.0195	-0.0044
C6	-0.0010	-0.0090	-0.0030	0.0259	0.0017	0.0142
C7	-0.0090	-0.0010	0.0000	0.0137	-0.0039	0.0031
C8	0.0810	-0.0090	0.0010	-0.3163	-1.1210	-1.1403
C9	-0.0050	-0.0030	0.0000	0.0219	-0.0034	0.0115
C10	0.0030	-0.0480	0.0050	0.0265	-0.0470	0.0091
AVG=	0.0194	0.0114	0.3018	0.0540	0.1233	0.1201
D1	0.0000	-0.0040	-0.5640	0.0082	0.0100	-0.5643
D2	-0.0050	0.0040	-0.5550	-0.0002	0.0223	-0.5815
D3	-0.0090	0.0070	-0.5750	0.0084	0.0297	-0.5980
D4	0.0040	0.0010	-0.5710	0.0118	0.0281	-0.5959

Point	Total Station - Laser Scanner			Total Station - Photogrammetry		
	X	Y	Z	X	Y	Z
D5	0.0010	-0.0080	-0.5670	0.0147	0.0282	-0.6015
D6	0.0060	-0.0020	0.0070	0.0208	0.0098	0.0033
D7	0.0010	0.0000	0.0020	0.0210	0.0063	-0.0009
D8	0.0150	-0.0090	0.0072	0.0242	0.0097	-0.0030
D9	0.0100	-0.0050	0.0000	0.0130	0.0262	-0.0274
D10	0.0020	-0.0040	-0.0180	0.0178	0.0218	-0.0229
AVG=	0.0053	0.0044	0.2866	0.0140	0.0192	0.2999
Total Average=	0.0098	0.0100	0.2051	0.0248	0.0383	0.1198

DISTANCE DISCREPANCY DATA

Laser Scanner

Point		Center Point A006			
		Total Station (ft.)	Laser Scanner (ft.)	Discrepancy (ft.)	Abs. Discrepancy (ft.)
A1	A008	9.2192	9.2243	0.0051	0.0051
A2	A013	8.6877	8.7091	0.0213	0.0213
A3	A016	7.9486	7.9575	0.0088	0.0088
A4	A028	7.1416	7.1344	-0.0072	0.0072
A5	A047	5.6950	3.9063	-1.7887	1.7887
A6	A053	6.2465	6.2390	-0.0075	0.0075
A7	A062	4.9969	4.9956	-0.0013	0.0013
A8	A064	2.7507	2.7503	-0.0003	0.0003
A9	A066	-	-	-	-
A10	A070	5.5915	5.5787	-0.0128	0.0128
B1	B007	6.3586	6.3597	0.0010	0.0010
B2	B008	5.1624	5.1644	0.0020	0.0020
B3	B009	4.1311	4.1323	0.0012	0.0012
B4	B013	5.7681	5.7627	-0.0053	0.0053
B5	B014	4.7240	4.7266	0.0026	0.0026
B6	B054	15.9217	15.9504	0.0287	0.0287
B7	B055	15.4597	15.4626	0.0029	0.0029
B8	B056	15.0932	15.0916	-0.0016	0.0016
B9	B060	17.2370	17.2450	0.0080	0.0080
B10	B061	16.9467	16.9435	-0.0032	0.0032
C1	C006	18.2621	17.3835	-0.8786	0.8786
C2	C007	17.7650	17.7794	0.0144	0.0144
C3	C016	17.4456	17.4708	0.0252	0.0252
C4	C023	18.6121	18.6217	0.0096	0.0096
C5	C028	17.9069	17.9877	0.0808	0.0808
C6	C035	18.7102	18.7218	0.0117	0.0117
C7	C036	18.8418	18.8468	0.0049	0.0049
C8	C039	18.4843	18.5792	0.0948	0.0948
C9	C044	19.4840	19.4934	0.0094	0.0094
C10	C047	19.0823	19.0950	0.0128	0.0128
D1	D009	18.1862	18.0420	-0.1442	0.1442
D2	D010	16.2082	16.0445	-0.1637	0.1637
D3	D012	13.0561	12.8407	-0.2154	0.2154
D4	D013	12.0830	11.8537	-0.2293	0.2293
D5	D014	11.2362	11.0241	-0.2121	0.2121

D6	D021	17.5161	17.5369	0.0208	0.0208
D7	D022	15.4417	15.4574	0.0157	0.0157
D8	D028	15.3131	15.3389	0.0258	0.0258
D9	D031	10.8326	10.8462	0.0136	0.0136
D10	D037	11.8780	11.8905	0.0125	0.0125
Point		**Center Point B013**			
		Total Station (ft.)	**Laser Scanner (ft.)**	**Discrepancy (ft.)**	**Abs. Discrepancy (ft.)**
A1	A008	11.9894	11.9756	-0.0138	0.0138
A2	A013	10.6325	10.6448	0.0123	0.0123
A3	A016	11.0620	11.0582	-0.0038	0.0038
A4	A028	7.9992	7.9832	-0.0160	0.0160
A5	A047	5.7069	6.0667	0.3599	0.3599
A6	A053	4.5540	4.5796	0.0256	0.0256
A7	A062	3.0644	3.0631	-0.0013	0.0013
A8	A064	3.6716	3.6719	0.0003	0.0003
A9	A066	5.7681	5.7627	-0.0053	0.0053
A10	A070	1.9142	1.9266	0.0124	0.0124
B1	B007	1.1963	1.1982	0.0019	0.0019
B2	B008	0.9304	0.9204	-0.0100	0.0100
B3	B009	1.9571	1.9475	-0.0096	0.0096
B4	B013	-	-	-	-
B5	B014	1.3350	1.3320	-0.0030	0.0030
B6	B054	12.6192	12.6439	0.0246	0.0246
B7	B055	12.5533	12.5540	0.0007	0.0007
B8	B056	12.6177	12.6143	-0.0034	0.0034
B9	B060	14.1161	14.1214	0.0053	0.0053
B10	B061	14.0651	14.0607	-0.0044	0.0044
C1	C006	15.3259	15.2251	-0.1008	0.1008
C2	C007	15.1334	15.1425	0.0092	0.0092
C3	C016	15.7757	15.7904	0.0147	0.0147
C4	C023	16.4183	16.4123	-0.0060	0.0060
C5	C028	16.5266	16.5994	0.0728	0.0728
C6	C035	16.9561	16.9560	-0.0001	0.0001
C7	C036	17.5428	17.5355	-0.0073	0.0073
C8	C039	18.1338	18.2115	0.0776	0.0776
C9	C044	19.2514	19.2466	-0.0048	0.0048
C10	C047	19.4652	19.4547	-0.0105	0.0105
D1	D009	17.7503	17.7388	-0.0115	0.0115
D2	D010	16.0333	16.0193	-0.0140	0.0140
D3	D012	13.6089	13.5925	-0.0165	0.0165
D4	D013	13.0702	13.0542	-0.0160	0.0160
D5	D014	13.1154	13.1271	0.0117	0.0117
D6	D021	17.9423	17.9454	0.0031	0.0031

D7	D022	16.2485	16.2478	-0.0007	0.0007
D8	D028	16.5111	16.5156	0.0045	0.0045
D9	D031	13.6347	13.6303	-0.0044	0.0044
D10	D037	14.3744	14.3753	0.0009	0.0009
Point		**Center Point C035**			
		Total Station (ft.)	**Laser Scanner (ft.)**	**Discrepancy (ft.)**	**Abs. Discrepancy (ft.)**
A1	A008	17.8096	17.8091	-0.0004	0.0004
A2	A013	17.3197	17.3286	0.0089	0.0089
A3	A016	17.7574	17.7586	0.0012	0.0012
A4	A028	17.0004	17.0101	0.0097	0.0097
A5	A047	17.1410	17.4398	0.2988	0.2988
A6	A053	17.3595	17.3643	0.0048	0.0048
A7	A062	17.7878	17.8011	0.0133	0.0133
A8	A064	18.0639	18.0831	0.0192	0.0192
A9	A066	18.7102	18.7218	0.0117	0.0117
A10	A070	18.5920	18.6024	0.0104	0.0104
B1	B007	17.5959	17.6046	0.0087	0.0087
B2	B008	17.7163	17.7105	-0.0058	0.0058
B3	B009	17.9040	17.9006	-0.0033	0.0033
B4	B013	16.9561	16.9560	-0.0001	0.0001
B5	B014	17.1078	17.1171	0.0093	0.0093
B6	B054	8.1265	8.1124	-0.0142	0.0142
B7	B055	8.2254	8.1989	-0.0266	0.0266
B8	B056	8.5466	8.5251	-0.0215	0.0215
B9	B060	7.7886	7.7694	-0.0192	0.0192
B10	B061	7.8734	7.8378	-0.0356	0.0356
C1	C006	5.5929	5.9991	0.4062	0.4062
C2	C007	6.1670	6.1555	-0.0115	0.0115
C3	C016	3.9512	3.9426	-0.0086	0.0086
C4	C023	1.5993	1.6197	0.0204	0.0204
C5	C028	2.1344	2.1145	-0.0199	0.0199
C6	C035	-	-	-	-
C7	C036	1.5676	1.5696	0.0021	0.0021
C8	C039	4.5495	4.5594	0.0099	0.0099
C9	C044	5.3005	5.3019	0.0013	0.0013
C10	C047	7.1105	7.0855	-0.0250	0.0250
D1	D009	6.1335	6.2335	0.1000	0.1000
D2	D010	7.7808	7.8672	0.0864	0.0864
D3	D012	12.2380	12.3036	0.0656	0.0656
D4	D013	14.6831	14.7258	0.0427	0.0427
D5	D014	17.7998	17.8600	0.0602	0.0602
D6	D021	7.2780	7.2773	-0.0006	0.0006
D7	D022	8.7364	8.7405	0.0041	0.0041

D8	D028	9.4242	9.4125	-0.0116	0.0116
D9	D031	15.6378	15.6316	-0.0063	0.0063
D10	D037	13.6870	13.6951	0.0080	0.0080
Point		**Center Point D022**			
		Total Station (ft.)	**Laser Scanner (ft.)**	**Discrepancy (ft.)**	**Abs. Discrepancy (ft.)**
A1	A008	11.3954	11.3974	0.0020	0.0020
A2	A013	11.7348	11.7337	-0.0011	0.0011
A3	A016	11.5986	11.5969	-0.0017	0.0017
A4	A028	12.7964	12.8073	0.0108	0.0108
A5	A047	13.9303	13.6279	-0.3023	0.3023
A6	A053	15.0398	15.0238	-0.0160	0.0160
A7	A062	15.7503	15.7632	0.0129	0.0129
A8	A064	15.4766	15.4958	0.0192	0.0192
A9	A066	15.4417	15.4574	0.0157	0.0157
A10	A070	17.3576	17.3617	0.0041	0.0041
B1	B007	16.8748	16.8876	0.0127	0.0127
B2	B008	16.6565	16.6555	-0.0010	0.0010
B3	B009	16.5351	16.5357	0.0006	0.0006
B4	B013	16.2485	16.2478	-0.0007	0.0007
B5	B014	16.0710	16.0847	0.0137	0.0137
B6	B054	13.9963	14.0012	0.0049	0.0049
B7	B055	13.6599	13.6394	-0.0205	0.0205
B8	B056	13.4534	13.4338	-0.0197	0.0197
B9	B060	14.3471	14.3366	-0.0105	0.0105
B10	B061	14.1396	14.1100	-0.0295	0.0295
C1	C006	13.1059	12.3406	-0.7653	0.7653
C2	C007	13.1014	13.0999	-0.0015	0.0015
C3	C016	10.2230	10.2311	0.0081	0.0081
C4	C023	9.9823	10.0030	0.0206	0.0206
C5	C028	8.5009	8.5192	0.0183	0.0183
C6	C035	8.7364	8.7405	0.0041	0.0041
C7	C036	7.6210	7.6158	-0.0052	0.0052
C8	C039	6.4225	6.4812	0.0587	0.0587
C9	C044	5.8446	5.8409	-0.0037	0.0037
C10	C047	6.2275	6.2550	0.0275	0.0275
D1	D009	4.2316	3.8108	-0.4208	0.4208
D2	D010	3.2850	2.7280	-0.5570	0.5570
D3	D012	6.2831	6.0117	-0.2714	0.2714
D4	D013	8.6715	8.4678	-0.2038	0.2038
D5	D014	11.5113	11.4037	-0.1076	0.1076
D6	D021	2.6961	2.7015	0.0054	0.0054
D7	D022	-	-	-	-
D8	D028	1.3200	1.3148	-0.0052	0.0052

D9	D031	8.1646	8.1548	-0.0097	0.0097
D10	D037	5.7799	5.7848	0.0049	0.0049

Photogrammetry

Point		Center Point A006			
		Total Station (ft.)	Photogrammetry (ft.)	Discrepancy (ft.)	Abs. Discrepancy (ft.)
A1	A008	9.2192	9.2160	-0.0032	0.0032
A2	A013	8.6877	8.6936	0.0059	0.0059
A3	A016	7.9486	7.9459	-0.0028	0.0028
A4	A028	7.1416	7.1389	-0.0027	0.0027
A5	A047	5.6950	5.7072	0.0122	0.0122
A6	A053	6.2465	6.2520	0.0055	0.0055
A7	A062	4.9969	5.0004	0.0035	0.0035
A8	A064	2.7507	2.7528	0.0022	0.0022
A9	A066	-	-	-	-
A10	A070	5.5915	5.5928	0.0013	0.0013
B1	B007	6.3586	6.3802	0.0215	0.0215
B2	B008	5.1624	5.1634	0.0010	0.0010
B3	B009	4.1311	4.1278	-0.0032	0.0032
B4	B013	5.7681	5.7705	0.0024	0.0024
B5	B014	4.7240	4.7372	0.0133	0.0133
B6	B054	15.9217	15.9522	0.0305	0.0305
B7	B055	15.4597	15.4865	0.0268	0.0268
B8	B056	15.0932	15.1194	0.0262	0.0262
B9	B060	17.2370	17.2652	0.0283	0.0283
B10	B061	16.9467	16.9724	0.0257	0.0257
C1	C006	18.2621	18.2994	0.0373	0.0373
C2	C007	17.7650	17.8003	0.0352	0.0352
C3	C016	17.4456	17.4933	0.0477	0.0477
C4	C023	18.6121	18.6476	0.0355	0.0355
C5	C028	17.9069	18.0075	0.1007	0.1007
C6	C035	18.7102	18.7623	0.0521	0.0521
C7	C036	18.8418	18.8765	0.0346	0.0346
C8	C039	18.4843	18.0723	-0.4121	0.4121
C9	C044	19.4840	19.5203	0.0363	0.0363
C10	C047	19.0823	19.1105	0.0283	0.0283
D1	D009	18.1862	18.0573	-0.1289	0.1289
D2	D010	16.2082	16.0525	-0.1557	0.1557
D3	D012	13.0561	12.8657	-0.1903	0.1903
D4	D013	12.0830	11.8767	-0.2063	0.2063
D5	D014	11.2362	11.0550	-0.1813	0.1813
D6	D021	17.5161	17.5504	0.0344	0.0344
D7	D022	15.4417	15.4744	0.0327	0.0327
D8	D028	15.3131	15.3463	0.0332	0.0332

D9	D031	10.8326	10.8624	0.0297	0.0297
D10	D037	11.8780	11.9076	0.0296	0.0296
Point		**Center Point B013**			
		Total Station (ft.)	**Photogrammetry (ft.)**	**Discrepancy (ft.)**	**Abs. Discrepancy (ft.)**
A1	A008	11.9894	11.9814	-0.0079	0.0079
A2	A013	10.6325	10.6237	-0.0088	0.0088
A3	A016	11.0620	11.0463	-0.0157	0.0157
A4	A028	7.9992	7.9819	-0.0173	0.0173
A5	A047	5.7069	5.7106	0.0038	0.0038
A6	A053	4.5540	4.5515	-0.0025	0.0025
A7	A062	3.0644	3.0628	-0.0016	0.0016
A8	A064	3.6716	3.6678	-0.0038	0.0038
A9	A066	5.7681	5.7705	0.0024	0.0024
A10	A070	1.9142	1.9247	0.0104	0.0104
B1	B007	1.1963	1.2108	0.0145	0.0145
B2	B008	0.9304	0.9393	0.0089	0.0089
B3	B009	1.9571	1.9682	0.0111	0.0111
B4	B013	-	-	-	-
B5	B014	1.3350	1.3286	-0.0064	0.0064
B6	B054	12.6192	12.6461	0.0268	0.0268
B7	B055	12.5533	12.5760	0.0227	0.0227
B8	B056	12.6177	12.6381	0.0204	0.0204
B9	B060	14.1161	14.1386	0.0225	0.0225
B10	B061	14.0651	14.0876	0.0225	0.0225
C1	C006	15.3259	15.3566	0.0308	0.0308
C2	C007	15.1334	15.1647	0.0313	0.0313
C3	C016	15.7757	15.8193	0.0436	0.0436
C4	C023	16.4183	16.4509	0.0326	0.0326
C5	C028	16.5266	16.6310	0.1044	0.1044
C6	C035	16.9561	17.0032	0.0471	0.0471
C7	C036	17.5428	17.5730	0.0302	0.0302
C8	C039	18.1338	17.8306	-0.3032	0.3032
C9	C044	19.2514	19.2804	0.0291	0.0291
C10	C047	19.4652	19.4793	0.0141	0.0141
D1	D009	17.7503	17.7655	0.0152	0.0152
D2	D010	16.0333	16.0457	0.0124	0.0124
D3	D012	13.6089	13.6301	0.0211	0.0211
D4	D013	13.0702	13.0886	0.0184	0.0184
D5	D014	13.1154	13.1679	0.0525	0.0525
D6	D021	17.9423	17.9710	0.0287	0.0287
D7	D022	16.2485	16.2733	0.0248	0.0248
D8	D028	16.5111	16.5372	0.0261	0.0261
D9	D031	13.6347	13.6601	0.0254	0.0254

D10	D037	14.3744	14.3997	0.0254	0.0254
Point		**Center Point C035**			
		Total Station (ft.)	**Photogrammetry (ft.)**	**Discrepancy (ft.)**	**Abs. Discrepancy (ft.)**
A1	A008	17.8096	17.8272	0.0177	0.0177
A2	A013	17.3197	17.3368	0.0171	0.0171
A3	A016	17.7574	17.7722	0.0148	0.0148
A4	A028	17.0004	17.0297	0.0293	0.0293
A5	A047	17.1410	17.1931	0.0521	0.0521
A6	A053	17.3595	17.4153	0.0558	0.0558
A7	A062	17.7878	17.8435	0.0556	0.0556
A8	A064	18.0639	18.1250	0.0611	0.0611
A9	A066	18.7102	18.7623	0.0521	0.0521
A10	A070	18.5920	18.6513	0.0593	0.0593
B1	B007	17.5959	17.6477	0.0518	0.0518
B2	B008	17.7163	17.7744	0.0580	0.0580
B3	B009	17.9040	17.9615	0.0575	0.0575
B4	B013	16.9561	17.0032	0.0471	0.0471
B5	B014	17.1078	17.1614	0.0535	0.0535
B6	B054	8.1265	8.1414	0.0149	0.0149
B7	B055	8.2254	8.2446	0.0192	0.0192
B8	B056	8.5466	8.5705	0.0239	0.0239
B9	B060	7.7886	7.8048	0.0162	0.0162
B10	B061	7.8734	7.8784	0.0050	0.0050
C1	C006	5.5929	5.6146	0.0217	0.0217
C2	C007	6.1670	6.1918	0.0249	0.0249
C3	C016	3.9512	3.9614	0.0102	0.0102
C4	C023	1.5993	1.6032	0.0038	0.0038
C5	C028	2.1344	2.1376	0.0032	0.0032
C6	C035	-	-	-	-
C7	C036	1.5676	1.5661	-0.0015	0.0015
C8	C039	4.5495	5.2561	0.7066	0.7066
C9	C044	5.3005	5.2975	-0.0030	0.0030
C10	C047	7.1105	7.0914	-0.0191	0.0191
D1	D009	6.1335	6.2432	0.1097	0.1097
D2	D010	7.7808	7.8910	0.1102	0.1102
D3	D012	12.2380	12.3231	0.0851	0.0851
D4	D013	14.6831	14.7547	0.0716	0.0716
D5	D014	17.7998	17.8923	0.0925	0.0925
D6	D021	7.2780	7.2914	0.0134	0.0134
D7	D022	8.7364	8.7490	0.0126	0.0126
D8	D028	9.4242	9.4405	0.0164	0.0164
D9	D031	15.6378	15.6765	0.0386	0.0386

D10	D037	13.6870	13.7216	0.0345	0.0345
Point		**Center Point D022**			
		Total Station (ft.)	**Photogrammetry (ft.)**	**Discrepancy (ft.)**	**Abs. Discrepancy (ft.)**
A1	A008	11.3954	11.3997	0.0043	0.0043
A2	A013	11.7348	11.7429	0.0080	0.0080
A3	A016	11.5986	11.6051	0.0066	0.0066
A4	A028	12.7964	12.8179	0.0215	0.0215
A5	A047	13.9303	13.9643	0.0340	0.0340
A6	A053	15.0398	15.0779	0.0382	0.0382
A7	A062	15.7503	15.7866	0.0363	0.0363
A8	A064	15.4766	15.5209	0.0443	0.0443
A9	A066	15.4417	15.4744	0.0327	0.0327
A10	A070	17.3576	17.3936	0.0360	0.0360
B1	B007	16.8748	16.9115	0.0367	0.0367
B2	B008	16.6565	16.6916	0.0351	0.0351
B3	B009	16.5351	16.5692	0.0341	0.0341
B4	B013	16.2485	16.2733	0.0248	0.0248
B5	B014	16.0710	16.1081	0.0371	0.0371
B6	B054	13.9963	14.0047	0.0084	0.0084
B7	B055	13.6599	13.6695	0.0096	0.0096
B8	B056	13.4534	13.4676	0.0141	0.0141
B9	B060	14.3471	14.3580	0.0109	0.0109
B10	B061	14.1396	14.1391	-0.0004	0.0004
C1	C006	13.1059	13.1263	0.0204	0.0204
C2	C007	13.1014	13.1211	0.0197	0.0197
C3	C016	10.2230	10.2358	0.0128	0.0128
C4	C023	9.9823	9.9884	0.0060	0.0060
C5	C028	8.5009	8.5128	0.0119	0.0119
C6	C035	8.7364	8.7490	0.0126	0.0126
C7	C036	7.6210	7.6267	0.0057	0.0057
C8	C039	6.4225	7.2200	0.7975	0.7975
C9	C044	5.8446	5.8520	0.0074	0.0074
C10	C047	6.2275	6.2584	0.0309	0.0309
D1	D009	4.2316	3.8030	-0.4286	0.4286
D2	D010	3.2850	2.7046	-0.5804	0.5804
D3	D012	6.2831	6.0100	-0.2731	0.2731
D4	D013	8.6715	8.4785	-0.1930	0.1930
D5	D014	11.5113	11.4149	-0.0964	0.0964
D6	D021	2.6961	2.6948	-0.0013	0.0013
D7	D022	-	-	-	-
D8	D028	1.3200	1.3221	0.0021	0.0021
D9	D031	8.1646	8.1831	0.0185	0.0185

D10	D037	5.7799	5.7956	0.0157	0.0157

APPENDIX B

CASE STUDY: TEMPLE OF THE SEVEN DOLLS MERIDA, MEXICO

This sections includes the raw data that was collected during temple case study. The data is split into three sections according to the type of data. The first is section is for the actual raw data collected from each method. The second section is the discrepancies from the coordinate discrepancy method and the third contains the discrepancies from the distance discrepancy method.

RAW TOTAL STATION, LASER SCANNER, AND PHOTOGRAMMETRY DATA

Point		Easting (X)			Northing (Y)			Elevation (Z)		
		TS (ft.)	Laser (ft.)	Photo (ft.)	TS (ft.)	Laser (ft.)	Photo (ft.)	TS (ft.)	Laser (ft.)	Photo (ft.)
N1	N1	692.071	692.128	692.053	360.586	360.598	360.596	54.884	54.900	54.890
N2	N2	692.555	692.629	692.538	360.601	360.627	360.614	53.464	53.473	53.466
N3	N3	691.903	691.939	691.846	360.879	360.889	360.866	58.084	58.109	58.093
N4	N4	684.136	684.118	684.091	361.778	361.809	361.749	60.404	60.389	60.426
N5	N5	684.057	684.111	684.057	361.708	361.761	361.725	54.588	55.158	55.085
N6	N6	675.248	675.262	675.207	363.003	363.028	363.021	58.079	58.083	58.072
N7	N7	669.660	667.973	669.632	363.500	363.542	363.534	53.675	53.678	53.641
N8	N8	669.530	669.548	669.530	363.783	363.810	363.783	58.657	58.687	58.657
S1	S1	663.698	663.614	663.613	327.476	327.557	327.554	56.248	56.271	56.232
S2	S2	663.396	663.408	663.396	327.542	327.550	327.542	58.783	58.786	58.783
S3	S3	667.661	667.715	667.690	326.853	326.863	326.865	58.380	58.389	58.368
S4	S4	670.304	670.313	670.253	326.262	326.320	326.337	57.671	57.718	57.668
S5	S5	675.947	675.978	675.956	325.593	325.614	325.616	58.746	58.753	58.732
S6	S6	678.141	678.167	678.159	325.320	325.366	325.351	60.270	60.285	60.266
S7	S7	685.788	685.785	685.859	323.451	323.519	326.651	60.437	60.448	61.246
S8	S8	685.791	685.873	685.909	323.656	323.607	323.730	57.497	57.501	57.500
S9	S9	693.507	693.576	693.562	322.721	322.670	322.691	57.402	57.420	57.399
S10	S10	700.148	700.263	700.194	321.501	321.461	321.474	57.047	57.051	57.058
E1	E1	700.298	700.395	700.379	321.504	321.514	321.562	58.705	58.715	58.713
E2	E2	700.629	700.699	700.688	323.251	323.181	323.218	57.054	57.078	57.068
E3	E3	703.255	703.362	703.297	335.368	335.383	335.403	58.985	59.004	59.000
E4	E4	704.564	704.672	704.564	343.747	343.755	343.747	61.276	61.287	61.276
E5	E5	704.470	704.602	704.539	344.396	344.442	344.457	55.402	55.411	55.409
E6	E6	704.725	704.860	704.805	345.848	345.869	345.893	57.675	57.671	57.672
E7	E7	704.488	704.620	704.548	345.838	345.860	345.894	53.465	53.460	53.466

Point		Easting (X)			Northing (Y)			Elevation (Z)		
		TS (ft.)	Laser (ft.)	Photo (ft.)	TS (ft.)	Laser (ft.)	Photo (ft.)	TS (ft.)	Laser (ft.)	Photo (ft.)
E8	E8	705.462	705.591	705.516	351.873	351.886	351.926	54.505	54.512	54.515
E9	E9	713.295	713.446	713.416	360.883	360.906	360.971	48.547	48.540	48.564
E10	E10	715.038	715.175	715.136	360.675	360.716	360.756	46.482	46.503	46.508
E11	E11	717.248	717.394	717.352	361.018	361.031	361.103	43.402	43.419	43.424
E12	E12	706.290	706.423	706.339	368.145	368.130	368.162	46.210	46.223	46.234
W1	W1	669.480	669.456	669.414	363.308	363.256	363.285	54.437	54.445	54.421
W2	W2	669.413	669.056	669.020	362.381	362.343	362.350	58.707	58.708	58.677
W3	W3	667.683	667.662	667.611	354.485	354.420	354.475	57.348	57.357	57.307
W4	W4	666.948	666.937	666.889	349.674	349.619	349.684	53.892	53.903	53.877
W5	W5	666.726	666.722	666.675	349.373	349.331	349.385	59.258	59.294	59.226
W6	W6	665.041	665.036	665.017	338.826	338.808	338.839	57.750	57.789	57.733
W7	W7	664.186	664.208	664.180	333.613	333.621	333.638	56.130	56.150	56.116
W8	W8	663.637	663.642	663.637	330.378	330.354	330.377	57.473	57.511	57.473
W9	W9	663.308	663.311	663.298	327.695	327.659	327.672	55.040	55.059	55.031
W10	W10	663.271	663.274	663.263	327.720	327.679	327.701	58.264	58.307	58.258

COORDINATE DISCREPANCY DATA

Point	Total Station - Laser Scanner			Total Station - Photogrammetry		
	X	Y	Z	X	Y	Z
N1	0.0568	0.0118	0.0162	-0.0180	0.0094	0.0063
N2	0.0738	0.0260	0.0092	-0.0168	0.0126	0.0022
N3	0.0365	0.0103	0.0251	-0.0565	-0.0123	0.0096
N4	-0.0178	0.0307	-0.0152	-0.0447	-0.0290	0.0221
N5	0.0539	0.0527	0.5697	0.0000	0.0168	0.4964
N6	0.0137	0.0255	0.0038	-0.0416	0.0189	-0.0076
N7	-1.6870	0.0420	0.0030	-0.0277	0.0336	-0.0344
N8	0.0180	0.0267	0.0303	0.0000	0.0000	0.0000
AVG=	0.1957	0.0225	0.0673	0.0205	0.0133	0.0579
S1	-0.0835	0.0812	0.0235	-0.0849	0.0778	-0.0157
S2	0.0118	0.0083	0.0027	0.0000	0.0000	0.0000
S3	0.0542	0.0097	0.0090	0.0294	0.0118	-0.0116
S4	0.0088	0.0583	0.0472	-0.0513	0.0750	-0.0026
S5	0.0313	0.0215	0.0067	0.0098	0.0231	-0.0141
S6	0.0258	0.0456	0.0146	0.0180	0.0306	-0.0047
S7	-0.0031	0.0684	0.0111	0.0712	3.2000	0.8087
S8	0.0822	-0.0488	0.0043	0.1185	0.0737	0.0036
S9	0.0693	-0.0508	0.0183	0.0556	-0.0303	-0.0027
S10	0.1147	-0.0398	0.0043	0.0456	-0.0268	0.0110
AVG=	0.0485	0.0432	0.0142	0.0484	0.3549	0.0875
E1	0.0970	0.0105	0.0100	0.0808	0.0585	0.0077
E2	0.0698	-0.0698	0.0238	0.0584	-0.0333	0.0141
E3	0.1070	0.0151	0.0191	0.0422	0.0355	0.0152
E4	0.1082	0.0083	0.0106	0.0000	0.0000	0.0000
E5	0.1320	0.0457	0.0087	0.0692	0.0608	0.0070
E6	0.1350	0.0207	-0.0037	0.0801	0.0448	-0.0026
E7	0.1325	0.0225	-0.0050	0.0606	0.0562	0.0011
E8	0.1293	0.0127	0.0073	0.0547	0.0525	0.0101
E9	0.1510	0.0235	-0.0070	0.1208	0.0885	0.0174
E10	0.1375	0.0410	0.0210	0.0984	0.0806	0.0259
E11	0.1465	0.0135	0.0170	0.1047	0.0857	0.0221
E12	0.1330	-0.0150	0.0135	0.0494	0.0172	0.0245
AVG=	0.1232	0.0249	0.0122	0.0683	0.0511	0.0123
W1	-0.0236	-0.0519	0.0083	-0.0657	-0.0233	-0.0159
W2	-0.3569	-0.0378	0.0013	-0.3933	-0.0311	-0.0292
W3	-0.0209	-0.0650	0.0087	-0.0722	-0.0100	-0.0415

Point	Total Station - Laser Scanner			Total Station - Photogrammetry		
	X	Y	Z	X	Y	Z
W4	-0.0113	-0.0547	0.0113	-0.0595	0.0099	-0.0146
W5	-0.0040	-0.0415	0.0360	-0.0506	0.0127	-0.0319
W6	-0.0046	-0.0175	0.0393	-0.0232	0.0134	-0.0169
W7	0.0217	0.0085	0.0200	-0.0067	0.0258	-0.0143
W8	0.0047	-0.0235	0.0381	0.0000	0.0000	0.0000
W9	0.0029	-0.0356	0.0186	-0.0105	-0.0223	-0.0097
W10	0.0030	-0.0408	0.0433	-0.0085	-0.0189	-0.0054
AVG=	0.0454	0.0377	0.0225	0.0690	0.0167	0.0179
Total Average=	0.1032	0.0321	0.0290	0.0516	0.1090	0.0439

DISTANCE DISCREPANCY DATA

Laser Scanner

Point		Center Point N3			
		Total Station (ft.)	Laser Scanner (ft.)	Discrepancy (ft.)	Abs. Discrepancy (ft.)
N1	N1	3.218	3.228	0.010	0.010
N2	N2	4.674	4.694	0.020	0.020
N3	N3	-	-	-	-
N4	N4	8.156	8.198	0.043	0.043
N5	N5	8.629	8.411	-0.218	0.218
N6	N6	16.789	16.814	0.025	0.025
N7	N7	22.826	24.516	1.690	1.690
N8	N8	22.568	22.588	0.021	0.021
S1	S1	43.757	43.780	0.023	0.023
S2	S2	43.869	43.886	0.017	0.017
S3	S3	41.779	41.769	-0.010	0.010
S4	S4	40.804	40.778	-0.026	0.026
S5	S5	38.732	38.723	-0.008	0.008
S6	S6	38.191	38.161	-0.030	0.030
S7	S7	37.997	37.945	-0.052	0.052
S8	S8	37.726	37.777	0.051	0.051
S9	S9	38.198	38.260	0.063	0.063
S10	S10	40.245	40.311	0.066	0.066
E1	E1	40.265	40.277	0.012	0.012
E2	E2	38.640	38.726	0.086	0.086
E3	E3	27.937	27.961	0.024	0.024
E4	E4	21.541	21.582	0.042	0.042
E5	E5	20.900	20.932	0.032	0.032
E6	E6	19.761	19.818	0.057	0.057
E7	E7	20.148	20.206	0.058	0.058
E8	E8	16.666	16.744	0.078	0.078
E9	E9	23.422	23.540	0.118	0.118
E10	E10	25.882	25.974	0.092	0.092
E11	E11	29.291	29.390	0.099	0.099
E12	E12	20.020	20.087	0.067	0.067
W1	W1	22.847	22.902	0.055	0.055
W2	W2	22.548	22.937	0.389	0.389
W3	W3	25.060	25.135	0.075	0.075
W4	W4	27.674	27.745	0.072	0.072
W5	W5	27.706	27.765	0.059	0.059

W6	W6	34.757	34.806	0.049	0.049
W7	W7	38.929	38.941	0.012	0.012
W8	W8	41.589	41.635	0.046	0.046
W9	W9	43.910	43.967	0.057	0.057
W10	W10	43.810	43.871	0.061	0.061
Point		**Center Point S5**			
		Total Station (ft.)	**Laser Scanner (ft.)**	**Discrepancy (ft.)**	**Abs. Discrepancy (ft.)**
N1	N1	38.723	38.724	0.001	0.001
N2	N2	39.107	39.129	0.022	0.022
N3	N3	38.732	38.723	-0.008	0.008
N4	N4	37.138	37.135	-0.003	0.003
N5	N5	37.248	37.225	-0.023	0.023
N6	N6	37.422	37.427	0.004	0.004
N7	N7	38.758	39.094	0.336	0.336
N8	N8	38.726	38.733	0.007	0.007
S1	S1	12.642	12.759	0.117	0.117
S2	S2	12.701	12.718	0.017	0.017
S3	S3	8.389	8.365	-0.024	0.024
S4	S4	5.783	5.802	0.019	0.019
S5	S5	-	-	-	-
S6	S6	2.686	2.683	-0.002	0.002
S7	S7	10.213	10.171	-0.042	0.042
S8	S8	10.110	10.174	0.063	0.063
S9	S9	17.844	17.892	0.048	0.048
S10	S10	24.604	24.696	0.092	0.092
E1	E1	24.692	24.759	0.067	0.067
E2	E2	24.851	24.897	0.046	0.046
E3	E3	29.006	29.075	0.069	0.069
E4	E4	33.984	34.042	0.058	0.058
E5	E5	34.327	34.424	0.097	0.097
E6	E6	35.209	35.293	0.085	0.085
E7	E7	35.388	35.472	0.084	0.084
E8	E8	39.747	39.814	0.067	0.067
E9	E9	52.386	52.476	0.089	0.089
E10	E10	53.938	54.024	0.086	0.086
E11	E11	56.534	56.611	0.076	0.076
E12	E12	53.746	53.773	0.027	0.027
W1	W1	38.508	38.445	-0.063	0.063
W2	W2	37.364	37.376	0.012	0.012
W3	W3	30.084	30.015	-0.069	0.069
W4	W4	26.162	26.106	-0.056	0.056
W5	W5	25.510	25.465	-0.045	0.045
W6	W6	17.177	17.168	-0.009	0.009

W7	W7	14.473	14.471	-0.002	0.002
W8	W8	13.268	13.274	0.006	0.006
W9	W9	13.337	13.352	0.015	0.015
W10	W10	12.862	12.878	0.017	0.017

Point		**Center Point E4**			
		Total Station (ft.)	**Laser Scanner (ft.)**	**Discrepancy (ft.)**	**Abs. Discrepancy (ft.)**
N1	N1	21.920	21.951	0.030	0.030
N2	N2	22.120	22.153	0.033	0.033
N3	N3	21.541	21.582	0.042	0.042
N4	N4	27.262	27.372	0.110	0.110
N5	N5	28.069	28.010	-0.060	0.060
N6	N6	35.219	35.308	0.089	0.089
N7	N7	40.820	42.382	1.562	1.562
N8	N8	40.444	40.530	0.086	0.086
S1	S1	44.273	44.422	0.149	0.149
S2	S2	44.312	44.402	0.090	0.090
S3	S3	40.689	40.738	0.049	0.049
S4	S4	38.632	38.694	0.062	0.062
S5	S5	33.984	34.042	0.058	0.058
S6	S6	32.229	32.275	0.046	0.046
S7	S7	27.661	27.693	0.032	0.032
S8	S8	27.755	27.815	0.060	0.060
S9	S9	24.070	24.138	0.068	0.068
S10	S10	23.071	23.117	0.046	0.046
E1	E1	22.794	22.794	0.000	0.000
E2	E2	21.293	21.373	0.080	0.080
E3	E3	8.784	8.776	-0.008	0.008
E4	E4	-	-	-	-
E5	E5	5.911	5.916	0.006	0.006
E6	E6	4.173	4.193	0.020	0.020
E7	E7	8.087	8.105	0.019	0.019
E8	E8	10.616	10.623	0.007	0.007
E9	E9	23.063	23.100	0.037	0.037
E10	E10	24.802	24.831	0.028	0.028
E11	E11	27.904	27.921	0.016	0.016
E12	E12	28.728	28.708	-0.020	0.020
W1	W1	40.747	40.832	0.085	0.085
W2	W2	39.867	40.257	0.390	0.390
W3	W3	38.613	38.716	0.103	0.103
W4	W4	38.789	38.895	0.106	0.106
W5	W5	38.307	38.409	0.102	0.102
W6	W6	39.984	40.096	0.112	0.112
W7	W7	41.947	42.029	0.082	0.082

W8	W8	43.222	43.328	0.105	0.105
W9	W9	44.706	44.817	0.112	0.112
W10	W10	44.396	44.510	0.113	0.113
Point		**Center Point W8**			
		Total Station (ft.)	**Laser Scanner (ft.)**	**Discrepancy (ft.)**	**Abs. Discrepancy (ft.)**
N1	N1	41.566	41.629	0.063	0.063
N2	N2	42.021	42.107	0.086	0.086
N3	N3	41.589	41.635	0.046	0.046
N4	N4	37.614	37.643	0.029	0.029
N5	N5	37.509	37.562	0.053	0.053
N6	N6	34.635	34.683	0.049	0.049
N7	N7	33.879	33.688	-0.191	0.191
N8	N8	33.942	33.994	0.051	0.051
S1	S1	3.150	3.060	-0.091	0.091
S2	S2	3.133	3.089	-0.044	0.044
S3	S3	5.425	5.436	0.011	0.011
S4	S4	7.838	7.799	-0.039	0.039
S5	S5	13.268	13.274	0.006	0.006
S6	S6	15.613	15.606	-0.007	0.007
S7	S7	23.397	23.359	-0.038	0.038
S8	S8	23.151	23.232	0.081	0.081
S9	S9	30.835	30.905	0.069	0.069
S10	S10	37.577	37.688	0.111	0.111
E1	E1	37.740	37.820	0.081	0.081
E2	E2	37.674	37.747	0.073	0.073
E3	E3	39.959	40.065	0.106	0.106
E4	E4	43.222	43.328	0.105	0.105
E5	E5	43.222	43.366	0.144	0.144
E6	E6	43.904	44.042	0.137	0.137
E7	E7	43.861	44.000	0.139	0.139
E8	E8	47.119	47.248	0.129	0.129
E9	E9	58.959	59.113	0.154	0.154
E10	E10	60.669	60.817	0.148	0.148
E11	E11	63.331	63.474	0.143	0.143
E12	E12	58.073	58.178	0.105	0.105
W1	W1	33.582	33.552	-0.030	0.030
W2	W2	32.544	32.466	-0.078	0.078
W3	W3	24.445	24.400	-0.045	0.045
W4	W4	19.903	19.875	-0.028	0.028
W5	W5	19.327	19.308	-0.019	0.019
W6	W6	8.568	8.573	0.004	0.004
W7	W7	3.545	3.584	0.039	0.039
W8	W8	-	-	-	-

W9	W9	3.636	3.659	0.022	0.022
W10	W10	2.797	2.815	0.018	0.018

Photogrammetry

Point		Center Point N3			
		Total Station (ft.)	photogrammetry (ft.)	Discrepancy (ft.)	Abs. Discrepancy (ft.)
N1	N1	3.218	3.222	0.004	0.004
N2	N2	4.674	4.686	0.012	0.012
N3	N3	-	-	-	-
N4	N4	8.156	8.146	-0.010	0.010
N5	N5	8.629	8.394	-0.235	0.235
N6	N6	16.789	16.778	-0.011	0.011
N7	N7	22.826	22.812	-0.014	0.014
N8	N8	22.568	22.513	-0.055	0.055
S1	S1	43.757	43.707	-0.049	0.049
S2	S2	43.869	43.822	-0.046	0.046
S3	S3	41.779	41.709	-0.070	0.070
S4	S4	40.804	40.728	-0.077	0.077
S5	S5	38.732	38.672	-0.060	0.060
S6	S6	38.191	38.123	-0.068	0.068
S7	S7	37.997	34.878	-3.119	3.119
S8	S8	37.726	37.613	-0.113	0.113
S9	S9	38.198	38.221	0.023	0.023
S10	S10	40.245	40.281	0.035	0.035
E1	E1	40.265	40.225	-0.040	0.040
E2	E2	38.640	38.687	0.046	0.046
E3	E3	27.937	27.934	-0.003	0.003
E4	E4	21.541	21.563	0.022	0.022
E5	E5	20.900	20.919	0.019	0.019
E6	E6	19.761	19.807	0.046	0.046
E7	E7	20.148	20.173	0.024	0.024
E8	E8	16.666	16.722	0.056	0.056
E9	E9	23.422	23.581	0.159	0.159
E10	E10	25.882	26.013	0.131	0.131
E11	E11	29.291	29.425	0.134	0.134
E12	E12	20.020	20.098	0.078	0.078
W1	W1	22.847	22.859	0.012	0.012
W2	W2	22.548	22.882	0.334	0.334
W3	W3	25.060	25.076	0.016	0.016
W4	W4	27.674	27.671	-0.003	0.003
W5	W5	27.706	27.689	-0.018	0.018
W6	W6	34.757	34.715	-0.042	0.042
W7	W7	38.929	38.868	-0.061	0.061
W8	W8	41.589	41.541	-0.047	0.047

W9	W9	43.910	43.889	-0.021	0.021
W10	W10	43.810	43.784	-0.026	0.026
Point		**Center Point S5**			
		Total Station (ft.)	**photogrammetry (ft.)**	**Discrepancy (ft.)**	**Abs. Discrepancy (ft.)**
N1	N1	38.723	38.697	-0.026	0.026
N2	N2	39.107	39.084	-0.023	0.023
N3	N3	38.732	38.672	-0.060	0.060
N4	N4	37.138	37.077	-0.061	0.061
N5	N5	37.248	37.186	-0.062	0.062
N6	N6	37.422	37.419	-0.003	0.003
N7	N7	38.758	38.777	0.019	0.019
N8	N8	38.726	38.705	-0.021	0.021
S1	S1	12.642	12.743	0.100	0.100
S2	S2	12.701	12.707	0.006	0.006
S3	S3	8.389	8.368	-0.021	0.021
S4	S4	5.783	5.847	0.064	0.064
S5	S5	-	-	-	-
S6	S6	2.686	2.697	0.011	0.011
S7	S7	10.213	10.269	0.056	0.056
S8	S8	10.110	10.205	0.094	0.094
S9	S9	17.844	17.897	0.053	0.053
S10	S10	24.604	24.646	0.042	0.042
E1	E1	24.692	24.757	0.064	0.064
E2	E2	24.851	24.903	0.052	0.052
E3	E3	29.006	29.041	0.035	0.035
E4	E4	33.984	33.964	-0.020	0.020
E5	E5	34.327	34.395	0.068	0.068
E6	E6	35.209	35.278	0.070	0.070
E7	E7	35.388	35.446	0.058	0.058
E8	E8	39.747	39.797	0.050	0.050
E9	E9	52.386	52.503	0.117	0.117
E10	E10	53.938	54.030	0.093	0.093
E11	E11	56.534	56.633	0.099	0.099
E12	E12	53.746	53.754	0.009	0.009
W1	W1	38.508	38.475	-0.033	0.033
W2	W2	37.364	37.383	0.019	0.019
W3	W3	30.084	30.076	-0.008	0.008
W4	W4	26.162	26.174	0.012	0.012
W5	W5	25.510	25.522	0.012	0.012
W6	W6	17.177	17.191	0.014	0.014
W7	W7	14.473	14.488	0.015	0.015
W8	W8	13.268	13.267	-0.001	0.001
W9	W9	13.337	13.348	0.011	0.011

W10	W10	12.862	12.873	0.011	0.011

Point		Center Point E4			
		Total Station (ft.)	photogrammetry (ft.)	Discrepancy (ft.)	Abs. Discrepancy (ft.)
N1	N1	21.920	21.936	0.016	0.016
N2	N2	22.120	22.138	0.018	0.018
N3	N3	21.541	21.563	0.022	0.022
N4	N4	27.262	27.275	0.014	0.014
N5	N5	28.069	27.966	-0.103	0.103
N6	N6	35.219	35.265	0.046	0.046
N7	N7	40.820	40.866	0.046	0.046
N8	N8	40.444	40.444	0.000	0.000
S1	S1	44.273	44.325	0.052	0.052
S2	S2	44.312	44.312	0.000	0.000
S3	S3	40.689	40.658	-0.031	0.031
S4	S4	38.632	38.644	0.012	0.012
S5	S5	33.984	33.964	-0.020	0.020
S6	S6	32.229	32.197	-0.032	0.032
S7	S7	27.661	25.340	-2.321	2.321
S8	S8	27.755	27.621	-0.134	0.134
S9	S9	24.070	24.071	0.001	0.001
S10	S10	23.071	23.086	0.015	0.015
E1	E1	22.794	22.721	-0.073	0.073
E2	E2	21.293	21.311	0.019	0.019
E3	E3	8.784	8.740	-0.044	0.044
E4	E4	-	-	-	-
E5	E5	5.911	5.910	-0.001	0.001
E6	E6	4.173	4.202	0.029	0.029
E7	E7	8.087	8.100	0.013	0.013
E8	E8	10.616	10.655	0.039	0.039
E9	E9	23.063	23.165	0.102	0.102
E10	E10	24.802	24.883	0.081	0.081
E11	E11	27.904	27.991	0.087	0.087
E12	E12	28.728	28.732	0.005	0.005
W1	W1	40.747	40.795	0.048	0.048
W2	W2	39.867	40.202	0.335	0.335
W3	W3	38.613	38.683	0.070	0.070
W4	W4	38.789	38.851	0.062	0.062
W5	W5	38.307	38.360	0.054	0.054
W6	W6	39.984	40.007	0.023	0.023
W7	W7	41.947	41.949	0.002	0.002
W8	W8	43.222	43.222	0.000	0.000
W9	W9	44.706	44.725	0.019	0.019
W10	W10	44.396	44.411	0.015	0.015

Point		Center Point W8			
		Total Station (ft.)	photogrammetry (ft.)	Discrepancy (ft.)	Abs. Discrepancy (ft.)
N1	N1	41.566	41.561	-0.006	0.006
N2	N2	42.021	42.019	-0.003	0.003
N3	N3	41.589	41.541	-0.047	0.047
N4	N4	37.614	37.567	-0.047	0.047
N5	N5	37.509	37.488	-0.021	0.021
N6	N6	34.635	34.639	0.004	0.004
N7	N7	33.879	33.911	0.032	0.032
N8	N8	33.942	33.942	0.000	0.000
S1	S1	3.150	3.085	-0.066	0.066
S2	S2	3.133	3.133	0.000	0.000
S3	S3	5.425	5.437	0.012	0.012
S4	S4	7.838	7.755	-0.083	0.083
S5	S5	13.268	13.267	-0.001	0.001
S6	S6	15.613	15.619	0.006	0.006
S7	S7	23.397	22.846	-0.551	0.551
S8	S8	23.151	23.243	0.092	0.092
S9	S9	30.835	30.897	0.061	0.061
S10	S10	37.577	37.628	0.050	0.050
E1	E1	37.740	37.805	0.065	0.065
E2	E2	37.674	37.738	0.063	0.063
E3	E3	39.959	40.006	0.047	0.047
E4	E4	43.222	43.222	0.000	0.000
E5	E5	43.222	43.307	0.085	0.085
E6	E6	43.904	43.995	0.091	0.091
E7	E7	43.861	43.937	0.076	0.076
E8	E8	47.119	47.190	0.072	0.072
E9	E9	58.959	59.104	0.145	0.145
E10	E10	60.669	60.788	0.119	0.119
E11	E11	63.331	63.456	0.125	0.125
E12	E12	58.073	58.116	0.043	0.043
W1	W1	33.582	33.549	-0.033	0.033
W2	W2	32.544	32.444	-0.099	0.099
W3	W3	24.445	24.423	-0.021	0.021
W4	W4	19.903	19.906	0.002	0.002
W5	W5	19.327	19.329	0.002	0.002
W6	W6	8.568	8.577	0.009	0.009
W7	W7	3.545	3.573	0.028	0.028
W8	W8	-	-	-	-
W9	W9	3.636	3.660	0.024	0.024
W10	W10	2.797	2.815	0.018	0.018

APPENDIX C

CASE STUDY: ZACH S. HENDERSON LIBRARY TERRACE

This sections includes the raw data that was collected during Recreation Activity Center storage building case study. The data is split into three sections according to the type of data. The first is section is for the actual raw data collected from each method. The second section is the discrepancies from the coordinate discrepancy method and the third contains the discrepancies from the distance discrepancy method.

RAW TOTAL STATION, LASER SCANNER, AND PHOTOGRAMMETRY DATA

Point		Easting (X)			Northing (Y)			Elevation (Z)		
		TS (ft.)	Laser (ft.)	Photo (ft.)	TS (ft.)	Laser (ft.)	Photo (ft.)	TS (ft.)	Laser (ft.)	Photo (ft.)
A1	A001	135.605		135.606	342.685		342.715	992.010		992.016
A2	A002	141.805	141.895	141.773	340.005	340.056	340.035	992.150	992.176	992.121
A3	A003	146.805	146.919	146.809	336.000	336.002	335.996	992.340	992.379	992.268
A4	A004	149.570	149.660	149.567	332.695	332.673	332.667	992.505	992.553	992.428
A5	A005	151.490		151.485	328.315		328.305	992.665		992.578
A6	A006	153.265	153.370	153.291	320.465	320.488	320.463	992.875	992.918	992.748
A7	A007	155.800	155.926	155.796	310.420	310.454	310.183	993.045	993.103	992.947
A8	A008	158.650		158.424	302.220		302.252	993.275		993.278
A9	A009	161.750		161.833	296.920		296.971	993.425		993.446
A10	A010	165.335		165.395	288.905		288.807	993.610		993.665
A11	A011	165.220	165.338	165.264	283.905	283.858	283.823	993.450	993.497	993.417
A12	A012	163.100	163.217	163.138	279.980	280.097	280.051	993.215	993.262	993.185
A13	A013	159.225	159.342	159.250	274.595	274.714	274.644	992.820	992.855	992.812
A14	A014	158.310	158.402	158.337	272.305	272.464	272.405	992.730	992.779	992.726
A15	A015	158.295	158.397	158.375	269.415	269.548	269.508	992.690	992.728	992.663
A16	A016	159.235	159.360	159.287	267.105	267.268	267.175	992.695	992.743	992.685
A17	A017	161.655	161.778	161.671	262.160	262.293	262.230	992.790	992.850	992.787
A18	A018	165.890		165.897	252.965		253.056	993.180		993.161
A19	A019	168.125	168.223	168.133	244.535	244.699	244.672	993.345	993.398	993.314
A20	A020	168.870		168.905	238.710		238.808	993.420		993.383
A21	A021	169.222			238.730			993.395		
B1	B001	135.465		135.229	346.875		346.992	997.775		997.680

Point		Easting (X)			Northing (Y)			Elevation (Z)		
		TS (ft.)	Laser (ft.)	Photo (ft.)	TS (ft.)	Laser (ft.)	Photo (ft.)	TS (ft.)	Laser (ft.)	Photo (ft.)
B2	B002	141.330	141.330	141.239	347.425	347.504	347.528	997.780	997.798	997.704
B3	B003	145.750		145.864	346.670		346.572	997.745		997.707
B4	B004	166.680	166.717	166.675	337.905	337.906	337.891	997.800	997.787	997.700
B5	B005	169.315	169.302	169.249	336.460	336.489	336.494	997.815	997.822	997.726
B6	B006	179.420	179.436	179.415	327.700	327.750	327.751	997.830	997.821	997.733
B7	B007	181.060	181.060	181.023	324.550	324.647	324.620	997.865	997.858	997.769
B8	B008	201.805		201.831	256.845		256.990	997.865		997.797
B9	B009	202.460		202.444	254.895		255.101	997.200		997.133
C1	C001	134.580	134.668	134.576	352.560	352.538	352.529	999.900	999.903	999.879
C2	C002	146.585	146.677	146.570	353.845	353.819	353.832	999.945	999.952	999.903
C3	C003	152.160	152.177	152.108	353.200	353.137	353.176	999.925	999.966	999.914
C4	C004	170.400	170.455	170.394	345.295	345.299	345.299	999.940	999.978	999.908
C5	C005	172.790	172.819	172.793	343.710	343.720	343.715	999.945	999.993	999.927
C6	C006	187.605	187.613	187.588	330.910	330.960	330.941	999.980	1000.006	999.954
C7	C007	189.515	189.557	189.508	328.225	328.265	328.234	999.970	1000.031	999.962
C8	C008	203.710		203.699	288.445		288.507	1000.015		1000.027
C9	C009	204.425	204.337	204.405	286.285	286.414	286.326	999.360	999.404	999.373
C10	C010	206.895	206.899	206.906	279.155	279.370	279.240	999.390	999.422	999.376
C11	C011	-			-			-		
C12	C012	209.085			272.685			998.710		
D1	D001	134.820	134.817	134.724	358.155	358.168	358.203	1001.540	1001.573	1001.540
D2	D002	154.250		154.162	360.315		360.413	1001.560		1001.545
D3	D003	156.865	156.845	156.781	359.760	359.980	359.839	1001.575	1001.600	1001.555
D4	D004	174.665	174.628	174.588	351.620	351.697	351.710	1001.595	1001.621	1001.557
D5	D005	177.550	177.505	177.475	350.115	350.182	350.202	1001.585	1001.621	1001.559
D6	D006	193.320	193.284	193.287	336.380	336.499	336.482	1001.590	1001.610	1001.546
D7	D007	196.115	196.141	196.078	332.695	332.828	332.803	1001.585	1001.604	1001.539
D8	D008	207.730		206.340	303.325		308.338	1001.570		1001.506
D9	D009	208.600		208.595	301.010		301.056	1000.895		1000.878
D10	D010	211.915	211.887	211.881	292.705	292.730	292.635	1000.875	1000.913	1000.859
E1	E001	134.085	134.093	134.010	363.805	364.016	363.829	1002.935	1002.968	1002.954
E2	E002	157.985	158.003	157.959	366.550	366.575	366.612	1003.030	1003.072	1003.026
E3	E003	161.960		161.901	366.050		366.089	1003.035		1003.028
E4	E004	183.821		183.789	355.445		355.487	1003.030		1003.011
E5	E005	193.995		193.918	346.510		346.505	1002.995		1002.980
E6	E006	195.840	195.833	195.825	344.805	344.765	344.814	1002.335	1002.367	1002.307
E7	E007	203.765	203.739	203.734	337.865	337.843	337.879	1002.385	1002.419	1002.347
E8	E008	206.095	206.085	206.105	334.190	334.140	334.227	1002.390	1002.420	1002.346
E9	E009	213.220	213.220	213.193	319.200	318.964	319.212	1002.390	1002.405	1002.343
F1	F001	133.455	133.532	133.432	369.630	369.545	369.595	1005.915	1005.944	1005.924
F2	F002	139.425	139.510	139.414	370.305	370.267	370.302	1005.925	1005.984	1005.943

Point		Easting (X)			Northing (Y)			Elevation (Z)		
		TS (ft.)	Laser (ft.)	Photo (ft.)	TS (ft.)	Laser (ft.)	Photo (ft.)	TS (ft.)	Laser (ft.)	Photo (ft.)
F3	F003	141.630	141.719	141.643	370.510	370.434	370.436	1005.285	1005.332	1005.305
F4	F004	156.650	156.672	156.619	371.905	371.889	371.965	1005.355	1005.406	1005.368
F5	F005	158.835	158.837	158.786	372.215	372.171	372.234	1004.710	1004.799	1004.705
F6	F006	163.335		163.268	372.690		372.734	1004.705		1004.700
F7	F007	167.500		167.453	372.190		372.209	1004.700		1004.699
F8	F008	173.955	173.990	173.917	368.995	368.960	368.990	1004.045	1004.083	1004.033
F9	F009	181.435	181.394	181.344	365.335	365.308	365.327	1003.380	1003.411	1003.358
F10	F010	226.630			281.080			1001.330		
F11	F011	233.315			275.555			997.615		
F12	F012	232.085			243.410			997.320		
F13	F013	211.830			243.410			995.375		
F14	F014	206.180			230.225			994.070		

COORDINATE DISCREPANCY DATA

Point	Total Station - Laser Scanner			Total Station - Photogrammetry		
	X	Y	Z	X	Y	Z
A1	0.0903	0.0511	0.0255	-0.0319	0.0297	-0.0292
A2	0.0904	-0.0216	0.0482	-0.0025	-0.0284	-0.0771
A3	0.1054	0.0225	0.0433	0.0255	-0.0022	-0.1274
A4	0.1183	-0.0472	0.0473	0.0435	-0.0822	-0.0328
A5	0.1170	0.1188	0.0350	0.0247	0.0491	-0.0084
A6	0.1017	0.1329	0.0380	0.0795	0.0935	-0.0272
A7	0.1232	0.1326	0.0595	0.0158	0.0702	-0.0034
A8	0.0980	0.1642	0.0528	0.0083	0.1365	-0.0314
A9	0.0004	0.0793	0.0178	-0.0911	0.1032	-0.0765
A10	0.0366	0.0009	-0.0132	-0.0050	-0.0137	-0.1004
AVG=	0.0881	0.0771	0.0381	0.0328	0.0609	0.0514
B1	-0.0128	0.0295	0.0068	-0.0665	0.0339	-0.0887
B2	0.0160	0.0499	-0.0095	-0.0054	0.0514	-0.0975
B3	-0.0005	0.0967	-0.0073	-0.0374	0.0704	-0.0959
B4	0.0878	-0.0218	0.0030	-0.0041	-0.0315	-0.0208
B5	0.0922	-0.0261	0.0074	-0.0154	-0.0125	-0.0417
B6	0.0172	-0.0634	0.0408	-0.0516	-0.0241	-0.0111
B7	0.0290	0.0099	0.0482	0.0028	0.0052	-0.0179
B8	0.0083	0.0499	0.0256	-0.0171	0.0314	-0.0256
B9	0.0419	0.0403	0.0612	-0.0067	0.0089	-0.0077
B10	0.0036	0.2152	0.0321	0.0114	0.0854	-0.0144
AVG=	0.0309	0.0603	0.0242	0.0218	0.0355	0.0421
C1	-0.0258	-0.0222	0.0344	-0.0306	0.0141	-0.0377
C2	-0.0101	-0.0496	0.0300	0.0102	0.0369	-0.0443
C3	0.0004	-0.2362	0.0154	-0.0265	0.0116	-0.0466
C4	0.0772	-0.0852	0.0294	-0.0227	-0.0352	0.0088
C5	0.0850	-0.0379	0.0586	-0.0109	-0.0033	0.0180
C6	0.0887	-0.0761	0.0467	0.0134	-0.0736	0.0204
C7	0.0224	-0.0161	0.0507	-0.0307	0.0600	0.0128
C8	0.0018	-0.0444	0.0889	-0.0490	0.0189	-0.0050
C9	0.0349	-0.0352	0.0382	-0.0383	-0.0052	-0.0118
C10	-0.0405	-0.0274	0.0305	-0.0912	-0.0080	-0.0222
AVG=	0.0387	0.0630	0.0423	0.0324	0.0267	0.0228
D1	-0.0027	0.0135	0.0332	-0.0964	0.0476	0.0001
D2	-0.0196	0.2203	0.0248	-0.0840	0.0786	-0.0201
D3	-0.0367	0.0766	0.0255	-0.0773	0.0899	-0.0384
D4	-0.0445	0.0667	0.0364	-0.0745	0.0865	-0.0262

Point	Total Station - Laser Scanner			Total Station - Photogrammetry		
	X	Y	Z	X	Y	Z
D5	-0.0362	0.1189	0.0201	-0.0334	0.1025	-0.0436
D6	0.0261	0.1328	0.0191	-0.0370	0.1081	-0.0460
D7	-0.0282	0.0246	0.0382	-0.0339	-0.0696	-0.0164
D8	0.0079	0.2114	0.0334	-0.0753	0.0238	0.0186
D9	0.0184	0.0249	0.0422	-0.0255	0.0618	-0.0044
D10	-0.0075	-0.0401	0.0316	-0.0151	0.0091	-0.0284
AVG=	0.0228	0.0930	0.0304	0.0553	0.0678	0.0242
Total Average=	0.0451	0.0733	0.0337	0.0356	0.0477	0.0351

DISTANCE DISCREPANCY DATA

Laser Scanner

Point		Center Point A011			
		Total Station (ft.)	Laser Scanner (ft.)	Discrepancy (ft.)	Abs. Discrepancy (ft.)
A1	A002	60.8043	60.9062	0.1019	0.1019
A2	A019	39.4772	39.2648	-0.2124	0.2124
A3	B002	68.0020	68.1598	0.1578	0.1578
A4	B007	43.8453	43.9307	0.0853	0.0853
A5	C001	75.4581	75.4898	0.0317	0.0317
A6	C010	42.3633	42.2197	-0.1437	0.1437
A7	D001	80.6391	80.7393	0.1001	0.1001
A8	D010	48.0936	47.9632	-0.1303	0.1303
A9	E001	86.2749	86.5528	0.2778	0.2778
A10	F001	92.2668	92.2433	-0.0236	0.0236
B1	A006	38.4693	38.5396	0.0704	0.0704
B2	A011	-	-	-	-
B3	B004	54.1946	54.2356	0.0410	0.0410
B4	B005	52.8947	52.9576	0.0629	0.0629
B5	C006	52.4709	52.5085	0.0376	0.0376
B6	D005	67.8378	67.9184	0.0805	0.0805
B7	E006	68.7411	68.6895	-0.0516	0.0516
B8	E009	60.2467	60.0374	-0.2093	0.2093
B9	F003	90.5372	90.5172	-0.0200	0.0200
B10	F009	83.6204	83.6071	-0.0134	0.0134
C1	A004	51.2472	51.1983	-0.0490	0.0490
C2	A013	11.0911	10.9263	-0.1648	0.1648
C3	A017	22.0452	21.8930	-0.1522	0.1522
C4	C002	72.6708	72.6228	-0.0480	0.0480
C5	C007	50.9610	51.0238	0.0628	0.0628
C6	D004	68.8540	68.9273	0.0734	0.0734
C7	D006	60.0791	60.1688	0.0897	0.0897
C8	E007	66.9121	66.8840	-0.0281	0.0281
C9	E004	89.2142	89.2029	-0.0113	0.0113
C10	F008	86.1908	86.1644	-0.0265	0.0265
D1	A015	16.0777	15.9233	-0.1545	0.1545
D2	B006	46.2474	46.3029	0.0554	0.0554
D3	C003	70.8116	70.8139	0.0023	0.0023
D4	C005	60.6311	60.6765	0.0454	0.0454
D5	D003	76.7450	77.0222	0.2771	0.2771

D6	D007	58.3193	58.4174	0.0981	0.0981
D7	E002	83.5124	83.5919	0.0795	0.0795
D8	E008	65.4161	65.3318	-0.0843	0.0843
D9	F002	91.0273	91.0471	0.0198	0.0198
D10	F005	89.2536	89.2701	0.0164	0.0164
Point		**Center Point B007**			
		Total Station (ft.)	**Laser Scanner (ft.)**	**Discrepancy (ft.)**	**Abs. Discrepancy (ft.)**
A1	A002	42.5732	42.4685	-0.1047	0.1047
A2	A019	81.1797	81.0942	-0.0855	0.0855
A3	B002	45.8448	45.8354	-0.0094	0.0094
A4	B007	-	-	-	-
A5	C001	54.3055	54.1693	-0.1363	0.1363
A6	C010	52.2540	52.1542	-0.0998	0.0998
A7	D001	57.2795	57.2351	-0.0444	0.0444
A8	D010	44.4432	44.4787	0.0356	0.0356
A9	E001	61.4273	61.4976	0.0703	0.0703
A10	F001	66.0549	65.8793	-0.1756	0.1756
B1	A006	28.5333	28.4321	-0.1012	0.1012
B2	A011	43.8453	43.9307	0.0853	0.0853
B3	B004	19.6251	19.5329	-0.0922	0.0922
B4	B005	16.7271	16.6879	-0.0391	0.0391
B5	C006	9.3680	9.3500	-0.0180	0.0180
B6	D005	26.0716	26.0544	-0.0171	0.0171
B7	E006	25.4695	25.3636	-0.1058	0.1058
B8	E009	32.9145	32.9742	0.0597	0.0597
B9	F003	61.0090	60.8279	-0.1811	0.1811
B10	F009	41.1579	41.0397	-0.1182	0.1182
C1	A004	32.9650	32.8655	-0.0995	0.0995
C2	A013	54.7514	54.5932	-0.1582	0.1582
C3	A017	65.5349	65.3676	-0.1673	0.1673
C4	C002	45.2885	45.2018	-0.0867	0.0867
C5	C007	9.4564	9.5233	0.0668	0.0668
C6	D004	28.0641	28.1498	0.0857	0.0857
C7	D006	17.4394	17.4992	0.0598	0.0598
C8	E007	26.7065	26.6794	-0.0271	0.0271
C9	E004	53.8000	53.7828	-0.0173	0.0173
C10	F008	45.4316	45.3969	-0.0347	0.0347
D1	A015	59.8740	59.7980	-0.0760	0.0760
D2	B006	3.5515	3.5025	-0.0491	0.0491
D3	C003	40.7465	40.6240	-0.1225	0.1225
D4	C005	20.9720	20.8867	-0.0853	0.0853
D5	D003	42.8825	42.9976	0.1151	0.1151
D6	D007	17.5166	17.5618	0.0452	0.0452

D7	E002	48.1989	48.1326	-0.0663	0.0663
D8	E008	27.2058	27.1517	-0.0541	0.0541
D9	F002	62.3856	62.2384	-0.1472	0.1472
D10	F005	53.0354	52.9202	-0.1152	0.1152
Point		**Center Point D003**			
		Total Station (ft.)	**Laser Scanner (ft.)**	**Discrepancy (ft.)**	**Abs. Discrepancy (ft.)**
A1	A002	26.5687	26.6326	0.0640	0.0640
A2	A019	116.0660	116.1312	0.0651	0.0651
A3	B002	20.1963	20.2688	0.0725	0.0725
A4	B007	42.8825	42.9976	0.1151	0.1151
A5	C001	23.4791	23.4545	-0.0246	0.0246
A6	C010	94.8944	94.9107	0.0164	0.0164
A7	D001	22.1034	22.1025	-0.0009	0.0009
A8	D010	86.7604	86.9061	0.1458	0.1458
A9	E001	23.1763	23.1482	-0.0281	0.0281
A10	F001	25.7736	25.5707	-0.2029	0.2029
B1	A006	40.4073	40.5848	0.1775	0.1775
B2	A011	76.7450	77.0222	0.2771	0.2771
B3	B004	24.2534	24.4797	0.2264	0.2264
B4	B005	26.6839	26.8563	0.1725	0.1725
B5	C006	42.1878	42.3248	0.1370	0.1370
B6	D005	22.8231	22.8659	0.0428	0.0428
B7	E006	41.7526	41.8579	0.1053	0.1053
B8	E009	69.4382	69.7219	0.2837	0.2837
B9	F003	19.0114	18.7623	-0.2491	0.2491
B10	F009	25.2591	25.1856	-0.0736	0.0736
C1	A004	29.4618	29.4445	-0.0172	0.0172
C2	A013	85.6463	85.5280	-0.1184	0.1184
C3	A017	98.1116	97.9805	-0.1311	0.1311
C4	C002	11.9717	11.9047	-0.0671	0.0671
C5	C007	45.4209	45.4209	0.0000	0.0000
C6	D004	19.5729	19.5078	-0.0651	0.0651
C7	D006	43.3081	43.2135	-0.0946	0.0946
C8	E007	51.7654	51.7520	-0.0134	0.0134
C9	E004	12.7215	12.7209	-0.0006	0.0006
C10	F008	19.5820	19.6008	0.0188	0.0188
D1	A015	90.7921	90.8798	0.0877	0.0877
D2	B006	39.3776	39.5400	0.1624	0.1624
D3	C003	8.2397	8.4439	0.2041	0.2041
D4	C005	22.6686	22.8503	0.1817	0.1817
D5	D003	-	-	-	-
D6	D007	47.6768	47.7641	0.0873	0.0873
D7	E002	7.0339	6.8555	-0.1784	0.1784

D8	E008	55.4805	55.6138	0.1334	0.1334
D9	F002	20.8392	20.6290	-0.2103	0.2103
D10	F005	12.9937	12.7594	-0.2343	0.2343
Point		**Center Point E007**			
		Total Station (ft.)	**Laser Scanner (ft.)**	**Discrepancy (ft.)**	**Abs. Discrepancy (ft.)**
A1	A002	62.8361	62.7256	-0.1105	0.1105
A2	A019	100.3116	100.0926	-0.2190	0.2190
A3	B002	63.3303	63.3212	-0.0092	0.0092
A4	B007	26.7065	26.6330	-0.0735	0.0735
A5	C001	70.7720	70.6622	-0.1099	0.1099
A6	C010	58.8696	58.6346	-0.2350	0.2350
A7	D001	71.8736	71.8615	-0.0121	0.0121
A8	D010	45.9144	45.8678	-0.0466	0.0466
A9	E001	74.3538	74.4040	0.0502	0.0502
A10	F001	77.2332	77.1133	-0.1199	0.1199
B1	A006	54.2536	54.1155	-0.1380	0.1380
B2	A011	66.9121	66.8478	-0.0644	0.0644
B3	B004	37.3674	37.3114	-0.0560	0.0560
B4	B005	34.7802	34.7689	-0.0113	0.0113
B5	C006	17.7567	17.6987	-0.0580	0.0580
B6	D005	28.9470	29.0016	0.0546	0.0546
B7	E006	10.5343	10.5088	-0.0256	0.0256
B8	E009	20.9232	21.1261	0.2029	0.2029
B9	F003	70.2486	70.1228	-0.1258	0.1258
B10	F009	35.4150	35.4201	0.0051	0.0051
C1	A004	55.3303	55.2351	-0.0952	0.0952
C2	A013	77.9641	77.7965	-0.1675	0.1675
C3	A017	87.1583	86.9770	-0.1812	0.1812
C4	C002	59.4211	59.3251	-0.0960	0.0960
C5	C007	17.3731	17.3080	-0.0651	0.0651
C6	D004	32.1968	32.2622	0.0654	0.0654
C7	D006	10.5799	10.5982	0.0183	0.0183
C8	E007	-	0.0483	-	-
C9	E004	58.2011	58.1761	-0.0250	0.0250
C10	F008	43.1331	43.0851	-0.0481	0.0481
D1	A015	82.7461	82.5474	-0.1987	0.1987
D2	B006	26.7723	26.7144	-0.0578	0.0578
D3	C003	53.8915	53.8383	-0.0531	0.0531
D4	C005	31.6159	31.5672	-0.0487	0.0487
D5	D003	51.7654	51.8630	0.0975	0.0975
D6	D007	9.2678	9.1404	-0.1273	0.1273
D7	E002	54.0283	54.0159	-0.0124	0.0124
D8	E008	4.3514	4.3830	0.0316	0.0316

D9	F002	72.1424	72.0377	-0.1047	0.1047
D10	F005	56.6042	56.5710	-0.0331	0.0331

Photogrammetry

Point		Center Point A011			
		Total Station (ft.)	Photogrammetry (ft.)	Discrepancy (ft.)	Abs. Discrepancy (ft.)
A1	A002	60.8043	60.9365	0.1322	0.1322
A2	A019	39.4772	39.2564	-0.2208	0.2208
A3	B002	68.0020	68.2198	0.2178	0.2178
A4	B007	43.8453	43.9515	0.1062	0.1062
A5	C001	75.4581	75.5247	0.0666	0.0666
A6	C010	42.3633	42.3158	-0.0475	0.0475
A7	D001	80.6391	80.8148	0.1756	0.1756
A8	D010	48.0936	48.0233	-0.0703	0.0703
A9	E001	86.2749	86.4217	0.1468	0.1468
A10	F001	92.2668	92.3389	0.0721	0.0721
B1	A006	38.4693	38.5524	0.0832	0.0832
B2	A011	-	-	-	-
B3	B004	54.1946	54.2562	0.0616	0.0616
B4	B005	52.8947	52.9972	0.1025	0.1025
B5	C006	52.4709	52.5478	0.0769	0.0769
B6	D005	67.8378	67.9820	0.1442	0.1442
B7	E006	68.7411	68.7965	0.0554	0.0554
B8	E009	60.2467	60.2439	-0.0028	0.0028
B9	F003	90.5372	90.5602	0.0230	0.0230
B10	F009	83.6204	83.6680	0.0476	0.0476
C1	A004	51.2472	51.3134	0.0662	0.0662
C2	A013	11.0911	10.9900	-0.1011	0.1011
C3	A017	22.0452	21.8985	-0.1467	0.1467
C4	C002	72.6708	72.7523	0.0814	0.0814
C5	C007	50.9610	51.0195	0.0586	0.0586
C6	D004	68.8540	69.0062	0.1522	0.1522
C7	D006	60.0791	60.2032	0.1241	0.1241
C8	E007	66.9121	66.9465	0.0344	0.0344
C9	E004	89.2142	89.3677	0.1535	0.1535
C10	F008	86.1908	86.2612	0.0704	0.0704
D1	A015	16.0777	15.9037	-0.1741	0.1741
D2	B006	46.2474	46.3530	0.1055	0.1055
D3	C003	70.8116	70.8881	0.0765	0.0765
D4	C005	60.6311	60.7138	0.0828	0.0828
D5	D003	76.7450	76.9193	0.1743	0.1743
D6	D007	58.3193	58.4343	0.1150	0.1150
D7	E002	83.5124	83.6642	0.1518	0.1518
D8	E008	65.4161	65.4854	0.0692	0.0692

D9	F002	91.0273	90.5602	-0.4671	0.4671
D10	F005	89.2536	89.3639	0.1103	0.1103
Point		**Center Point B007**			
		Total Station (ft.)	**Photogrammetry (ft.)**	**Discrepancy (ft.)**	**Abs. Discrepancy (ft.)**
A1	A002	42.5732	42.5444	-0.0287	0.0287
A2	A019	81.1797	81.1037	-0.0760	0.0760
A3	B002	45.8448	45.9077	0.0629	0.0629
A4	B007	-	-	-	-
A5	C001	54.3055	54.2275	-0.0781	0.0781
A6	C010	52.2540	52.2676	0.0136	0.0136
A7	D001	57.2795	57.3200	0.0405	0.0405
A8	D010	44.4432	44.5515	0.1083	0.1083
A9	E001	61.4273	61.4361	0.0088	0.0088
A10	F001	66.0549	65.9850	-0.0698	0.0698
B1	A006	28.5333	28.4881	-0.0452	0.0452
B2	A011	43.8453	43.9515	0.1062	0.1062
B3	B004	19.6251	19.5442	-0.0809	0.0809
B4	B005	16.7271	16.7216	-0.0055	0.0055
B5	C006	9.3680	9.3719	0.0039	0.0039
B6	D005	26.0716	26.1024	0.0308	0.0308
B7	E006	25.4695	25.4456	-0.0239	0.0239
B8	E009	32.9145	32.9415	0.0270	0.0270
B9	F003	61.0090	60.8820	-0.1270	0.1270
B10	F009	41.1579	41.0897	-0.0682	0.0682
C1	A004	32.9650	32.9044	-0.0606	0.0606
C2	A013	54.7514	54.7382	-0.0132	0.0132
C3	A017	65.5349	65.5123	-0.0226	0.0226
C4	C002	45.2885	45.2207	-0.0678	0.0678
C5	C007	9.4564	9.4802	0.0238	0.0238
C6	D004	28.0641	28.0997	0.0356	0.0356
C7	D006	17.4394	17.4752	0.0358	0.0358
C8	E007	26.7065	26.6941	-0.0124	0.0124
C9	E004	53.8000	53.8031	0.0030	0.0030
C10	F008	45.4316	45.3693	-0.0623	0.0623
D1	A015	59.8740	59.8025	-0.0715	0.0715
D2	B006	3.5515	3.5200	-0.0315	0.0315
D3	C003	40.7465	40.6946	-0.0519	0.0519
D4	C005	20.9720	20.9045	-0.0675	0.0675
D5	D003	42.8825	42.9221	0.0397	0.0397
D6	D007	17.5166	17.5452	0.0285	0.0285
D7	E002	48.1989	48.1956	-0.0033	0.0033
D8	E008	27.2058	27.2463	0.0405	0.0405
D9	F002	62.3856	60.8820	-1.5036	1.5036

D10	F005	53.0354	53.0058	-0.0296	0.0296
Point		**Center Point D003**			
		Total Station (ft.)	**Photogrammetry (ft.)**	**Discrepancy (ft.)**	**Abs. Discrepancy (ft.)**
A1	A002	26.5687	26.5788	0.0101	0.0101
A2	A019	116.0660	116.0183	-0.0477	0.0477
A3	B002	20.1963	20.1974	0.0011	0.0011
A4	B007	42.8825	42.9221	0.0397	0.0397
A5	C001	23.4791	23.4374	-0.0417	0.0417
A6	C010	94.8944	94.9388	0.0445	0.0445
A7	D001	22.1034	22.1180	0.0146	0.0146
A8	D010	86.7604	86.9067	0.1463	0.1463
A9	E001	23.1763	23.1606	-0.0157	0.0157
A10	F001	25.7736	25.6794	-0.0943	0.0943
B1	A006	40.4073	40.4995	0.0922	0.0922
B2	A011	76.7450	76.9193	0.1743	0.1743
B3	B004	24.2534	24.3811	0.1278	0.1278
B4	B005	26.6839	26.7408	0.0569	0.0569
B5	C006	42.1878	42.2691	0.0813	0.0813
B6	D005	22.8231	22.8284	0.0052	0.0052
B7	E006	41.7526	41.8417	0.0891	0.0891
B8	E009	69.4382	69.5237	0.0855	0.0855
B9	F003	19.0114	18.8554	-0.1560	0.1560
B10	F009	25.2591	25.2330	-0.0262	0.0262
C1	A004	29.4618	29.5576	0.0959	0.0959
C2	A013	85.6463	85.6776	0.0312	0.0312
C3	A017	98.1116	98.1234	0.0118	0.0118
C4	C002	11.9717	11.9614	-0.0104	0.0104
C5	C007	45.4209	45.5244	0.1036	0.1036
C6	D004	19.5729	19.5743	0.0014	0.0014
C7	D006	43.3081	43.3378	0.0297	0.0297
C8	E007	51.7654	51.8408	0.0754	0.0754
C9	E004	12.7215	12.7127	-0.0087	0.0087
C10	F008	19.5820	19.5836	0.0017	0.0017
D1	A015	90.7921	90.7807	-0.0114	0.0114
D2	B006	39.3776	39.4522	0.0746	0.0746
D3	C003	8.2397	8.3017	0.0619	0.0619
D4	C005	22.6686	22.7814	0.1128	0.1128
D5	D003	-	-	-	-
D6	D007	47.6768	47.6988	0.0220	0.0220
D7	E002	7.0339	7.0305	-0.0034	0.0034
D8	E008	55.4805	55.5829	0.1024	0.1024
D9	F002	20.8392	18.8554	-1.9838	1.9838

D10	F005	12.9937	12.9455	-0.0482	0.0482
Point		**Center Point D007**			
		Total Station (ft.)	**Photogrammetry (ft.)**	**Discrepancy (ft.)**	**Abs. Discrepancy (ft.)**
A1	A002	62.8361	62.8365	0.0004	0.0004
A2	A019	100.3116	100.1833	-0.1283	0.1283
A3	B002	63.3303	63.4063	0.0760	0.0760
A4	B007	26.7065	26.6941	-0.0124	0.0124
A5	C001	70.7720	70.7361	-0.0359	0.0359
A6	C010	58.8696	58.7996	-0.0700	0.0700
A7	D001	71.8736	71.9457	0.0721	0.0721
A8	D010	45.9144	45.9954	0.0810	0.0810
A9	E001	74.3538	74.3996	0.0458	0.0458
A10	F001	77.2332	77.2079	-0.0254	0.0254
B1	A006	54.2536	54.2224	-0.0312	0.0312
B2	A011	66.9121	66.9465	0.0344	0.0344
B3	B004	37.3674	37.3498	-0.0176	0.0176
B4	B005	34.7802	34.8217	0.0415	0.0415
B5	C006	17.7567	17.7360	-0.0207	0.0207
B6	D005	28.9470	29.0172	0.0702	0.0702
B7	E006	10.5343	10.5193	-0.0150	0.0150
B8	E009	20.9232	20.9272	0.0040	0.0040
B9	F003	70.2486	70.1713	-0.0772	0.0772
B10	F009	35.4150	35.4366	0.0216	0.0216
C1	A004	55.3303	55.3139	-0.0164	0.0164
C2	A013	77.9641	77.9005	-0.0636	0.0636
C3	A017	87.1583	87.0834	-0.0749	0.0749
C4	C002	59.4211	59.3995	-0.0216	0.0216
C5	C007	17.3731	17.3522	-0.0209	0.0209
C6	D004	32.1968	32.2715	0.0747	0.0747
C7	D006	10.5799	10.5711	-0.0088	0.0088
C8	E007	-	-	-	-
C9	E004	58.2011	58.2307	0.0296	0.0296
C10	F008	43.1331	43.1255	-0.0076	0.0076
D1	A015	82.7461	82.6187	-0.1274	0.1274
D2	B006	26.7723	26.7455	-0.0268	0.0268
D3	C003	53.8915	53.8996	0.0081	0.0081
D4	C005	31.6159	31.5801	-0.0359	0.0359
D5	D003	51.7654	51.8408	0.0754	0.0754
D6	D007	9.2678	9.2217	-0.0461	0.0461
D7	E002	54.0283	54.0497	0.0215	0.0215
D8	E008	4.3514	4.3542	0.0028	0.0028
D9	F002	72.1424	70.1713	-1.9710	1.9710

D10	F005	56.6042	56.6231	0.0189	0.0189